Master's thesis

NTNU
Norwegian University of Science and Technology
Faculty of Engineering
Department of Marine Technology

Kristoffer Lund

Online Optimization of a Hybrid Electric Marine Power Plant Using Mixed Integer Linear Programming

Master's thesis in Marine Technology
Supervisor: Roger Skjetne
June 2020

NTNU
Norwegian University of
Science and Technology

Kristoffer Lund

Online Optimization of a Hybrid Electric Marine Power Plant Using Mixed Integer Linear Programming

Master's thesis in Marine Technology
Supervisor: Roger Skjetne
June 2020

Norwegian University of Science and Technology
Faculty of Engineering
Department of Marine Technology

NTNU

Kunnskap for en bedre verden

NTNU Trondheim
Norwegian University of Science and Technology
Department of Marine Technology

MASTER OF TECHNOLOGY THESIS DEFINITION (30 SP)

Name of the candidate: Kristoffer Lund

Field of study: Marine control engineering

Thesis title (Norwegian): Norsk tittel

Thesis title (English): Online Optimization of a Hybrid Marine Power Plant using Mixed Integer Linear Programming

Background
Hybrid electric ships are becoming more popular with foreseen potentials of reduced emissions, maintenance, and fuel costs. Combining electrical propulsion with a mechanical shaft line gives various options when designing and configuring the marine power system. This can be done in a number of ways, and depends highly on the nature of the vessel, such as vessel type and operational profile. Adding also Energy Storage Devices (ESDs), such as battery banks, introduces more options for optimizing the plant operation. Given a hybrid electric vessel with a known operational profile, the design of the marine power system for the vessel can be optimized with respect to a number of variables. Optimization performance objectives can be fuel consumption, total emission, total cost, engine running hours, numbers of starts/stops, or other characteristics. The optimization variables can be scheduling of the power sources (connect/disconnect), engine speed and torque/load, battery charge/discharge, and opening/closing of bus-tie breakers. Choosing an optimal design of a marine power system, as opposed to an inferior design, and thereby optimally controlling the given power system, can introduce great savings for the ship owner, as well as reducing emissions to the environment.

Work description
1. Perform a background and literature review to provide information and relevant references on:
   - Hybrid electric power and propulsion systems, incl. ESDs and power converters.
   - Power management systems, battery management systems and energy & emission management systems (including system architecture and relevant functions).
   - Control of hybrid power systems.
   - Optimization used for power plant control.

   Write a list with abbreviations and definitions of terms and symbols, relevant to the literature study and project report.

2. Define some relevant marine power plant cases in terms of equipment, configurations (by single line diagrams), and load profiles on the main bus. Get data for the load profiles and specifications of the equipment, incl. SFOC curves (and possibly SNOx curves) for each engine. Also get specifications of the battery banks.

3. Study and present the Marine Power Plant Simulator developed at NTNU, and set up a simulation model for each case configuration that you have proposed:
   - This needs only to simulate the gensets, ESDs, relevant converters, and the main buses – with a power load profile inserted on each bus.
   - The simulation model should at least include the engine SFOC maps as lookup tables and output measurement of FOC during the simulation.

4. Study Mixed-Integer Linear Programming (MILP) used for energy and emission management applications. Consider a simplified marine power plant (not a simulation model) and the task of genset scheduling. Formulate the corresponding MILP optimization problem for the optimization objectives:
   - Minimizing online capacity.

- Minimizing running hours of gensets.
- Minimizing connections/disconnections of gensets.

5. Extend the optimization problem formulation to also consider the load sharing problem between active gensets. Develop and verify a MILP algorithm for optimal load sharing in a simplified marine power plant by demonstrating the performance on 1) a deterministic load profile, and 2) one of your realistic load profiles.

6. Study the functions in the Marine Power Plant Simulator related to connecting/disconnecting gensets by breakers and load sharing between generators. Develop functionality in order to perform droop-based load sharing and switching breakers on and off.

7. Implement the MILP optimization algorithm in the Marine Power Plant Simulator environment.

8. Run the simulation models on your load profiles in a fixed configuration (e.g., all connected), and a "non-fixed" configuration, using the MILP optimization algorithm for connecting/disconnecting gensets and load sharing between connected gensets. Define some key performance indicators (KPIs) used to measure the performance in each simulation case. Compare the different configurations with a given load profile using your KPIs.

Specifications

Every weekend throughout the project period, the candidate shall send a status email to the supervisor and co-advisors, providing two brief bulleted lists: 1) work done recent week, and 2) work planned to be done next week.

The scope of work may prove to be larger than initially anticipated. By the approval from the supervisor, described topics may be deleted or reduced in extent without consequences with regard to grading.

The candidate shall present personal contribution to the resolution of problems within the scope of work. Theories and conclusions should be based on mathematical derivations and logic reasoning identifying the various steps in the deduction.

The report shall be organized in a logical structure to give a clear exposition of background, problem, design, results, and critical assessments. The text should be brief and to the point, with a clear language. Rigorous mathematical deductions and illustrating figures are preferred over lengthy textual descriptions. The report shall have font size 11 pts., and it is not expected to be longer than 70 A4-pages, 100 B5-pages, from introduction to conclusion, unless otherwise agreed upon. It shall be written in English (preferably US) and contain the elements: Title page, abstract, acknowledgement, project definition, list of symbols and acronyms, table of contents, introduction (project motivation, objectives, scope and delimitations), background/literature review, problem formulation, method, results, conclusions with recommendations for further work, references, and optional appendices. Figures, tables, and equations shall be numerated. The original contribution of the candidate and material taken from other sources shall be clearly identified. Work from other sources shall be properly acknowledged using quotations and a Harvard citation style (e.g. *natbib* Latex package). The work is expected to be conducted in an honest and ethical manner, without any sort of plagiarism and misconduct, which is taken very seriously by the university and cause consequences. NTNU can use the results freely in research and teaching by proper referencing, unless otherwise agreed upon.

The thesis shall be submitted with an electronic copy to the main supervisor and department according to NTNU administrative procedures. The final revised version of this thesis description shall be included after the title page. Computer code, pictures, videos, dataseries, etc., shall be included electronically with the report.

Start date: 15 January, 2020 **Due date:** As specified by the administration.

Supervisor: Roger Skjetne
Co-advisor(s): Mehdi Zadeh, Laxminarayan Thorat

Trondheim, 15.03.2020

_____
Roger Skjetne
Supervisor

Abstract

This thesis presents a literature review of the hybrid electric power and propulsion system and the fields of optimization and control of hybrid marine power systems. Components, characteristics and control layers of hybrid electric power and propulsion systems are described, and several optimization and control methods of hybrid power systems are explored.

An optimization method using mixed integer linear programming (MILP) is studied, and a MILP formulation of the scheduling and load sharing problem for a marine power plant is presented. This results in a MILP optimization algorithm implemented in Matlab. The MILP optimization algorithm has the possibility to optimize the power plant with respect to several optimization objectives, including minimizing online capacity, running hours of gensets and numbers of connections/disconnections of gensets. The proposed optimization algorithm is verified in Matlab by optimizing a simplified marine power plant with a deterministic load profile.

The Marine Vessel and Power Plant System Simulator (MVPPSS) is studied and presented, in order to make a simulation model of marine power plants. Further on, the MILP optimization algorithm is implemented in the simulation environment of the MVPPSS. This introduces the possibility to include an online optimization layer in a simulation model in the MVPPSS, and makes it possible to optimize a simulation model of a marine power plant.

A case study is conducted, comparing three different marine power plants using the same realistic load profile. The three power plants are simulated in fixed configuration (i.e. all gensets connected throughout the whole simulation and no power control present in the model) and in non-fixed configuration (i.e. gensets are connected/disconnected and controlled by the optimal setpoints provided by the MILP optimization algorithm). The marine power plants are compared with respect to a set of chosen key performance indicators (KPIs), and an optimal design for a marine power plant for the given load profile is proposed. The comparison yields a proposed configuration of a marine power plant consisting of six gensets and a battery energy storage device (ESD). The simulations show that all three marine power plants experience a reduction in fuel consumption in non-fixed configuration vs fixed configuration, indicating that using the developed optimization algorithm reduces the fuel consumption of marine power plants. The case study demonstrates the possibility to use the MILP optimization algorithm for optimal design purposes, as well as online optimization of a marine power plant.

Sammendrag

Denne masteroppgaven presenterer et litteraturstudie om temaene hybrid-elektriske kraft- og fremdriftssystemer og optimalisering og regulering av hybride kraftsystemer. Komponenter, karakteristikker og reguleringslag ved hybrid-elektriske kraft- og fremdriftssystemer blir beskrevet, og flere optimaliserings- og reguleringsmetoder for hybride kraftsystemer utforskes.

En optimaliseringsmetode ved bruk av MILP utforskes, og en MILP-formulering for allokerings- og lastfordelingsproblemet for et marint kraftsystem blir presentert. Dette resulterer i en MILP optimaliseringsalgoritme som blir implementert i Matlab. MILP optimaliseringsalgoritmen kan optimalisere kraftsystemet med hensyn til flere optimaliseringsmål, inkludert å minimere online kapasitet, kjøretid for generatorsett og antall tilkoblinger/frakoblinger av generatorsett. Den foreslåtte optimaliseringsalgoritmen blir verifisert i Matlab ved å optimalisere et forenklet marint kraftsystem med et deterministisk lastprofil.

MVPPSS studeres og presenteres, slik at en simuleringsmodell av marine kraftsystemer kan lages. Videre blir MILP optimaliseringsalgoritmen implementert i MVPPSS. Dette gir muligheter for å inkludere et online optimaliseringslag i en simuleringsmodell i MVPPSS, og gjør det mulig å optimalisere en simuleringsmodell av et marint kraftsystem.

Et casestudie blir gjennomført, der tre ulike marine kraftsystemer med samme realistiske lastprofil blir sammenlignet. De tre kraftsystemene blir simulert i fixed konfigurasjon (det vil si alle generatorsett er tilkoblet gjennom hele simuleringen og det er ingen kraftregulering av generatorsett i modellen) og ikke-fixed konfigurasjon (det vil si generatorsett blir tilkoblet/frakoblet og regulert ved bruk av optimale settpunkt beregnet av optimaliseringsalgoritmen). De marine kraftsystemene blir sammenlignet ved å bruke valgte ytelsesindikatorer, og et optimalt design for et marint kraftsystem med det gitte lastprofilet blir foreslått. Sammenligningen gir en foreslått konfigurasjon av kraftsystemet bestående av seks generatorsett og ett batteri. Simuleringene viser at alle tre kraftsystemer opplever en reduksjon i drivstofforbruk i ikke-fixed konfigurasjon vs fixed konfigurasjon. Dette indikerer at den utviklede optimaliseringsalgoritmen reduserer drivstofforbruket til marine kraftsystemer. Casestudiet demonstrerer muligheten for å bruke MILP optimaliseringsalgoritmen som et ledd i optimale designformål, i tillegg til å bruke den som online optimalisering av et marint kraftsystem.

Preface

This master's thesis is the concluding submission of a Master of Science degree in Marine Technology, written at NTNU, Trondheim in the spring of 2020.

My summer internship with ABB during the summer of 2019 provided me with a curiosity and interest in marine power systems. This made me follow the desire to immerse myself in the field of optimization and control of hybrid marine power systems when choosing the topic for my master's thesis.

The work of this thesis is a continuation of the work I did in my project thesis during the fall of 2019. Thus, the continuation of the literature review, and further development of the implemented computer methods used in the project thesis have been in focus. The thesis presents a literature review of hybrid electric power and propulsion systems and optimization and control of hybrid power system. Then, an optimization method using mixed integer linear programming is implemented, before the optimization algorithm is connected with a realistic marine power system simulator.

The thesis has been written during the challenging and strange times of spring 2020, a time when the whole world has seen restrictions in everyday life due to the ongoing Corona virus situation. This has of course affected the course of the work with the thesis, as the university closed from mid-March. This has resulted in less collaboration and discussions with fellow students and office mates than desired. However, measures have been taken by the university, and supervision has been carried out digitally, providing the students with the needed guidance and supervision.

The project process started mid-January and started with further literate review of the relevant topics and the simulation environment used in the thesis. The work has been carried out mainly through using relevant literature and conducting simulations. Professor Roger Skjetne, my main supervisor, has guided me in finding out which direction the work of the thesis should evolve, and has been a valuable discussion partner for understanding research questions and methods used for power plant control. Professor Skjetne has helped with formulations and implementations of control methods in the chosen simulation environment. Laxminarayan Thorat has overseen and quality checked some mathematical formulations of optimization methods. Lastly, Daeseong Park has provided insight and clarifications on the contents of the power system simulator used in this thesis.

Acknowledgements

Firstly, I would like to thank professor Roger Skjetne for introducing me to the field of optimization of hybrid marine power systems and guiding me through the work of this thesis. Professor Skjetne has through his experience and competence in this field of study given valuable inputs when questions have occurred and clarifications have been needed.

I would also like to thank my co-supervisor, Laxminarayan Thorat, who has helped with quality checks of some of my work. Also, Daeseong Park's time and effort in helping me with clarifications and insight in the contents of the MVPPSS have been invaluable, and are much appreciated. I am also grateful for the possibility of using the MVPPSS for my master's thesis, which is a simulator developed at NTNU by Torstein Bø.

Lastly, I would like to thank my office mates for the great work and social environment we had in our office until mid-March. Especially, thanks go to Olav Fiksdahl for great collaboration on our joint work in our theses.

Table of Contents

List of Tables

List of Figures

Abbreviations

AC	=	Alternating Current
AVR	=	Automatic Voltage Regulator
BMS	=	Battery Management System
DC	=	Direct Current
DP	=	Dynamic Positioning
ECMS	=	Equivalent Cost Minimization Strategy
EEMS	=	Energy and Emission Management System
EMF	=	Electromotive Force
ESD	=	Energy Storage Device
Genset	=	Generator Set
GWO	=	Grey Wolf Optimization
KPI	=	Key Performance Indicator
LNG	=	Liquefied Natural Gas
LP	=	Linear Programming
MCR	=	Maximum Continuous Rating
MILP	=	Mixed Integer Linear Programming
MPC	=	Model Predictive Control
MSS	=	Marine Systems Simulator
MVPPSS	=	Marine Vessel and Power Plant System Simulator
NLP	=	Nonlinear Programming
P.U.	=	Per Unit
PSO	=	Particle Swarm Optimization
PID	=	Proportional, Integral and Derivative
PMP	=	Potryagin's Minimum Principle
PMS	=	Power Management System
PWL	=	Piecewise Linear
PWM	=	Pulse Width Modulation
QP	=	Quadratic Programming
RMS	=	Root Mean Square
ROV	=	Remotely Operated Vehicle
SFOC	=	Specific Fuel Oil Consumption
SLD	=	Single Line Diagram
SoC	=	State of Charge

Chapter 1

Introduction

1.1 Motivation

Hybrid electric ships are increasing in numbers and complexity, as the development of hybrid electric power and propulsion systems has sky rocketed since the industry fully adopted the shipboard electric power systems in the 1980s. The use of electric power systems aboard ships has introduced the possibility of optimizing the operation of the marine power plant in a way which previously was not possible. Also, hybrid marine power systems, which include several power sources, e.g. ESDs, introduce various options when designing and configuring the power plant. This can be done in a number of ways, using different optimization methods, and depends highly on the nature of the vessel, such as vessel type and operational profile. A marine power plant can be optimized with respect to several characteristics. Such optimization objectives can be fuel consumption, total emission, life cycle costs, engine running hours or numbers of connections/disconnections. Online optimization of a marine power plant, i.e. calculating optimal setpoints to power producers while the vessel is in operation, can be computationally demanding, but has the potential of reducing emissions and saving expenses for the ship owner due to lower fuel consumption and the reduction of wear and tear on the equipment.

This motivates for an investigation of optimization methods and the development of an optimization algorithm which can be used for optimizing the operation of a marine power plant. The potential of such an optimization algorithm can be assessed by a simulation model of a marine power plant. Simulations should be carried out and tested carefully before implementing an optimization algorithm in the control systems of a real vessel and testing it in reality.

1.2 Problem Formulation and Objectives

This thesis tries to answer how a hybrid marine power plant can be optimized with respect to a set of optimization objectives using mixed integer linear programming. To answer this research question, the following main objectives are formulated:

- Review literature within hybrid electric power and propulsion systems, control of hybrid power systems and optimization used for power plant control.
- Formulate the corresponding MILP optimization problem to the task of genset scheduling and load sharing of a marine power plant, resulting in a MILP optimization algorithm.
- Study the MVPPSS, developed at NTNU, and implement the developed MILP optimization algorithm in the simulator. Use the MVPPSS as a simulation environment for evaluating the performance of the optimization of a marine power plant.

1.3 Scope and Delimitations

The scope of the thesis is to perform a background study and retrieve relevant references on hybrid electric power systems, including control and optimization of said systems. Further, a MILP optimization formulation considering genset scheduling and load sharing should be implemented. This work is done in Matlab. Using the developed code for the MILP optimization algorithm, an optimization layer should be added to a simulation model of a marine power plant using the MVPPSS as simulation environment. This is done using Simulink. When a functional simulation model of a marine power plant including the optimization layer is developed, a case study comparing different marine power plant configurations should be conducted. The different configurations should be evaluated using a set of chosen KPIs.

Some of the delimitations of this thesis are:

- Power plants are limited to include gensets and battery ESDs connected directly to a bus. Only active power is considered.
- Battery is modeled including battery dynamics. However, the battery's contribution to the power plant is considered as a reduction in demanded load according to the delivered power from the battery. This means that no battery control system is included, meaning the battery can not be controlled and the different usage strategies of a battery can not be utilized.
- Fuel consumption is estimated using a piecewise (PWL) linear function as an approximation of the specific fuel oil consumption (SFOC)-curve. The SFOC-values are included in the optimization algorithm as lookup-tables.
- The developed MILP optimization algorithm only optimizes the scheduling and load sharing of gensets. Other power producers are not included in the optimization.

1.4 Contributions of the Thesis

The contributions of the thesis are:

- A MILP optimization algorithm has been implemented in Matlab, following the method proposed by Thorat and Skjetne (2018). The optimization algorithm can be simulated on a simplified power plant using the developed code.
- The developed MILP optimization algorithm has been implemented in the simulation environment of the MVPPSS, thus connecting the optimization method with a realistic simulation model of a marine power plant.
- The conducted case study demonstrates the performance of the MILP optimization algorithm on several marine power systems (and shows that using the algorithm leads to a significant reduction of fuel consumption for all configurations simulated).

1.5 Outline of the Thesis

Chapter 1

Introduces the thesis to the reader. Describes the motivation behind the thesis, the objectives, scope and delimitations of the thesis and the contributions of the thesis.

Chapter 2

Provides relevant background theory on components, characteristics and control layers of hybrid electric power and propulsion systems.

Chapter 3

Provides relevant background theory on optimization and control of hybrid power systems.

Chapter 4

Presents the corresponding MILP formulation to the task of genset scheduling and load sharing of a marine power plant, as proposed by Thorat and Skjetne (2018). Thorat and Skjetne (2018)'s formulation is implemented as Matlab code, giving rise to the MILP optimization algorithm used for optimization in this thesis.

Chapter 5

Presents the MVPPSS, including background theory and mathematical modeling of components. The implementation of the MILP optimization algorithm in the simulation environment of the MVPPSS is also described in this chapter.

Chapter 6

Verifies the MILP optimization algorithm, ensuring that its provided solutions are correct and its behavior is as expected according to the chosen optimization objectives.

Chapter 7

Conducts a case study consisting of comparing three different marine power plant configurations with respect to chosen KPIs. Shows how the MILP optimization can be used in the design process of a marine power plant regarding choosing an optimal design. Also verifies the use of the MILP optimization algorithm as an online optimization method of a marine power plant.

Chapter 8

Presents conclusions and recommendations for further work.

Chapter 2

Hybrid Electric Power and Propulsion Systems

Parts of this chapter are based on my project thesis (Lund, 2019), written at NTNU during the fall of 2019.

2.1 Background - A Brief History of Marine Electric Power Systems

The most essential purpose of a ship is transfer from one place to another by sea travel. All ships need an energy source of potential energy (e.g. chemical (fuel) or electric (on board electricity)). The potential energy is converted to kinetic energy through for instance diesel engines, electrical motors or turbines. In turn, the motion of the propulsors leads to the movement of the ship itself. Electric propulsion is a feature used in many ships, and the propulsion system is often powered by electricity generated on board by diesel engines or gas turbines (Ådnanes, 2003). A diesel-electric propulsion system is characterized by a diesel engine being connected to a generator, which provides power to the electrical grid on board (Wu et al., 2018). The electrical grid provides distribution of electricity to the electrical motors which drive the thrusters. Also, in a diesel-electric propulsion system, there may or may not be thrusters present that are driven directly by the diesel engine, through a drive shaft.

A hybrid power system combines two or more power sources for producing power. This thesis will focus on the hybrid-electric power system, containing a traditional power source, diesel engine(s), and ESD, a battery pack. Often, batteries are used as ESDs. There are different ESD usage strategies, which will be reviewed later.

The birth of the marine vessel power grid dates back to the 1830s, when German inventor Moritz Hermann von Jacobi experimented with a direct current (DC) motor on a small ferry using electric propulsion, powered by a battery (Skjong et al., 2015). In 1880, the *SS Columbia* was the first ship to have a shipboard electrical system (DC) installed, where the electrical system powered a lighting system on board the ship
(Skjong et al., 2015). Onward, the $US\ Bureau\ of\ Navigation$ ordered the installation of lights on board vessels (Skjong et al., 2016). In this period, most of the shipboard electrical power systems used DC, because the alternating current (AC) motors had not yet been properly developed. In 1885, the first successful electrically powered vessel, the $Elektra$, was built by German $Siemens\ \&\ Halske$. The US pushed the development of electric drives in the beginning of the 1900s, and installed the first turbo-electric drive on the $Joseph\ Medill$ in 1908. A turbo-electric power plant is a power plant which produces the electricity from generators driven by steam turbines. Therefore, instead of directly connecting the propeller shaft to the steam turbine, which was how the propulsion systems of steam powered ships traditionally were operated, the turbine drives generators creating electricity, which powers electrical motors which in turn run the propellers. Four years after the first turbo-electric driven ship, the US Navy installed a turbo-electric propulsion system on the collier $USSJupiter$ which was the first naval vessel using turbo-electric propulsion. As this was a success, the US Navy decided to upgrade all their front line battle ships to use electric power systems. The use of turbo-electric propulsion spread from navy vessels to passenger vessels, and by the 1920s several civilian ships had converted to the technology, among others in the US, Sweden and Britain (Smith, 2013; Skjong et al., 2016). Rudolf Diesel patented the diesel engine in 1892, and the first diesel electric propulsion system was made in 1903. Throughout the periods of World War 1 and World War 2, there was an arms race between the different parts in the wars. Especially submarines were developed with electric propulsion systems.

In the early 1900s, the mercury pool rectifier was developed and with it came a new method for power conversion instead of mechanical power conversion (Herskind and Morack, 1987). A rectifier is a device which converts AC to DC, which the electrical motors running the propulsors often use. Solid state power electronics were invented and made available in the 1960s and 1970s and meant great development and evolving of shipboard power systems. Using power electronics for optimizing power systems by minimizing fuel consumption became mainstream in the 1980s and was widely used in off-shore vessels. Off-shore vessels often use dynamic positioning (DP) for complex operations and are dependent on advanced and refined control systems for maintaining the desired position during operation. Diesel-electric propulsion systems became the most used configuration. Moving towards present time, fuel cell ESDs have made their appearance on the market, pushing the ship industry towards greener operations and less emissions. The world's first fully electric passenger- and car-ferry, the $MFAmpere$ was finished in 2015 (Skjong et al., 2016).

2.2 Motivation for Electric Power and Propulsion systems

Using electric propulsion has become the industry standard for many types of vessels, including cruise vessels, ferries, DP vessels, thruster assisted moored floating production vessels, shuttle tankers, supply vessels and war ships among others (Ådnanes, 2003). The main reason for using electric propulsion in ships is that it introduces great potential of fuel savings, as opposed to using a mechanically driven propulsion where the prime mover is directly connected to the propulsor (Hansen and Wendt, 2015). Every engine has an optimal load factor, which states for what operating point the engine consumes the least amount of fuel. This optimal operating point is usually around 80 % of the maximum continuous rating (MCR), and can be seen from the SFOC-curves for the engine. The utilization of running the gensets at their optimal running point is what causes the fuel savings when using electric propulsion. As opposed to land based electrical grids where the loads are easily anticipated and somewhat constant, at least for periods of time, a shipboard electrical grid can experience big variations in load level. This is due to the fact that vessels often have fluctuations in their operational profiles and can also be because of varying environmental loads for a dynamically positioned vessel. Given the property of the varying operational profiles and fluctuating demanded loads from thrusters and other power consumers, by using electric propulsion, the gensets can be operated at their optimal running point nevertheless. Thus, running the engines at their optimal condition, and switching components on and off in accordance with the power demand, will lead to less fuel consumption, meaning savings in cost and emissions (Hansen and Wendt, 2015). The electric propulsion system also makes way for podded propulsion, where the electric motor driving the propeller is submerged within the pod itself, saving space, cost and emissions and improving comfort onboard (ABB, 2019).

Other advantages of the electric power and propulsion system, as stated by Ådnanes (2003), are for instance space-savings on board the ship and flexibility of placing thrusters since the power to the thrusters is delivered through cables so there is no need for the thrusters being placed directly behind a prime mover because of a gear transmission. Also, improved maneuvering due to the use of azimuthing thrusters and less vibrations and noise due to gensets running on fixed speed (optimal operating point) are advantages of electric power and propulsion systems. Lastly, less cavitation on the pulling propellers and shorter rotating shafts in the propulsion system are also introduced in electric power and propulsion systems.

Installing an ESD, e.g. battery or supercapacitor, in a diesel-electric propulsion system can introduce several benefits. As stated by Miyazaki et al. (2016), “ESD is a device that stores energy and is able to consume and deliver power on demand”. A so called hybrid-electric power and propulsion system, by including an ESD, may introduce benefits like reduced fuel consumption (Lindtjørn et al., 2014). For a battery or supercapacitor to be utilized, there is need of an electric power and propulsion system.

2.3 Generator Sets

A generator set (genset) is a combination of a prime mover and an electric generator. Often, the prime mover is a diesel engine, but could also be natural gas engines or steam turbines. The purpose of the genset is to convert the chemical energy in the fuel (diesel, gas, hydrogen) to mechanical energy which runs the generator. The generator in turn produces electrical power from the mechanical energy. The generator is similar to the principle of an electric motor, using a stator and a rotor and utilizing the relations between a magnetic field, magnetic force and flux. However, a generator uses mechanical energy to produce electrical energy, as opposed to an electric motor which produces mechanical energy from electrical energy. The electricity produced by the generator is used to run electric motors which run the propulsors of the ship. The most common configuration of gensets is to have multiple gensets of the same size and specifications (Hansen and Wendt, 2015). Another way is to use gensets of different size and specifications. Wu (2017) explored the difference in performance by evaluating fuel consumption for a hybrid power plant using low-power vs. high power engines. By using several gensets, one assures redundancy, as well as the ability to produce power for several operating conditions, which often means different load demands.

2.4 Energy Storage Devices

As described earlier, an ESD is a device which can store energy and produce and consume power. There are several types of ESDs, and multiple usage strategies for delivering and consuming power. The most commonly used ESDs in hybrid-electric power systems are batteries and supercapacitors, where batteries experience a small preference because of the development within chemical and cooling technology. In general, batteries are preferred for energy intensive operation conditions whereas supercapacitors are preferred in repetitive and power intensive conditions (Lindtjørn et al., 2014).

A supercapacitor is a high-capacity capacitor. A capacitor stores energy by using electrostatics, as opposed to batteries which store energy as chemical energy. Capacitors deliver and consume power very quickly, and are lighter than batteries, providing the same amount of power. Capacitors can be charged and discharged without being worn out. The main drawback for capacitors is the amount of energy they are able to store, which is a small amount compared to the abilities of a battery.

A battery is a device storing chemical energy. By using electrochemical cells, the battery can store energy and release it as electrical power. Batteries can store great amounts of energy, but can not deliver and consume power as quick as capacitors. Batteries are also heavy. Using battery as an ESD is further explored in Section 2.6.5, where the usage strategies of battery ESDs and usual constraints and functions are addressed.

Flywheels are mechanical devices designed to store kinetic energy. By utilizing the moment of inertia of a flywheel, energy can be stored and released from the flywheel.

2.5 Power Converters

Power electronic converters are an important part of modern power plants. The main purpose of power electronic converters is to "perform a power conditioning to meet certain requirements of different applications" (Blaabjerg, 2018). Power electronic converters are used for changing the properties of the electrical energy, i.e. delivering the desired voltage and current of different magnitude and frequency. Different components need different types of electrical energy, and by introducing power electronic converters, one can change the power within the power grid for use in different types of applications. There are four types of power conversion of electrical energy between AC and DC. These power conversions include AC-DC converters, called rectifiers, AC-AC converters, called transformers, DC-DC converters and DC-AC converters, called inverters.

The **AC-DC converter**, or rectifier, converts a varying sinusoidal AC voltage to a constant DC voltage. This is one of the most frequently used power converters, as the land based electrical grid uses AC, while most devices, ranging from cell phones to refrigerators, use DC.

AC-AC converters, or transformers, convert power from an AC power source to an AC power load of a different voltage or current level, with respect to the signal's amplitude, frequency or phase. Some AC-AC converters have a DC-link in the conversion, meaning the AC power is converted to DC, and then back to AC (Wilson, 2000). Often, transformers are used when redistributing the power from the electrical distribution network to a subgrid, for instance a residential area.

A **DC-DC converter** changes the level of the DC input voltage to a higher or lower level of voltage for the DC output voltage. The basic functionality of the DC-DC converter is the utilization of semiconductor switches which are turned on and off at high frequencies (Blaabjerg, 2018). The DC output voltage from a DC-DC converter can be regulated by tuning the duration of the switch turned on. This is called pulse width modulation (PWM) control.

DC-AC converters convert electrical power from DC to AC. The AC power output is produced with a desired signal, given wanted amplitude, frequency and phase.

2.6 System Architecture of Control Layers

This section is written in collaboration with Olav Fiksdahl, see Fiksdahl (2020).

An autonomous ship has several layers of autonomy functions. This section focuses on the system structure of the power system of an autonomous ship, and defines the system structure for the energy and emission management system (EEMS), power management system (PMS), and the battery management system (BMS). The main functions of these systems and what is controlled by each of the control layers are also addressed in this section.

2.6.1 System Structure

Reddy et al. (2019) define the system structure of control layers for a hybrid power and propulsion system of an autonomous ship. The system structure of the control layers can be seen in Figure 2.1. The control layers are divided into three layers. The top level is the mission layer, where the vessel mission management system is located. The vessel mission management system supervises the vessel mission and objectives, and commands the lower level systems to act in accordance with these criteria. The next level is the online optimization layer. Here, the EEMS performs online optimization of the hybrid power and propulsion system. The last level, the real-time control execution layer, consists of the PMS and the BMS. Both the PMS and the BMS provide safe operation of the hybrid power system. The PMS ensures that the power system delivers power according to the load requirement, and it prevents blackout if a fault occurs. The BMS ensures safe and reliable operation of the batteries (Reddy et al., 2019). See also Figure 2.2 for the control and communication architecture of the control layers of an autonomous ship.

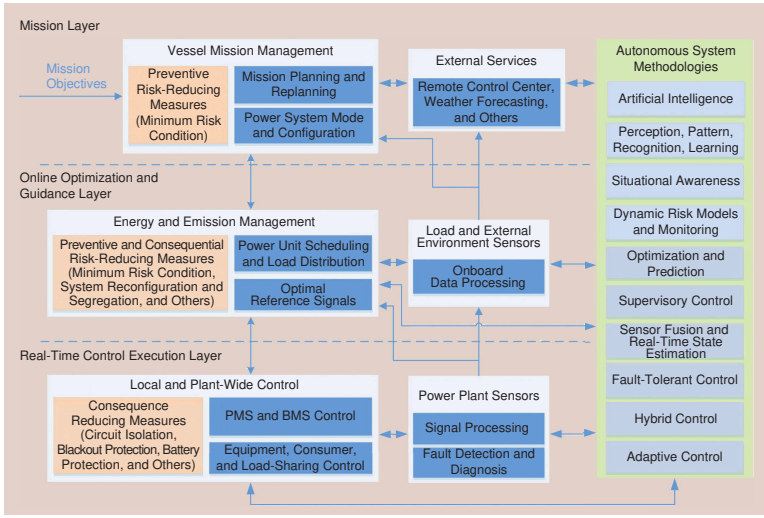

Figure 2.1: Control system layout of an autonomous ship and its power system. Courtesy: Roger Skjetne, NTNU AMOS. See also Reddy et al. (2019).

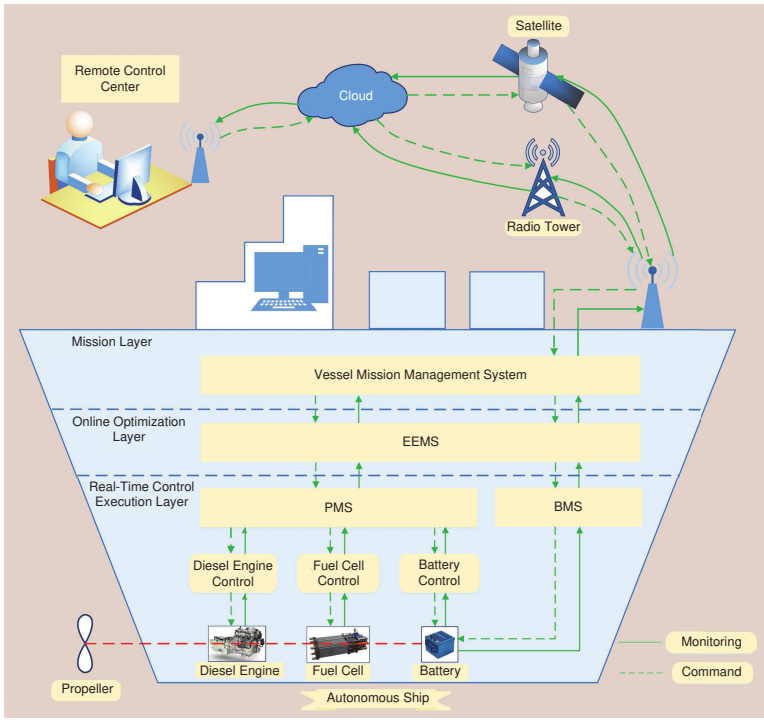

Figure 2.2: Control and communication architecture of an autonomous ship. Courtesy: Roger Skjetne, NTNU AMOS. See also Reddy et al. (2019).

2.6.2 Energy and Emission Management System

An EEMS is defined by Reddy et al. (2019) as a "high-level control system that commands the operation of a hybrid power plant to minimize energy usage and emissions while maintaining safety and resilience requirements and fulfilling the objectives of the vessel's mission". The EEMS distributes the required load power between several energy sources such that the energy sources are used in an optimal manner and the emissions from the power system are minimized. The optimal use of the different energy sources is determined by the EEMS by monitoring and controlling the energy flows in the power system, and a decision is made with respect to for instance minimizing the fuel consumption or other optimization objectives such as optimal load sharing or optimal connections/disconnections of power producers. Within the EEMS lie many opportunities of implementing different optimization algorithms, utilizing the capabilities of each algorithm and considering different optimization objectives. The EEMS performs online optimization of the power system, meaning that the optimization problem contains no or limited knowledge of the future information about the states of the optimization variables. Due to this fact, the online optimization uses an instantaneous cost function for optimization (Reddy et al., 2019), using instantaneous measurements of variables at the time instant the optimization is conducted. Therefore, an online optimization approach is suitable for optimizing the

operation of a marine power system, as the loads experienced by the system are unpredictable and estimated at best. This means that an optimization which uses measurements from the power system throughout the optimization fits this purpose. Examples of such measurements are power loads and power outputs from the different energy sources.

In Figure 2.3, an illustration of the objectives of an EEMS is seen, ranging from minimizing fuel consumption to minimizing life-cycle operating costs.

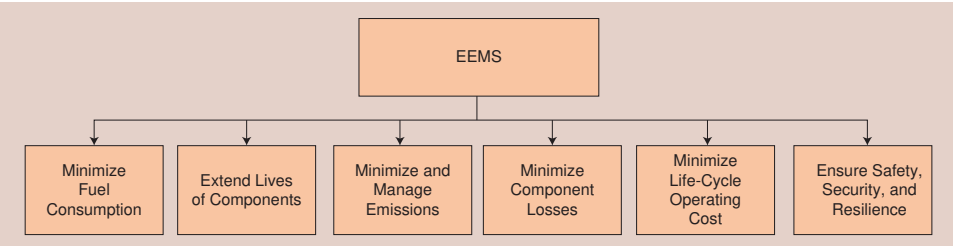

Figure 2.3: Objectives of an EEMS. Courtesy: Roger Skjetne, NTNU AMOS. See also Reddy et al. (2019).

The EEMS uses three different control strategies, and a classification of these strategies can be seen in Figure 2.4. As can be seen from the figure, the EEMS is divided into a rule based, an optimization based and a learning based strategy. Both theses, Fiksdahl (2020) and this thesis, will focus on online optimization, using model predictive control (MPC) and MILP optimization, respectively. Other online optimization methods include the equivalent cost minimization strategy (ECMS), Potryagin's minimum principle (PMP), linear programming (LP), quadratic programming (QP) and nonlinear programming (NLP).

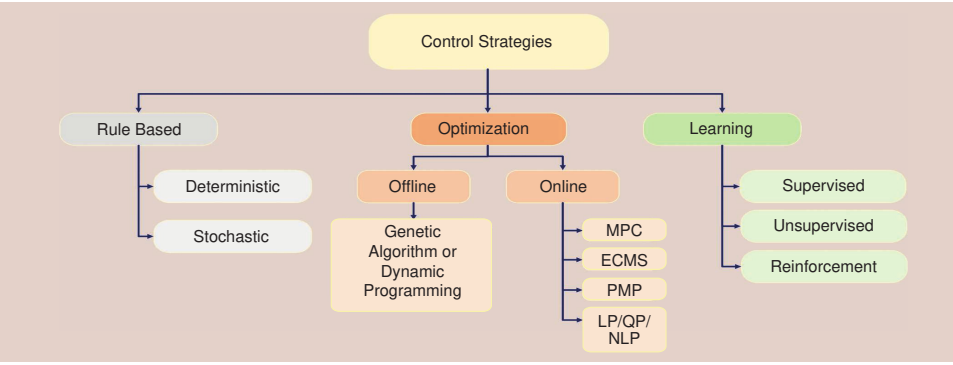

Figure 2.4: Classification of control strategies for the EEMS. Courtesy: Roger Skjetne, NTNU AMOS. See also Reddy et al. (2019).

2.6.3 Power Management System

The purpose of a PMS is to ensure that there is enough power available in the power grid (Ådnanes, 2003). Given the operating condition, the PMS ensures there are enough gensets running to provide power for the demanded load. Hence, the PMS has a very important job in the marine power plant; to ensure that faults are avoided, which in ultimate consequence can mean blackout. Also, if a blackout occurs, the PMS will restore power as soon as possible (Bø et al., 2015a). The PMS is responsible for starting and connecting new gensets if needed, and can even perform disconnections of loads in dangerous situations, by for instance disconnecting power consumers of low importance, such as pumps or hotel loads. The PMS gives references to the main power sources and ESDs, and does this in real-time in order to ensure a safe and reliable operation of the power sources.

The most important functions of the PMS are (Skjetne, 2012):

- *Blackout restoration*: A function which, as its name implies, brings the power system back online if a blackout should occur.
- *Load shedding*: Means disconnecting non-essential power consumers from the power system, in the near event of a blackout. The load shedding function is an important part of the PMS when it comes to preventing blackouts.
- *Under- and over-voltage detection and handling:* Ensures that the voltage levels of the power system (component-wise and the power system as a whole) are kept within the appropriate, predetermined voltage levels. This is also an important feature in preventing blackouts from happening.
- *Under- and over-frequency detection and handling:* Takes the frequency of the power system into consideration, and ensures these levels are kept within the allowed interval. As the under- and over-voltage detection, this function also prevents blackouts in the power system.
- *Active and reactive power load sharing:* Distributes the active and reactive power between power sources. This is done by for instance droop control or isochronous control.

2.6.4 Battery Management System

The BMS works in parallel with the PMS, as seen in Figures 2.1 and 2.2. The BMS ensures that the batteries operate in a safe and reliable manner, by avoiding over-current, over-voltage, and over-charging/-discharging of the battery, as this will accelerate the aging process and increases the risk of fire and explosion (Reddy et al., 2019; Simonsen, 2019). The BMS works in real-time, and monitors the status of the battery and gives commands to the battery. According to Andrea (2010), a classic BMS needs to measure and monitor the following states of the battery: cell voltage, pack temperature and pack current. This is an absolute minimum in order to have a sufficient BMS.

Gulsvik (2017) has proposed a robust BMS for a remotely operated vehicle (ROV), and defines the BMS as a device or system whose purpose is to monitor, control, and/or optimize a battery, ensuring a safe and efficient operation of the battery.

2.6.5 Battery as an Energy Storage Device

Batteries are the most common ESD in all-electric and hybrid ships (Reddy et al., 2019). The most important function of a battery is to consume or deliver power, thus manipulating the experienced load to the remaining power producers.

Common strategies for using the battery are, according to Sorensen et al. (2017) and Hansen (2019):

- *Enhanced dynamic performance*: The ESD can supply energy to the power plant during large load steps, so that the generator will be loaded gradually, which gives better performance and reduced risk of blackout. This strategy can for instance be used in ”slower” energy sources like liquefied natural gas (LNG) and fuel cells, since it supplies the power instantly.

- *Peak-shaving*: The genset power supply is bounded between a lower and an upper limit, and the ESD supplies the power outside these bounds. This method leads to both a reduction in fuel consumption and emissions, and it improves safety. When the load is below the lower limit, the battery is charged, and when it is above, the battery is discharged. See Figure 2.5a for a visual explanation of the peak-shaving principle.

- *Power smoothing*: This strategy is a form of peak-shaving, where fluctuations in the load are smoothed out. A band-pass filter can be used to control the battery load, where only the power variations in a given frequency range are counteracted by the battery, and the gensets consume the smoothed out load. This method has been used by Bø (2016), and Figure 2.5b illustrates power smoothing.

- *Spinning reserve*: An ESD works as a backup power to running generators. Class regulations from 2015 opened up for an ESD being used as a spinning reserve, where the ESD must be able to provide the necessary power to the plant for at least 30 minutes in case of a single fault (DNV GL, 2015).

- *Strategic loading*: Cyclic charging and discharging the ESD to strategically load the gensets to their optimal operating point, such that the total fuel consumption is reduced. Strategic loading has been studied in depth by Miyazaki (2017), and it is found to be an efficient strategy for reducing emissions.

- *Zero emissions operation*: Shutting down the generators and only use the ESD, which requires a large ESD installed on the vessel.

- *Enhanced ride through*: Use ESD as a short-time backup power in case of a failure.

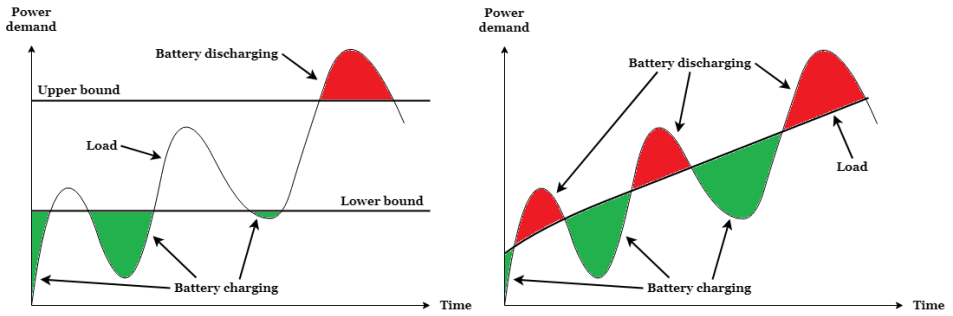

(a) Peak-shaving

(b) Power smoothing

Figure 2.5: Illustration of peak-shaving and power smoothing.

When using the battery, it is assumed that the sum of the genset and battery load is equal to the consumed power, according to

$$P_{gen} + P_{batt} = P_{load} \tag{2.1}$$

where P_{gen} is the generator power, P_{batt} is the battery power and P_{load} is the consumed power. In this way, the battery is used to change the genset load, and it can therefore, if used correctly, be efficient for reducing fuel consumption and emissions.

Typical constraints for the battery are temperature and state of charge (SoC), which should be kept within a lower and upper limit. Bø (2016) uses both SoC and temperature as battery constraints, but the temperature constraint can also be neglected. This was done in the work of Miyazaki (2017), which only included a constraint on the SoC. Another constraint in the battery can also be the battery power, with limits for the maximum charge and maximum discharge power, as stated by Dinh et al. (2018).

When it comes to inputs and outputs of the battery, Gulsvik (2017) has developed a thorough battery model, where the input is used to control the battery, and the output is used for measurements. In his battery model, the input was the battery current, and the output of the model was the voltage.

Chapter 3

Optimization and Control of Hybrid Power Systems

Parts of this chapter are based on my project thesis (Lund, 2019), written at NTNU during the fall of 2019.

3.1 Control of Hybrid Power Systems

Hybrid power systems introduce the need for more complex control strategies as there are several types of power source components involved in the power plant, and the loads affecting the power systems should be distributed in a reasonable way.

An advanced control design methodology is the MPC. MPC can handle multi-variable processes, satisfy constraints and implement appropriate response to time delays and model disturbance (Planakis et al., 2018). Mayne et al. (2000) describe the process of MPC as: "Model predictive control is a form of control in which the current control action is obtained by solving, at each sampling instant, a finite horizon open-loop optimal control problem, using the current state of the plant as the initial state; the optimization yields an optimal control sequence and the first control in this sequence is applied to the plant". Hence, at a time instant, an optimization problem for optimal control of the plant is solved for a finite time horizon. The control input sequence for the time horizon is calculated when solving the optimization problem, i.e. an optimal control sequence for the finite time horizon is calculated. However, only the first control input is implemented in the plant. Then, for the next time instant, a new optimization problem is solved for the rest of the time horizon, by using the measurements from the current state of the plant as the initial state. Thus, by solving the finite horizon optimization problem at each time instant, using the current state as the initial state, feedback is introduced (Foss and Heirung, 2016). This whole procedure relies on having a mathematically modeled approximation of the plant dynamics, which for measurements and inputs can produce responses and measurements

similar to those of the realistic process. An illustration of how an MPC algorithm works is shown in Figure 3.1.

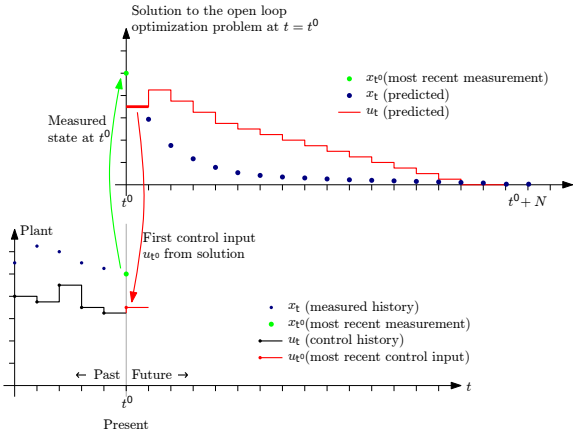

Figure 3.1: The process of model predictive control. Courtesy: Foss and Heirung (2016).

Shipboard electric propulsion systems are subject to large fluctuations of the loads, due to large variations in the influence from environmental conditions, such as wind, waves and current. This makes many of the strategies used for control of hybrid electric systems for land based vehicles inapplicable for ship propulsion systems (Hou et al., 2014). Hou et al. (2014) propose a new solution to account for the fluctuating load conditions for shipboard electrical propulsion systems. The fluctuation in the loads are both rapidly and slowly varying, due to the nature of environmental loads in a marine environment. Thus, Hou et al. (2014) introduce a hybrid energy storage system, containing both a battery and a supercapacitor, to utilize their different capabilities and characteristics as described in section 2.4. Using MPC for controlling the hybrid energy storage system, Hou et al. (2014) showed that utilization of a hybrid energy storage system meant great benefits in terms of reducing fluctuation and sustaining self-operation.

Hansen (2000) proposed a nonlinear control law and a model based predictive control strategy for a power generation plant.

An important attribute in an electrical power grid is whether the electricity in the grid is AC or DC. Both options have their advantages and limitations. DC grids in marine power plants have become more frequently used lately, which means that the engines can be operated at any frequency and the problem of synchronization with the electric grid is solved. However, DC components tend to be more expensive. AC on the other side have more components, manufacturers and general knowledge of the AC electric grid available. AC systems also have an advantage in that it is easier to implement breakers, which serve as protection towards overload or short circuits in the power plant. AC systems are usually operated by controlling the bus frequency and voltage (Rejani Miyazaki et al., 2016).

In (Radan, 2008), a focus towards control of marine electrical power systems for increased overall vessel performance led to the proposal of a new observer-based fast load reduction system for blackout prevention. Radan (2008) showed that the performance of

the load reduction system could detect blackouts faster and give faster and more precise load reduction compared to existing load reduction systems, and proved the system's reliability. Also, a new strategy to completely dampen the frequency and voltage fluctuations on the power network was proposed. The strategy called *power redistribution control* was investigated, and was made by improving the frequency control in the marine power plant by using dynamic feedback from the power plant to the electrical thrusters. This controller reduced the fluctuations in loads to the marine power plant caused by power consumers such as electrical thrusters. This control strategy can be used to detect bad performing thrusters causing load fluctuations in the plant and decrease their load, and then redistribute this energy to other power consumers. Radan (2008) also explored speed control of thrusters and propulsion engines, propulsion load control, energy management control and load limiting controllers for reduction in wear and tear on propulsors, and has proposed various designs on control laws and control strategies used for these purposes.

3.2 Opitimization Used for Power Plant Control

Optimization used for power plant control plays a big part in developing the control strategies for a power plant. In a marine power plant, there are several optimization objectives that can be looked into, and many control strategies utilizing optimization of the operation can be chosen depending on what components and equipment are used. Whether or not there are ESDs present, what types of ESDs are used and also the characteristics of the prime movers are among the considerations that need to be adressed. Optimization objectives are often to minimize the fuel consumption, minimizing running hours of gensets, scheduling of power sources, optimal engine speed and torque/load, battery charge/discharge and opening/closing of bus-tie breakers. In this section, using MILP optimization for power plant control will be explored, as well as other optimization strategies that have proven to be advantageous in power plant control.

3.2.1 Mixed Integer Linear Programming

MILP is an extension to LP, in which some of the variables are constrained to be integers. Using MILP formulations introduces flexibility in optimization, i.e. the possibility to easily formulate, model and solve many realistic problems, such as scheduling problems, the traveling salesman problem and production planning. MILP is especially suited for solving unit commitment problems, due to the binary characteristics of either using or not using a resource. This makes MILP especially applicable for genset scheduling, which is the area of application in this thesis.

Using MILP optimization for power plant control is proposed by Skjong (2017) and Thorat and Skjetne (2018). Skjong (2017) used MILP for unit commitment strategies and suggested a method for unit commitment in a marine power plant, which included the use of fixed speed gensets, variable speed and ESDs. Thorat and Skjetne (2018) proposed an approach for optimal genset scheduling and load sharing using MILP. This approach

included the optimization objectives of minimizing online capacity, minimizing running hours of gensets and minimizing connections/disconnections of gensets. The proposed method also included the possibility of a redundancy margin in order to ensure that in case of a failure of the biggest genset, the rest of the gensets should be able to deliver extra power accordingly to the power delivered by the biggest genset without overloading the remaining gensets. Thorat and Skjetne (2018)'s method is further explored in detail in Chapter 4 and is the method used as a basis for developing a MILP optimization algorithm in this thesis.

3.2.2 Other Optimization Methods - A Brief Overview

An optimization algorithm minimizing fuel consumption and an efficiency analysis of a DC hybrid power system containing diesel engines and a battery was done by Zahedi et al. (2014). The optimization algorithm proposed uses the strategy of calculating optimal value for the average power of the DC source, and finding the optimal value for the power ripple of the DC source. Power ripple is periodic variation of the levels of the DC voltage from a power supply, which has been converted from an AC source. The optimization strategy finds the optimal loading conditions regarding average power and power ripple, and determines the operating modes of the gensets; either charge-discharge mode or continuous mode. Charge-discharge mode is an operating mode with keeping the SoC of the battery within a chosen level as objective. In continuous mode, the ESD only delivers power according to the power ripple. Continuous mode is chosen when the operating point of the DC source correlates with the minimum SFOC, and otherwise charge-discharge mode is chosen (Zahedi et al., 2014). By using this optimization algorithm, Zahedi et al. (2014) showed that the DC hybrid power system provided about 15 % fuel savings compared to conventional AC systems, and 7 % fuel savings compared to the same DC system without ESD.

Bø (2016) explored scenario- and optimization-based control of marine electric power systems. By identifying and modeling fault scenarios, such as actuator faults, sensor faults or internal faults, a scenario-based model predictive controller was proposed. The scenario-based MPC uses dynamic safety constraints, by explicitly including the fault scenarios in the controller. Thus, the optimal control sequence calculated by the MPC is constrained by the fault scenarios. The scenario-based MPC detects faults and identifies faults that the system is not able to recover from, which can be used by the controller for changing the control objective or proactive reconfiguration of the modeled plant (Bø, 2016). Including the fault scenarios in the controller itself results in a scenario-based MPC which "[...] controls the states to a state set where the plant is recoverable if faults occur" (Bø, 2016). Also, a control strategy for peak shaving with a battey as ESD is proposed. The control of the peak shaving was done by combining an MPC with a power spectrum analysis in order to cancel out as much as possible of load fluctuations, while also ensuring the temperature of the battery does not get too high. Battery temperature can become an issue if the power demanded is too large. Thus, Bø (2016) proposed several good control strategies which are applicable to common problems and operations of marine power systems.

Another optimization method for power plant control is using a genetic algorithm. Wu et al. (2018) compared the fuel consumption between hybrid marine power plants consisting of low-power or high-power engines. A genetic algorithm was used for finding optimal operating points for the gensets. A genetic algorithm is a search heuristic which is similar to how evolution works in practice, and the law of "survival of the fittest". The algorithm starts with proposing a solution to the optimization problem by choosing individuals from an initial population. These individuals produce children, which inherit the characteristics of their parents. Thus, the genetic algorithm is an algorithm which produces a solution from generation to generation, and compares it with previous solutions to find the optimal one. A genetic algorithm uses three genetic operators; selection, crossover and mutation. The selection phase indicates that the fittest individuals (solutions) are allowed to pass on their genes to the next generation. Crossover means that the genes passed on to the next generation are chosen randomly from within the parents' genes, thus randomizing the produced offspring. Mutation consists of the genes from the parents to the offspring being altered randomly, and means that the next generation can include genes that the parents do not have. The advantage of a genetic algorithm is that it is allowed to escape from a local optimum due to its randomized characteristics, and is therefore a good choice for solving complex, multi-variable optimization problems. A disadvantage with a genetic algorithm is that it might not ever find a global optimum, as well as being computationally demanding (Wu et al., 2018).

Al-Falahi et al. (2018) proposed two optimization techniques for power management optimization of hybrid power systems in electric ferries; a power management method called rule-based control and a meta-heuristic power management method called Grey Wolf Optimization (GWO). The rule-based strategy for controlling the power sharing in the power system uses predetermined operational conditions. This is a computationally easy control strategy and is often easy to implement. However, since the strategy uses predetermined conditions which can change over the time of operation, it might not give the optimal solution of power management at all times. The meta-heuristic approach, GWO, mimics the social behavior of the grey wolf, by organizing the proposed solutions according to the social hierarchy of the wolf pack. The hierarchy contains, from top to bottom, the alpha, beta, delta and omega. The leader of the wolf pack is the alpha, where the betas are counselors to the alpha and bring orders down to the lower level of delta and omega. The search for a solution to the optimization problem is done by storing three solutions, one for alpha, beta and delta, and then telling the alpha, beta and delta where to search for the next solution based on the location of the current optimal solution. Since the alpha is the leader, the solution found by the alpha is considered the best solution. However, the beta, delta and omega are also involved in search of the optimal solution. The GWO algorithm was first proposed by Mirjalili et al. (2014). Al-Falahi et al. (2018) proposed a GWO to minimize the fuel consumption of the gensets in a hybrid power system subject to a set of constraints, for instance battery constraints, greenhouse gases emissions constraints and blackout prevention constraints. The proposed GWO provided more optimal operation than a traditional rule based optimization, with respect to minimization of fuel consumption.

An interesting approach for optimal control of power management is presented by Seenumani et al. (2010), who proposed a hierarchical optimal control strategy for power management of hybrid power systems in all electric ship applications. This control strategy's advantage is that it takes into account both the long time optimal power demand planning and short term disturbance rejection, which the controller can calculate in real-time without computational delay. As stated in (Seenumani et al., 2010), an MPC approach to solving the optimal control problem is common. The drawback of an MPC however, is the risk of the controller making short-sighted decisions not optimal for the entire time horizon, since the power demand for the entire time horizon, available for mission planning, is not utilized. The proposed hierarchical optimal control strategy consists of three levels, where the two first levels calculate the optimal power trajectories for the time horizon and the third level ensures the trajectory is followed optimally by using an offset free MPC to ensure disturbance rejection. The first level solves a static optimization problem, a quadratic program, ignoring the power source dynamics, determining the sub-optimal power split between the ESD (a battery) and other power sources for the entire time horizon. The second level includes the power source dynamics, and decides the optimal power split between fuel cell and gas turbine. Since an assumption is that battery power can be drawn instantaneously, the second level commands are only done for the fuel cell and gas turbine. Thus, the second level provides an optimal power trajectory for the fuel cell and gas turbine for the time horizon. The third level linearizes the power trajectory from the second level and formulates the trajectory tracking problem as an offset free MPC. All three steps in the hierarchical optimal control strategy use algorithms or utilize assumptions which ensure real-time computational efficiency.

Skjong (2017) proposed an MPC strategy for generating an active power filter that minimizes the harmonic distortions of a system consisting of multiple buses, whereas normally, an active power filter only locally compensate load current harmonic distortions on a single bus. Thus, by using an MPC strategy, the proposed controller mitigates harmonic distortions on a system-level. Skjong (2017) also proposed unit commitment strategies, one based on logics and one based on MILP.

Chapter 4

Optimal Genset Scheduling and Load Sharing Using Mixed Integer Linear Programming Optimization

This chapter introduces the MILP optimization problem corresponding to genset scheduling and load sharing of a marine power plant. Through this chapter, the mathematics behind the MILP optimization algorithm implemented in this thesis is presented. Parts of this chapter are based on my project thesis (Lund, 2019), written at NTNU during the fall of 2019.

Considering a simplified marine power plant and the task of genset scheduling, the optimization problem can be solved using MILP. The formulation of the optimization problem presented in this section is based on the results from Thorat and Skjetne (2018). As stated by Thorat and Skjetne (2018); "the scheduling problem is an optimal allocation of resources (online gensets) to activities (load demand) over an interval of time". Thus, the ultimate goal in the genset scheduling problem is to optimally connect and disconnect the gensets such that they meet the demands of the current load condition. In addition, an optimization objective of minimizing the fuel consumption, for the given scheduling scheme, can be added to the optimization problem. Thus, the overall goal of the optimization is to optimize the scheduling of the gensets, and for this particular scheduling, optimize the load sharing between the connected gensets given their specific fuel consumption.

Considering a general power plant of M parallel gensets, where each genset has index j, where $j \in \{1, 2, ..., M\}$. Let C be the binary scheduling vector containing the connection status of each genset, where $C_j \in \mathbb{I} := \{0, 1\}$, and C_j takes the value 1 if genset j is connected, 0 otherwise. A key idea of the optimization is that the active power from the connected gensets must be equal to or greater than the power demanded by the bus load, written in equation form as $\sum C_j P_j \geq P_{load}$. Later in the optimization schedule, we want

to opimize the power load sharing between the connected gensets. Thus, we normalize the power vectors to give rise to the load sharing vector we will optimize for active power sharing between the connected gensets. The equation thus becomes

$$\sum_{j \in \{1..M\}} \frac{C_j P_{b,j}}{P_{b,bus}} p_j \geq \frac{P_{load}}{P_{b,bus}} \tag{4.1}$$

where P_j is the supplied active power from genset j, $P_{b,j}$ is the rated 100 % active (base) power for genset j, $P_{b,bus}$ is the total amount of power possible to provide from the gensets and p_j is the per-unit supplied active power from genset j, defined as $p_j := \frac{P_j}{P_{b,j}}$.

4.1 MILP Formulation of the Genset Scheduling Problem Minimizing Online Capacity

The simplest form of optimizing the scheduling of gensets is to minimize the number of online gensets. Also, introducing a weighted cost function that takes value according to the genset capacity, ensures that the solution found is an optimal solution with the tightest gap to the demanded load. Thus, we minimize the online power delivered from the gensets. Given the scheduling vector C, the number of gensets is $N = 1_M^\top C$, where $1_M \in \mathbb{R}^M$ is a vector of ones. The optimal loading condition for a genset is usually around 80 % MCR. Introducing an optimal loading factor for genset j, e.g. $\gamma_j = 0.8$, the optimal loading condition of genset j can be written $P_{opt,j} = \gamma_j P_{b,j}$. The constraint which corresponds to the power plant delivering enough active power in accordance with the demanded active power on the bus can then be written as

$$P_b^\top \Gamma C \geq P_{load} \tag{4.2}$$

where $P_b = [P_{b,1}, P_{b,2}, ..., P_{b,M}]^\top$ and $\Gamma = \text{diag}([\gamma_1, \gamma_2, ..., \gamma_M])$. In addition to assuring the delivered active power is greater than the demanded active power, a constraint ensuring that at least a number of N_{min} gensets are connected, e.g. that at least one genset is connected at all times, i.e. $N_{min} = 1$. This constraint can be written as

$$1_M^\top C \geq N_{min} \tag{4.3}$$

Using the L1 norm of the P_b, i.e. $|P_b| = \text{sum}(P_b)$, the mixed integer linear program can be formulated as shown in Equation 4.4.

$$\begin{aligned} \min_C \quad & \frac{P_b^\top}{|P_b|} C \\ \text{s.t.} \quad & -P_b^\top \Gamma C \leq -P_{load} \\ & -1_M^\top C \leq -N_{min} \end{aligned} \tag{4.4}$$

From this MILP optimization problem, the scheduling vector C is found. Thus, the optimal scheduling is obtained at the time instant the optimization is done. Minimizing the weighted cost function rather than minimizing only the scheduling vector C, will in a

way favorize connecting the smaller gensets, since the scheduling vector is weighted with the maximum capacity of the gensets and this is a minimizing problem.

4.2 MILP Formulation of the Genset Scheduling Problem Minimizing Running Hours and/or Number of Connections/Disconnections

It is possible to add additional minimization objectives to the MILP optimization in eq. (4.4) in order to optimize the genset scheduling with different optimization objectives. Thorat and Skjetne (2018) introduce the optimization objectives of minimizing the running hours of the gensets and the number of connections and disconnections of the gensets. Depending on the marine operation, there may be huge variations in the load demanded from the power system of a ship. This can cause many connections and disconnections of the gensets, which may lead to unnecessary wear and tear on the equipment. On the other hand, other types of marine operations can lead to situations where the same gensets are connected all the time, meaning some gensets always are disconnected. This can also cause wear and tear of the gensets. Therefore, for some operations, configurations and type of equipment, the most advantageous genset scheduling might be one that takes factors like running hours and numbers of connections and disconnections into account.

In order to optimize the genset scheduling while not only considering minimizing the online capacity, but also minimizing the running hours and/or the connections and disconnections of the gensets, one can introduce penalties on the running time and connections and disconnections (Thorat and Skjetne, 2018). A variable that counts the running time for each genset is introduced as

$$d_j(k) = d_j(k-1) + C_j(k-1)T_s, \quad d_j(0) = 0, \tag{4.5}$$

where T_s is the time since the last execution of the optimization algorithm and k is the current time index. $d_j(k)$ is a variable which at every time instant k of the optimization horizon contains the total running time of Genset j. On vector form, the running time variable becomes

$$d(k) = d(k-1) + T_s C(k-1), \quad d(0) = 0. \tag{4.6}$$

Introducing variables that contain the accumulated connections and disconnection of Genset j, s_j^{on} and s_j^{off} respectively. On vector form, these variables become

$$s^{on} := \text{col}(s_1^{on}, ..., s_M^{on}), \quad s^{off} := \text{col}(s_1^{off}, ..., s_M^{off}) \tag{4.7}$$

In order to sum up all connections and disconnections of the gensets, the variable ΔC_k is defined as

$$\Delta C_k = C(k) - C(k-1) \tag{4.8}$$

where $C(k)$ is the scheduling vector at time instant k. Splitting ΔC_k up into two variables, where one variable contains 1 for the +1 elements and the other contains 1 for the -1 elements according to

$$\Delta C_k = \Delta C_k^+ - \Delta C_k^- \tag{4.9}$$

ensures that both the connections and disconnections are properly stored. This definition is derived from the fact that $\Delta c_j(k)$ is positive (1) for connecting genset j between time instant $k-1$ and k and negative (-1) for disconnecting genset j between time instant $k-1$ and k. The accumulated cost of connecting and disconnecting gensets can then be written

$$s^{on} = W_{connect} \sum_{i=1}^{k} \Delta C_i^+, \quad s^{off} = W_{disconnect} \sum_{i=1}^{k} \Delta C_i^- \tag{4.10}$$

Including the variables counting running time and connections and disconnections in the objective function of the MILP formulation in Equation (4.4), a new MILP formulation containing the newly introduced optimization objectives is expressed as

$$\begin{aligned} \min_{C} \quad & \left(w_1 \frac{P_b^\top}{|P_b|} + w_2 \frac{d}{|d| + \varepsilon} + w_3 \frac{s^{on}}{|s^{on}| + \varepsilon} + w_4 \frac{s^{off}}{|s^{off}| + \varepsilon} \right)^\top C \\ \text{s.t.} \quad & - P_b^\top \Gamma C \leq -P_{load} \\ & - 1_M^\top C \leq -N_{min} \end{aligned} \tag{4.11}$$

where w_1, w_2, w_3 and w_4 are relative weights between each optimization objective term and $\epsilon > 0$ is a small constant to avoid division by zero. In Equation 4.11, the first term represents minimizing online capacity, the second term represents minimizing running hours of gensets, the third term represents minimizing connections of gensets, and the fourth term represents minimizing disconnections of gensets. Thus, a new MILP formulation including the optimization objectives of minimizing running time and/or connections and disconnections has been established, as proposed by Thorat and Skjetne (2018).

4.3 LP Formulation of Load Sharing Between Online Gensets

If an optimization of both the scheduling vector, C, and the load sharing vector, p, is being performed, this often leads to an NLP. The goal is to solve this optimization using MILP. Hence, we simplify the optimization problem by optimizing in two stages. Solving the mixed integer linear program in Equation (4.11) results in the optimal scheduling vector. This is stage 1 of the optimization, whereas stage 2 consists of minimizing the fuel consumption per power unit produced (i.e., the SFOC), given the optimal load sharing vector C from stage 1. In other words, stage 2 defines an optimal load sharing vector p.

Generating the optimal load sharing vector p that minimizes the SFOC, means minimizing the SFOC-curves for each connected genset, provided that demanded active power is met with produced active power. Following the results from Thorat and Skjetne (2018), the SFOC-curves are given by

$$f_{SFOC,j} = h_j(p_j) \tag{4.12}$$

where $h_j(\,\cdot\,)$ is a convex curve for Genset j. This curve is populated by pairs of points according to $(p_j, f_{SFOC,j})$, measured as steady state values from testing the engine in a laboratory. This gives rise to a PWL function. Assuming the curve $f_{SFOC,j}(p_j)$ for genset j is populated by the $m_j + 1$ points

$$\begin{aligned} p_j &= \left\{p_{j,0}, p_{j,1}, \ldots, p_{j,m_j}\right\}, \quad p_{j,k-1} < p_{j,k} \\ f_{SFOC,j} &= \left\{z_{j,0}, z_{j,1}, \ldots, z_{j,m_j}\right\} \end{aligned} \tag{4.13}$$

where the assumption is that the interval $[p_{j,0}, p_{j,m_j}]$ is the power region allowed for Genset j for which the SFOC-curve is defined. Also assuming that $z_{j,0} = \max_k(z_{j,k})$ (Thorat and Skjetne, 2018). The linear curve coefficients are defined by

$$\left.\begin{aligned} a_{j,k} &= \tfrac{z_{j,k} - z_{j,k-1}}{p_{j,k} - p_{j,k-1}} \\ b_{j,k} &= z_{j,k-1} - a_{j,k} p_{j,k-1} \end{aligned}\right\}, \quad k = 1, 2, \ldots, m_j \tag{4.14}$$

The m_j linear curves for Genset j can then be expressed as

$$h_{j,k}\left(p_j\right) = a_{j,k} p_j + b_{j,k} \tag{4.15}$$

In this case, the optimization is performed directly on the PWL curve. For a given load p_j, the SFOC is given by

$$h_j(p_j) = f_{SFOC,j} = \max_k h_{j,k}(p_j) \tag{4.16}$$

The collection of the M PWL curves for all M gensets in one vector yields

$$h(p) := \operatorname{col}\left(h_1\left(p_1\right), h_2\left(p_2\right), \ldots, h_M\left(p_M\right)\right) \tag{4.17}$$

Minimizing the fuel consumption per power unit produced for M gensets with scheduling according to schedule vector C from stage 1, means minimizing the cost function according to Eq. (4.18).

$$\min_{C,p} \quad J_{SFOC}(C,p) = \sum_{j=1}^{M} C_j h_j\left(p_j\right) = C^\top h(p) \tag{4.18}$$

Given that the scheduling vector C is known from Stage 1, Equation (4.18) is an optimization problem of $N = 1_M^\top C$ separable convex functions, where each SFOC-function is a PWL function. This is solved as a new LP problem. The minimization of one single PWL SFOC-curve for a genset is done by (Ferris et al., 2007):

$$\begin{aligned} \min_{p_j,\mu_j} \quad & \mu_j \\ \text{s.t.} \quad & a_{j,k}p_j + b_{j,k} \leq \mu_j, \quad k = 1, 2, \ldots, m_j \\ & P_{b,j}p_j = P_{load} \\ & p_{j,0} \leq p_j \leq p_{j,m_j} \end{aligned} \tag{4.19}$$

where μ is an auxiliary variable. If the scheduling vector C containing the connection status of the gensets is included in the optimization, the linear program is formulated as

$$\begin{aligned} \min_{p_j,\mu_j} \quad & C_j\mu_j \\ \text{s.t.} \quad & a_{j,k}p_j + b_{j,k} \leq \mu_j, \quad k = 1, 2, \ldots, m_j \\ & P_{b,j}p_j = P_{load} \\ & C_jp_{j,0} \leq p_j \leq C_jp_{j,m_j} \end{aligned} \tag{4.20}$$

This allows for an optimal solution to be found, in which $p_j = 0$ for disconnected gensets. As seen from the linear program in Equation (4.20), a disconnected genset j, for which $C_j = 0$, the feasible solution is $p_j = 0$ and $\mu_j \geq b_{j,k}$ free. As whole, the stage 2 optimization problem can be expressed as

$$\min_{p,\mu} \quad C^\top \mu \tag{4.21}$$

$$\text{s.t.} \quad Ap + E\mu \leq -b \tag{4.22}$$

$$(C \circ P_b)^\top p = P_{load} \tag{4.23}$$

$$C \circ (p_j^- - \Delta p) \leq p \leq C \circ (p_j^- + \Delta p) \tag{4.24}$$

$$C \circ p_{min} \leq p \leq C \circ p_{max} \tag{4.25}$$

where $\circ$ means the Hadamard elementwise vector product. In the linear program in Equations (4.21) through (4.25), the variables are defined as:

$$A := \begin{bmatrix} a_1 & 0_{m_1\times 1} & \cdots & 0_{m_1\times 1} \\ 0_{m_2\times 1} & a_2 & & 0_{m_2\times 1} \\ \vdots & & \ddots & \vdots \\ 0_{m_j\times 1} & 0_{m_j\times 1} & \cdots & a_M \end{bmatrix}$$

$$E := \begin{bmatrix} -1_{m_1} & 0_{m_1\times 1} & \cdots & 0_{m_1\times 1} \\ 0_{m_2\times 1} & -1_{m_2} & & 0_{m_2\times 1} \\ \vdots & & \ddots & \vdots \\ 0_{m_j\times 1} & 0_{m_j\times 1} & \cdots & -1_{m_M} \end{bmatrix}$$

$$b := \begin{bmatrix} b_1 \\ \vdots \\ b_M \end{bmatrix}, \quad p_{min} := \begin{bmatrix} p_{1,0} \\ \vdots \\ p_{M,0} \end{bmatrix}, \quad p_{max} := \begin{bmatrix} p_{1,m_1} \\ \vdots \\ p_{M,m_M} \end{bmatrix}$$

where

$$a_j := \begin{bmatrix} a_{j,1} \\ \vdots \\ a_{j,m_j} \end{bmatrix} \in \mathbb{R}^{m_j}, \quad b_j = \begin{bmatrix} b_{j,1} \\ \vdots \\ b_{j,m_j} \end{bmatrix} \in \mathbb{R}^{m_j} \tag{4.26}$$

Equation (4.22) together with the minimization of the auxiliary variable μ in (4.21) ensure minimization of the PWL SFOC-curves. Equation (4.23) ensures that the active power delivered from the gensets corresponds to the demanded active power on the bus. Equation (4.24) ensures that the active power delivered for this instant of the optimization does not exceed the maximum absolute value of rate of change, where p_j^- is the active power value when the optimization is initiated for this time instant. Δp is the maximum allowable rate of change over the optimization period. Equation (4.25) ensures that the disconnected gensets are set to zero active power, and that the connected gensets do not exceed their minimum and maximum power levels. This completes stage 2 of the optimization. Thus, the goal of optimizing the scheduling as well as optimizing the load sharing between the connected gensets is reached, as proposed by Thorat and Skjetne (2018). The process of the optimization process can be seen illustrated using a flowchart diagram, presented in fig. 4.1.

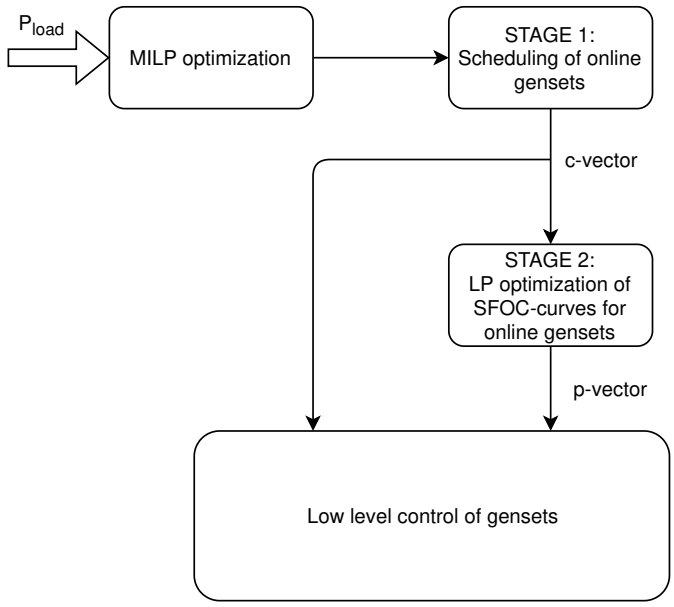

Figure 4.1: Flowchart describing the process of the optimization of the genset scheduling and load sharing.

4.4 Implementation of MILP optimization problem formulation in Matlab

The MILP optimization problem formulation is implemented in Matlab, and gives rise to a MILP optimization algorithm. This Matlab implementation, which is later used for verification of the MILP optimization, is done using a simplified marine power plant consisting of six equal gensets. See Appendix A.1 for Matlab code, $milp\_optimization\_algorithm.m$. The MILP optimization algorithm is later implemented in the simulation environment of the MVPPSS, see Section 5.3. The implementation of the LP optimization problem as proposed by Thorat and Skjetne (2018) required some creative thinking. The proposed method yields correct results and is shown in Appendix A.2. Note that the method, i.e. the optimization problem formulation as a whole, is based on the work presented by Thorat and Skjetne (2018), but the code for simulating an optimization of a simplified marine power plant and the implementation of the MILP optimization algorithm in a simulation environment is a contribution of this thesis.

Chapter 5

Marine Vessel and Power Plant System Simulator

This chapter investigates and introduces the MVPPSS. This chapter's focus is to explore the simulator's capabilities and limitations, as well as understanding the MVPPSS by exploring the simulator's outline and structure, modeling and assumptions. Parts of this chapter are based on my project thesis (Lund, 2019), written at NTNU during the fall of 2019.

5.1 Background and Outline

The Marine Vessel and Power Plant System Simulator (MVPPSS) (Bø et al., 2015a), developed at NTNU, is a simulator developed as an extension to the Marine Systems Simulator (Tristan et al., 2006). There exist several previously developed marine power plant and marine dynamics simulation solutions (Bø et al., 2015a) such as **Marine Cybernetics' Cybersea** technology platform, **U.S. Office of Naval Research's** Electric Ship Research and Development Consortium (Xie et al., 2009), **Marine System Simulator** library and simulator for Matlab/Simulink (MSS, 2010), **Italian Integrated Power Plant Ship Simulator** Simulink environment (Bosich et al., 2012), **NTNU models** thruster power consumption and power management system functions (Hansen et al., 2001) and **NTNU bond graph** model library (Pedersen and Pedersen, 2012). Whereas these solutions mainly focus on the electrical power system or the positioning system/vessel dynamics separately, the MVPPSS is a simulator combining the two systems by extending the Marine Systems Simulator (MSS). The MVPPSS is a modular system simulator. This means that its purpose is to model the system as a whole, including interactions between the positioning system and the electrical power system by modeling subsystems as modules and connecting them as a whole system. This gives possibilities of simulating a vessel with realistic interactions between power plant, hydrodynamics, steering gear, vessel motion, thruster drive dynamics, machinery system and high-level plant controllers such as PMS and DP

(Bø et al., 2015b).

Some use cases of the MVPPSS include: *realistic power consumption profile*; the power load fluctuations are represented in a realistic way since the thruster models and DP controller are connected to the power plant, *fault consequence analysis*; plant behavior if an electrical fault occurs, such as a loss of a power source, *operation optimization*; optimization of operation with regards to emissions, maintenance or fuel consumption due to the detailed level of modeling such as temperature and power output and *concept evaluation*; investigation of new power sources and their effect on control and performance of the system since new subsystems such as ESDs can be introduced in the simulator (Bø et al., 2015a).

The MVPPSS can simulate several operations of a marine vessel. Some examples include transit operation, maneuvering of the vessel and DP operation. According to Bø et al. (2015b), the simulator is designed using the following assumptions:

Steady-state electrical system: This means that the electrical systems are assumed to be in steady state during simulations. This means that some features can not be simulated, such as phase imbalance, transient voltage fault, short circuit and harmonic distortion. However, the simulator provides real-time capabilities of simulating the electrical system, which means it is possible to simulate faults such as under/over-frequency, slow under-/over voltage fault and reverse power.

Mean-value engine model: The diesel engine models are modeled based on physical laws. The in-cylinder process is modeled using simplifications which means it only provides a cycle average output of shaft torque, and mass and energy flow of the combustion gas.

Power management system: A PMS is included in the simulations. The PMS's primary objective is to ensure that there is enough power available for the electrical system, given the loading condition. The PMS controls which power producers that should be turned on, and can start additional power producers if there is not enough power available in the plant. It can also command loads to reduce power or to be disconnected if the power consumption is too big compared to the available power.

Protection relay: Protection relays are not modeled in the MVPPSS. Because of this, in order to simulate a partial blackout, a total loss of power to an area, there is need of implementing some custom protection relays. Another alternative is to post-process the results to find out when breakers should be opened, and then run a new simulation with open breakers at the given time.

Fixed pitch, variable speed thrusters: The thrusters are assumed to be fixed pitch propellers, running with variable speed. Both azimuth thrusters and fixed thrusters can be simulated.

To better understand the architecture of a simulation model in the MVPPSS, an example of a simulation model of a DP controlled semi-submersible is shown in Figure 5.1. This shows the complexity of the modular simulator.

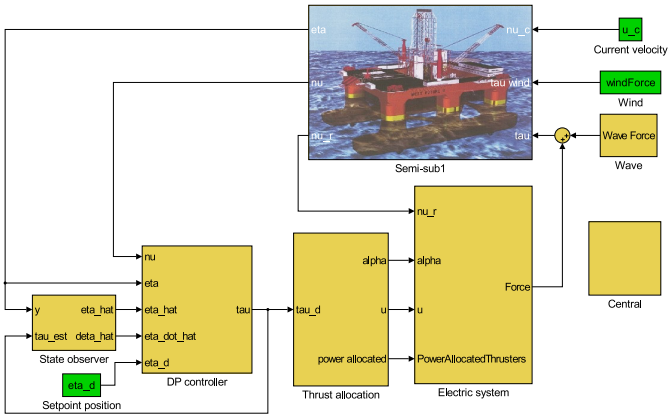

Figure 5.1: Overview of a typical simulation model in the MVPPSS. This system contains a vessel model, observer, DP controller, thrust allocation and electrical system. Central block is used for calculations. Courtesy: Bø et al. (2015a).

A brief explanation of the components modeled by subsystems in Figure 5.1;

Vessel dynamics: Contains the vessel dynamics which calculate the vessel position and velocities using equations of motions. The vessel motion is calculated by taking into account all the forces acting on the vessel, including thruster forces and environmental forces.

Observer: Estimates the position and velocity of the vessel from measurements. A frequently used state estimator is the Kalman filter (Fossen and Perez, 2009).

DP Controller: Calculates the generalized forces (in surge, sway and yaw for a 3-DOF model) based on the current states of the vessel (position, velocity) and the setpoint (desired position).

Thrust allocation: Distributes the generalized forces among the thrusters. Calculates the forces each thruster needs to produce and the angles assigned to azimuth thrusters.

Electric system: Converts the commanded forces for each thruster to actual thrust as well as calculating the electrical power consumption.

Environmental model: Generates environmental loads affecting the vessel, such as forces from current, wind and waves.

The content of the electrical system block seen in Figure 5.1 is shown in Figure 5.2.

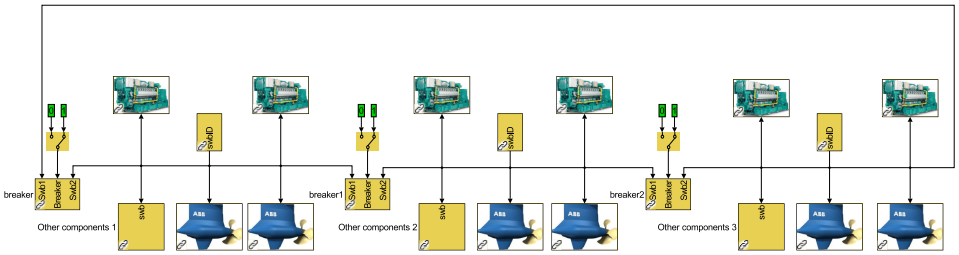

Figure 5.2: Typical set up of the electrical system in the MVPPSS. This electrical system contains bus-tie breakers, thrusters, generator sets and ”other loads”-block. Courtesy: Bø et al. (2015a).

The electric power plant modeled in the electrical system block in the MVPPSS mimics a single line diagram (SLD) (Bø et al., 2015b). This makes it intuitive to design and model a power plant according to technical drawings and industry standards. The SLD makes it easy and intuitive to understand the configuration of the power plant, as well as the power flow between components. Even though the electrical system looks like an SLD, there are no signals containing information sent between the components. This is merely done for the visualization of the marine power plant configuration. The structural layout of subsystems in Simulink means that if each component had been connected to every other component it interacts with, a very messy Simulink diagram would be the result. The components in the electrical system, seen in Figure 5.2, according to Bø et al. (2015a) consist of;

Generator set: Includes a prime mover, e.g. a diesel engine, a generator, a speed governor and an automatic voltage regulator (AVR).

Thruster drives: Includes a frequency converter, an electric motor, a propeller and a controller.

Other components: Includes for example hotel and drilling loads which are modeled as power consumption. Can also be used to model ESDs such as batteries with a frequency converter. When a battery is modeled in this block, the load is negative when the battery delivers power (discharges) and positive when the battery consumes power (charges).

Switchboards: The purpose of the switchboards is to connect all power loads and power producers.

Breakers: Responsible for connecting and disconnecting components in the electrical system to the bus(es).

5.2 Mathematical Modeling and Simulator Implementation

This section provides a deeper insight in the MVPPSS and explores the mathematical equations and assumptions on which the processes in the MVPPSS are based on. The mathematical background and dynamic models presented in this section are based on the findings presented in (Skjetne, 2017).

5.2.1 Mechanical System

The mechanical system, i.e. the engine, provides mechanical energy delivered to a generator, which in turn converts the mechanical energy to electrical energy. The mechanical dynamics are governed by the *swing equation* (Skjetne, 2017)

$$J_m\dot{\omega}_m = T_m - T_e - T_d, \tag{5.1}$$

where T_m is the mechanical torque provided by the engine, T_e is the electrical load torque from the generator and T_d is a damping torque (Skjetne, 2017). Given that the goal is to develop a system dependent on electrical variables instead of mechanical variables, the following conversions and relations are applied:

$$\theta_e = \frac{N_p}{2}\theta_m \tag{5.2}$$

$$\omega_e = \dot{\theta}_e = \frac{N_p}{2}\dot{\theta}_m = \frac{N_p}{2}\omega_m \tag{5.3}$$

$$\omega_{m,b} = \frac{2}{N_p}\omega_b = \frac{4\pi}{N_p}f_b \quad [\mathrm{rad/s}] \tag{5.4}$$

$$n_{m,b} = 30\frac{\omega_{m,b}}{\pi} = \frac{120}{N_p}f_b \quad [\mathrm{rpm}], \tag{5.5}$$

where Equation 5.2 and Equation 5.3 describe the relationships between mechanical angle, θ_m, and electrical angle, θ_e, where N_p is the number of poles in the generator and ω_m is the mechanical rotor velocity. Equation 5.4 and Equation 5.5 describe the relationships between the bases, where $\omega_{m,b}$ and $n_{m,b}$ represent the rotor mechanical base velocity of the engine, in [rad/s] and [rpm] respectively, and ω_b is the electric base frequency of the genset/bus.

To convert the expression in Equation 5.1 to per-unit, Equation 5.1 is divided by T_b, the base torque of the genset:

$$\frac{J_m}{T_b}\dot{\omega}_m = \frac{T_m}{T_b} - \frac{T_e}{T_b} - \frac{T_D}{T_b} = t_m - t_e - t_d, \tag{5.6}$$

where the lower-case letters indicate variables are presented in per-unit. Defining

$$H := \frac{\frac{1}{2}J_m\omega_{m,b}^2}{S_b} = \frac{\frac{1}{2}J_m\omega_{m,b}}{T_b} = \frac{\text{stored kinetic energy at nominal speed}}{\text{genset power rating}}, \tag{5.7}$$

which is the intertia constant, with unit in seconds. S_b is the three-phase base apparent power for the genset. Rearranging and inserting into Equation 5.6 yields

$$2\frac{H}{\omega_{m,b}}\dot{\omega}_m = t_m - t_e - t_d. \tag{5.8}$$

The inertia constant H typically is of magnitude 1-10 [s], while the inertia J_m varies widely from genset to genset (Glover et al., 2007). The damping term, t_d is according to Skjetne (2017) modeled as a linear term:

$$t_d := D_{fw}\omega \tag{5.9}$$

where $D_{fw} > 0$ is the damping gain due to friction and windage torques, and

$$\omega := \frac{\omega_e}{\omega_b} = \frac{\omega_m}{\omega_{m,b}} \tag{5.10}$$

is the per-unit angular velocity.

In order to use the electric load P_e from the generator as an input to the model, the following relation is used:

$$t_e = \frac{T_e}{T_b} = \frac{\omega_{m,b}}{\omega_m}\frac{P_e}{S_b} = \frac{\omega_b}{\omega_e}\frac{P_e}{S_b} = \frac{p_e}{\omega}, \quad p_e = \frac{P_e}{S_b} \tag{5.11}$$

Also, for the model to address the effects of electrical losses, the per-unit electric load from the generator is expressed as $p_e \approx p + p_{scl}$ where p is the supplied active power to the electrical network and p_{scl} is the stator conductor losses, given by

$$p_{scl} = 3r_s\hat{i}_a^2 = 3r_s\frac{|s_a|^2}{\hat{v}_{an}^2} = r_s\frac{|s|^2}{\hat{v}_{ll}^2} = r_s\frac{p^2+q^2}{\hat{v}_{ll}^2}, \tag{5.12}$$

where r_s is the per-unit stator resistance, $\hat{i}_a$ is the per-unit instantaneous induced root mean sqaure (RMS) current for the stator a-phase of the generator, s_a is the per-unit complex stator a-phase electric power produced by the generator, $\hat{v}_{an}$ is the per-unit RMS terminal voltage for the stator a-phase of the generator, s is the per-unit complex electric power produced by the generaor, $\hat{v}_{ll}$ is the per-unit bus line-to-line voltage when connected to the power network and q is the delivered reactive power.

Using the relations in Equations 5.3, 5.4 and 5.10 and inserting Equations 5.9, 5.11 and 5.12 into Equation 5.8 yields the following model (Skjetne, 2017):

$$2H\dot{\omega} = t_m - D_{fw}\omega - \frac{p + p_{scl}\left(p, q, \hat{v}_{ll}\right)}{\omega} \tag{5.13}$$

The dynamics from the fuel index u to the mechanical torque T_m is modeled in the frequency-domain (s-domain) as

$$\frac{T_m(s)}{U(s)} = \frac{k_u}{1+\tau_e s}e^{-\rho s}, \tag{5.14}$$

as proposed by Blanke (1981). Here, τ_e is a time constant of the cylinder, ρ is an average time delay from the fuel index setting to the corresponding fuel entering the cylinders and k_u is a gain (Skjetne, 2017). In (Blanke, 1981), τ_e is approximated as

$$\tau_e \approx \frac{0.9}{\omega_{m,b}}. \tag{5.15}$$

Modeling the delayed fuel input as $U_\rho(s) := U(s)e^{-\rho s}$ and denoting $t_m = \frac{T_m}{T_b}$ yields

$$t_m(s) = \frac{1}{(1+\tau_e s)} \frac{k_u}{T_b} U_\rho(s), \tag{5.16}$$

which in the time-domain is expressed as

$$\dot{t}_m = -\frac{1}{\tau_e}\left(t_m - \frac{k_u}{T_b}u_\rho\right), \tag{5.17}$$

where $u_\rho(t) = u(t-\rho)$.

The resulting engine model can be found by evaluating Equations 5.13 and 5.17 at steady state, which yields

$$\frac{k_u}{T_b}u_\rho = D_{fw}\omega + \frac{p_e}{\omega}. \tag{5.18}$$

Following the method in (Skjetne, 2017), calibrating $u_\rho = 1$ at the rated values of $\omega = 1$ and $p_e = 1$, yields

$$k_u = T_b\left(D_{fw} + 1\right). \tag{5.19}$$

As stated by Skjetne (2017), "It is not desired to implement the electrical angle θ_e in a simulator, since this will wind-up to large values with time. Instead it is common to use the power angle defined by $\delta := \theta_e - \theta_{bus}$ where θ_{bus} is the resulting electrical angle of the bus voltage". Hence, introducing ω_{bus}, the per-unit frequency of the bus voltage, the resulting dynamic mechanical system model is expressed as

$$\dot{\delta} = \omega_b\left(\omega - \omega_{bus}\right) \tag{5.20a}$$

$$2H\dot{\omega} = t_m - D_{fw}\omega - \frac{p}{\omega} - r_s\frac{p^2+q^2}{\omega\hat{v}_{ll}^2} \tag{5.20b}$$

$$\dot{t}_m = -\frac{1}{\tau_e}t_m + \frac{D_{fw}+1}{\tau_e}u_\rho. \tag{5.20c}$$

5.2.2 Speed Control

The engine speed, and thus frequency, is controlled by the engine speed controller, also known as the governor. The governor's objective is to keep the engine frequency within an acceptable range. The allowed range of variation in frequency, according to main class

regulations, is $\pm 5\%$ for steady load conditions and $\pm 10\%$ for transient load conditions (Skjetne, 2017). Often, the governor is a PID-controller. In Figure 5.3, a block diagram of the inner control loop of the speed controller is shown.

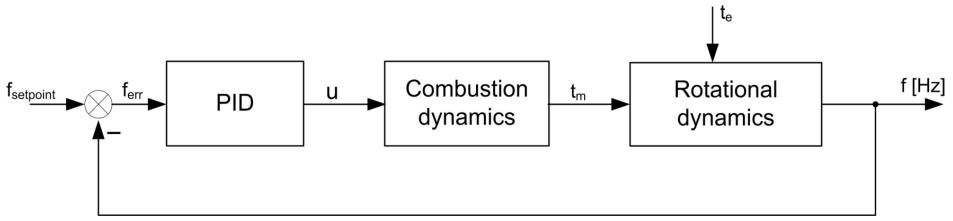

.

Figure 5.3: Inner speed control loop. Courtesy: Skjetne (2017)

The speed controller can operate in various modes, often *droop mode* or *isochronous mode* are applied. Briefly explained, isochronous mode means having the governor keep the same frequency for all power outputs, while the droop mode ensures a drop in the frequency level when the load increases and vice versa. For the purposes and goals of this thesis, the droop speed control is applied.

When using droop speed control, it is advantageous to normalize the active power P, such that the droop percentage can be used directly (Skjetne, 2017). The corrected setpoint frequency to the governor of Genset j is calculated as

$$f_{sp,j} = f_{ref,j} - \frac{d_{\%-\text{ Droop },j}}{100} \frac{P_j}{P_{n,j}} \tag{5.21}$$

where $P_{n,j}$ is the rated 100% active power value and $f_{ref,j}$ is the per-unit no-load frequency of Genset j. The block diagram of the control loop using droop speed control can be seen in Figure 5.4.

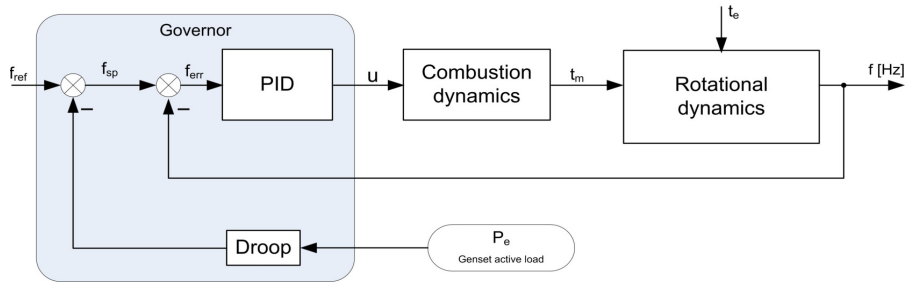

Figure 5.4: Droop speed control. Courtesy: Skjetne (2017).

5.2.3 Electrical System

The generator's stator and rotor both consist of windings. The rotor windings' objective is to induce a constant magnetic field which rotates with the shaft of the generator. The stator windings are set up in a configuration with a 120° relative angle to each other, in order to produce a 3-phase current delivered to the electrical network (Skjetne, 2017).

In Figure 5.5, an a-phase equivalent circuit of the generator can be seen, including the field excitation system (rotor).

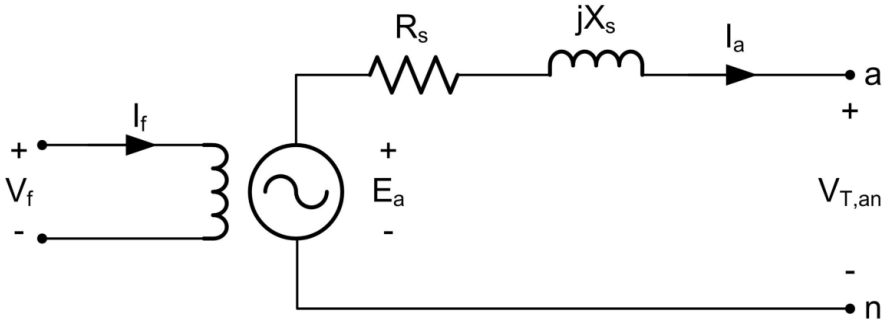

Figure 5.5: A-phase equivalent circuit of the generator, including the field excitation of the rotor. Courtesy: Skjetne (2017).

The induced voltage in the generator's stator is adjusted by controlling the excitation system through the DC field current I_f. Assuming that the generator is operated at constant frequency ω and that R_f and L_f are the resistance and self-inductance of the magnetizing field windings, respectively. Then, the field voltage V_f can be expressed in terms of the field current I_f:

$$V_f = R_f I_f + L_f \frac{dI_f}{dt}, \tag{5.22}$$

as proposed by Gönen (2011). By taking the Laplace transform of Equation 5.22, the field current I_f is related to the field voltage V_f by a stable linear filter (Skjetne, 2017):

$$\frac{I_f(s)}{V_f(s)} = \frac{k_f}{\tau_f s + 1}, \quad k_f = \frac{1}{R_f}, \quad \tau_f = \frac{L_f}{R_f}. \tag{5.23}$$

Since the rotations of the rotor relative to the stator windings depend on the angle $\theta_e(t)$, the magnetic flux induced by the rotation of the rotor near the stator will also rotate. The magnetic flux is experienced by the stator windings as

$$\Phi(t) = \Phi_{amp}(t) \sin \theta_e(t), \tag{5.24}$$

where $\Phi_{amp} = k_1 I_f(t)$, under the assumption that we have magnetic linearity without magnetic saturation and hysteresis effects (Skjetne, 2017). k_1 is some constant based on

the construction of the machine and its characteristics. By disregarding the rapid transient of Equation 5.22, by Faraday's law and Lenz's law, the induced electromotive force (EMF), $E_a(t)$, in the stator is according to Skjetne (2017):

$$E_a(t) = N\dot{\Phi}(t) = Nk_1 I_f(t)\omega_e(t)\cos\theta_e(t), \tag{5.25}$$

where N is the number of turns of the wire in the stator. This shows that the induced voltage has frequency $\dot{\theta}_e(t) = \omega_e(t)$ [rad/s] and an RMS value of

$$\hat{E}_a(t) = k\omega_e(t)I_f(t), \tag{5.26}$$

where $k = \frac{Nk_1}{\sqrt{2}}$ is a constant value.

In order to get all values in per-unit, the following transformations of the variables are done:

$$r_f := \frac{R_f}{Z_b}, \quad i_f := \frac{I_f}{I_b}, \quad \text{and} \quad v_f := \frac{V_f}{V_b}, \tag{5.27}$$

where Z_b is the base impedance for the genset, I_b is the base current for the genset and V_b is the electric base voltage (line-to-line) for the genset/bus. Applying these relations to Equation 5.22 yields

$$\frac{d}{dt}i_f = -\frac{1}{\tau_f}\left(i_f - \frac{1}{r_f}v_f\right) \tag{5.28}$$

$$\hat{e}_a = \frac{\hat{E}_a}{V_b} = \frac{k\omega_b\omega I_b}{V_b}i_f = \frac{k\omega_b}{Z_b}\omega i_f. \tag{5.29}$$

$\hat{e}_a$ is the per-unit RMS induced voltage for the stator a-phase of the generator.

In steady state, $i_f = \frac{v_f}{r_f}$ which means that $\hat{e}_a = k\frac{\omega_b v_f}{Z_b r_f}\omega$. Defining

$$k := \frac{r_f Z_b}{\sqrt{3}\omega_b} = \frac{R_f}{\sqrt{3}\omega_b} \quad \Longrightarrow \quad \hat{e}_a = \frac{r_f}{\sqrt{3}}\omega i_f \tag{5.30}$$

and choosing $\omega = 1$ and $r_f i_f = 1$ such that $\hat{e}_a = \frac{1}{\sqrt{3}}$ and $\hat{e}_{ll} = \sqrt{3}\hat{e}_a = 1$.

Equation 5.28 and Equation 5.30 forms a dynamic system where the per-unit field voltage in the rotor of the generator v_f is the control input from the AVR and the per-unit RMS induced voltage for the stator a-phase of the generator, $\hat{e}_a$, is the output of the generator (Skjetne, 2017).

The phasor line-to-neutral voltage at the terminals of the generator (bus line-to-neutral voltage), $\tilde{v}_{an}$, can, following Kirchoff's voltage law, be calculated as

$$\tilde{v}_{an} = -z_s\tilde{i}_a + \tilde{e}_a = -\left(r_s + j\omega x_s\right)\tilde{i}_a + \tilde{e}_a \tag{5.31}$$

where $\tilde{i}$ is the stator line current for the a-phase, $\tilde{e}_a = \hat{e}_a e^{j\theta_e}$, $r_s := \frac{R_s}{Z_b}$ is the per-unit resistance of the stator a-winding and

$$x_s := \frac{X_s}{Z_b} = \frac{\omega_b L_s}{Z_b} = \omega_b l_s \tag{5.32}$$

is the synchronous reactance at base frequency. In Equation 5.32, X_s is the stator synchronous reactance of the generator, L_s is the stator synchronous inductance of the generator and l_s is the per-unit stator synchronous inductance of the generator.

5.2.4 Voltage Control

The purpose of the AVR is to maintain the generator's terminal voltage, $\hat{V}_t$ within an acceptable range, by controlling the magnetization. As the speed governor, described in Section 5.2.2, the AVR often uses droop control in order to control the voltage. The droop curve is often chosen with a value of $\pm 2.5\%$ for the allowed variation of the voltage over the nominal reactive power range (Skjetne, 2017). Droop correction of the voltage level is also used for equal distribution of reactive power between the different gensets. For this application, the droop value is also often 2.5%. The reactive power, Q, is normalized, such that the droop-percent value can be used directly. Normalizing the reactive power, the corrected setpoint to the AVR of Genset j is calculated as

$$\hat{v}_{sp,j} = \hat{v}_{ref,j} - \frac{d_{\%-\mathrm{Droop},j}}{100} \frac{Q_j}{Q_{n,j}} \tag{5.33}$$

A block diagram of the control loop is illustrated in Figure 5.6.

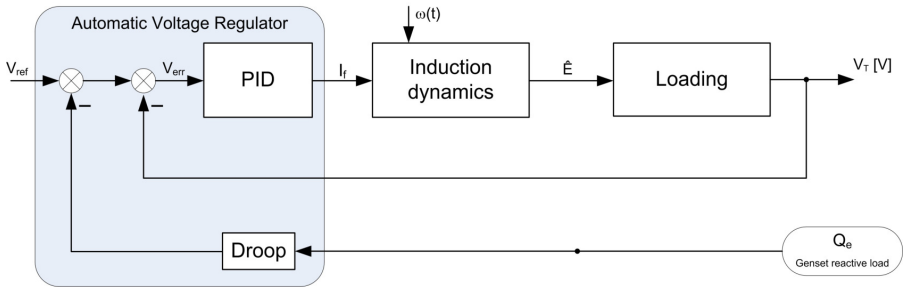

Figure 5.6: Droop control AVR. Courtesy: Skjetne (2017).

5.2.5 Power Load Sharing

The power load sharing between gensets is in the MVPPSS ensured using equivalent circuits, like the one illustrated in Figure 5.7.

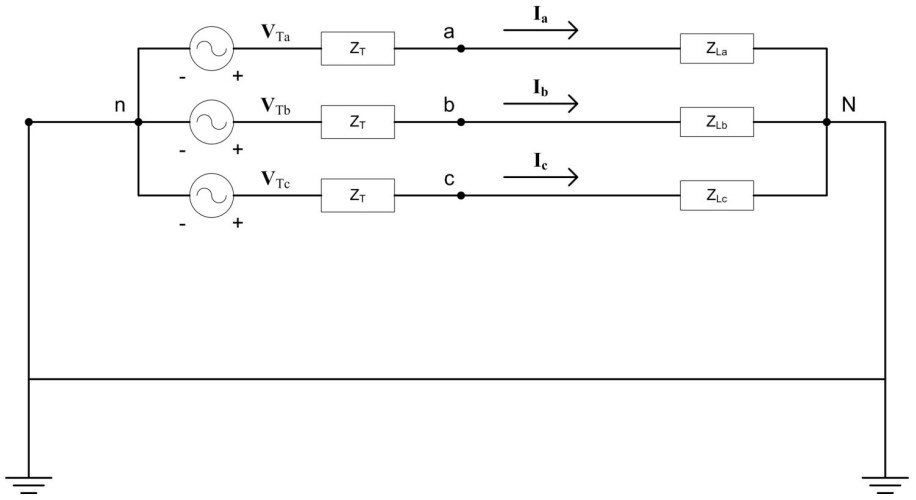

Figure 5.7: 3-phase equivalent circuit where the generators are represented by a Thevenin equivalent circuit and the consumers by a common load impedance. Courtesy: Skjetne (2017).

The steps in the power load sharing consist of the following steps (Skjetne, 2017):

1. Assuming the load is balanced, the load impedance for the a-phase, Z_L, is calculated. Usually, the knowledge of the bus voltage from the previous iteration is needed in order to do this. This problem is overcome by using a unit delay or low-pass filter with initial values.
2. The equivalent complex Thévenin voltage, $\tilde{V}_{Ta}$, and impedance, Z_T, are calculated for the connected generators. Equal frequency of the voltage output from each generator is assumed.
3. The resulting per-phase bus voltage $\tilde{V}_{an}$ is calculated.
4. The current $\tilde{I}_a$ and the active and reactive power levels, P and Q, supplied by each generator are calculated.

The mathematical derivations of each of these steps can be found in (Skjetne, 2017).

5.3 Implementation of MILP Optimization Algorithm

This section describes the implementation of the developed MILP optimization algorithm, based on the MILP optimization problem formulation of Chapter 4, in the MVPPSS. The different features and functions of the MILP optimization algorithm are addressed and explanations of how they are implemented within the simulation environment of the MVPPSS are provided.

In order to include MILP optimization of a simulation model in the MVPPSS, the developed MILP algorithm, described in Section 4.4, must be connected to the simulation model. The calculated optimal scheduling scheme and the optimal power levels for all gensets should be used as setpoints to the gensets in the simulation model. By using these as setpoints, the gensets in the marine power plant should be operated in an optimal manner, with respect to the chosen optimization objective and fuel consumption. Including the MILP optimization algorithm in the MVPPSS is done by using the Matlab-function block in Simulink. This block allows for the user to define own functions within the Simulink environment. The contents of the Matlab-function block is an adapted and altered version of the code presented in Section 4.4. One of the changes include that the demanded load is not fed directly to the optimization algorithm, like when implemented in Matlab, but the experienced load by the simulation model is sent in as an input to the algorithm. Also, the calculated optimal scheduling scheme and power levels are outputs from the algorithm, which are used as setpoints for the controllers in the simulator. Many of the calculations within the optimization algorithm depend on the previous values of variables, hence many variables are fed back as inputs to be used as previous values. To make sure the optimization does not execute for each tiny time step of the simulation in Simulink, a feature that keeps track of the last time the optimization was executed is implemented. This feature allows for the periodic execution of the optimization to be chosen, since a conditional statement stating that optimization should only be executed if the time since last optimization is bigger than a set value is included. This value is initially set to ten seconds, but can be changed, which is the case for the case study conducted later in this thesis. See Chapter 7. One drawback of this method is that the simulations in the MVPPSS use a variable step size in its solver, the ode15s solver (Bø et al., 2015b). This means that some of the step sizes of the solver might exceed the value of the periodic execution of the optimization. This means that the optimization might not execute as often as desired if a big step size occurs. However, evaluation of the step sizes after each simulation showed that the step sizes rarely exceeded a value of 10 seconds, 20 seconds at most, and for the most parts, the step sizes were less than 1 second. Efforts were given to run the simulations with predetermined fixed step sizes, i.e. other types of solvers, but the simulations were unable to finish as errors occured.

The initialization files used for initializing simulation models are based on an initialization file made by Torstein Bø, which is part of the MVPPSS installation package. Proper adjustments have been made in the initialization files in order to use them with desired power plant configurations. Therefore, the initialization files must be viewed as Torstein Bø's original work, whereas additions to these have been made through the work of this thesis. When optimizing a simulation model of a marine power plant in the MVPPSS,

the constants and variables needed for optimization are initialized by additions made to the initialization file. By adding the needed variables and constants to the initialization file, all variables needed for optimization and running the simulator are loaded to Matlab's workspace.

The Matlab function block with its inputs, outputs and feedback can be found in Appendix A.3. Its content, i.e. the implementation of the MILP optimization algorithm's code, can be found in Appendix A.4.

5.3.1 Genset Scheduling

The genset scheduling is stage 1 of the optimization algorithm. The optimal scheduling scheme is found by solving the mixed integer linear program, as formulated in Equation 4.11. To solve the mixed integer linear program, the Matlab function *intlinprog* is used. When running a model in Simulink, Simulink translates the block diagrams to C/C++ code and solves the corresponding equations in C/C++. The Matlab function *intlinprog* is not supported for code generation in Simulink. Therefore, the function must be declared as an extrinsic function, using the command *coder.extrinsic(intlinprog)*. By declaring the function extrinsic, the function call is executed using the Matlab engine instead of translating it to C/C++ code. This leads to more complex calculations and is more computationally demanding, thus affecting simulation time. However, it is an acceptable approach as the simulations performed in this thesis usually finish in minutes, some times up to half an hour. The alternative would be to write C/C++ code for *intlinprog*.

5.3.2 Load Sharing Between Active Gensets

The optimization of the load sharing with respect to minimizing the fuel consumption of the power plant is stage 2 of the optimization algorithm. The optimal load sharing is found by solving the linear program, seen in Equations 4.21 through 4.25. The linear program minimizes the total sum of the SFOC-curves for the gensets such that the power demand is met. The SFOC-curves are represented as PWL curves with discrete values in Matlab, and they are loaded to Matlab's workspace when running the initialization file that must be run before simulations in the MVPPSS. The linear program which minimizes the fuel consumption is solved by using the Matlab function *linprog*. This function must also be declared as an extrinsic function in Simulink, ref. previous section. The optimal power levels for each genset are outputs from the optimization algorithm, and are used as setpoints in the control of each genset. The gensets are controlled towards their optimal power levels using droop control.

5.3.3 Droop Control

When the MILP optimization algorithm has calculated the optimal power levels, these are used as setpoints for the control of the gensets. Using droop control, the gensets can be

controlled to a desired frequency according to Equation 5.21. The control input is the no-load frequency. Studying the contents of the genset model in the MVPPSS, it was discovered that the speed governor use a slightly different equation for calculating the frequency setpoint, namely

$$\omega_{sp} = \omega_{NL}(1 - \frac{d_{\%-Droop}}{100}p). \tag{5.34}$$

Rearranging this yields

$$\omega_{NL} = \frac{\omega_{sp}}{1 - \frac{d_{\%-Droop}}{100}p}. \tag{5.35}$$

Keeping ω_{sp} constant at 1.0 (p.u.), the no-load frequency corresponding to the given amount of active power (p.u.) can thus be calculated. Using this no-load frequency as the control input to the speed governor of the genset will ensure the genset's power level is controlled towards the optimal power level. Thus, the droop equation, shown in Equation 5.35, serves as a guidance function for mapping the setpoint of the power level to the commanded no-load frequency.

In Figure 5.8, a typical droop curve can be seen, using 4 % droop. The figure illustrates the idea behind droop control, and how the frequency and rated power are connected through the droop curve. It is essentially by changing the droop curve for each genset the power is controlled with the power level setpoints, as the no-load frequency is constantly calculated and updated. Thus, for each optimization, a different droop curve for each genset is made. This new droop curve fits the objective of controlling the genset towards the desired power level, through obtaining the desired frequency from calculating a new no-load frequency, as Equation 5.35 shows.

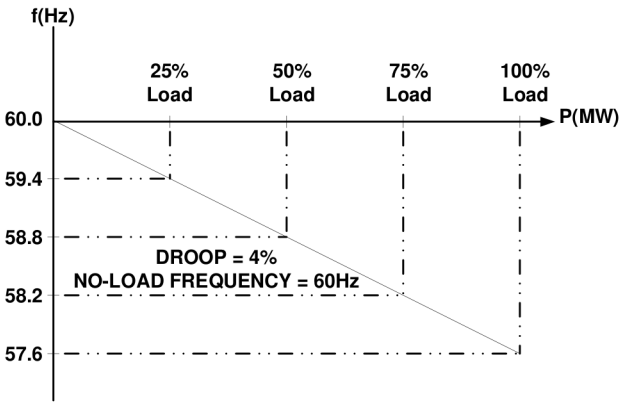

Figure 5.8: Droop curve using 4 % droop. No-load frequency at 60 Hz. Courtesy: (Cosse et al., 2011).

5.3.4 Estimation of Fuel Consumption

Estimating the fuel consumption of the gensets is done by including the SFOC-curves used in the load sharing optimization as lookup tables for the calculation of fuel consumption. The SFOC has unit g/kWh, thus the fuel consumption FC, can be calculated according to

$$FC = SFOC \cdot p \cdot P_b \tag{5.36}$$

where P_b is the rated base power of the genset and p is the active power (p.u.) of the genset. The SFOC-curves are PWL curves, which means if the active power of the genset is in between two data points of the PWL curve, the estimation will interpolate between the two data points to find an accurate SFOC value corresponding to the current active power level.

Chapter 6

Verification of MILP Optimization Algorithm

The task of optimal genset scheduling and load sharing of a marine power plant is considered in this thesis. The corresponding MILP optimization problem to genset scheduling and load sharing is formulated in Chapter 4. The MILP optimization problem is implemented in Matlab, and gives rise to a MILP optimization algorithm applicable for optimization of marine power plants. Onwards, the MILP optimization algorithm is incorporated into the simulation environment of the MVPPSS, as described in Section 5.3. This makes it possible to use the MILP optimization algorithm within a realistic marine power plant system simulator.

In this chapter, the MILP optimization algorithm made from the optimization problem formulation in Chapter 4 is verified. The MILP optimization algorithm can be used to find the optimal genset scheduling and load sharing for a marine power plant. The MILP optimization algorithm is verified in two steps. In the first step, the optimization algorithm is verified by optimizing the control of a simplified marine power plant with a deterministic load profile, ensuring that the correct results are obtained. Then, in the second step, the optimization algorithm is verified by optimizing the control of a simulation model of a marine power plant within the MVPPSS, also using a deterministic load profile. This second step verifies that the MILP optimization algorithm produces the desired results, also within the framework of the chosen simulation environment. Also, this demonstrates the ability of the MILP optimization algorithm to serve in an online optimization layer of a marine vessel and that the simulation model correctly controls the components using the optimal setpoints calculated by the MILP optimization algorithm.

6.1 Verification of Optimization of a Simplified Marine Power Plant

6.1.1 Background and Problem Formulation

The first step of verifying the MILP optimization algorithm verifies that the implemented MILP optimization algorithm works properly and provides results according to the desired behavior. Verification is conducted by simulating the genset scheduling and load sharing on a simplified marine power plant, using the MILP optimization problem formulation, expressed in Equation 4.11 and Equations 4.21 through 4.25. The simulation of the genset scheduling and load sharing is performed by iterating through an array containing the load profile for retrieving the current load, and for a given periodic time instant, solving the MILP optimization problem corresponding to the given time instant. The MILP optimization algorithm sends out two results; a scheduling vector containing the connection scheme of the gensets and a load sharing vector containing the load sharing between the connected gensets.

Load Profile

The capabilities of the MILP optimization are demonstrated using a deterministic load profile. The deterministic load profile provides a possibility to verify and validate the optimization algorithm's performance, as it is easy to anticipate the scheduling behavior for a deterministic load profile with known values and development of the demanded load. The deterministic load profile is a load profile linearly increasing from zero load, before decreasing linearly to zero load over the time horizon of the simulation, which is 4000 s. The deterministic load profile used for the first step of verification can be seen in Figure 6.1.

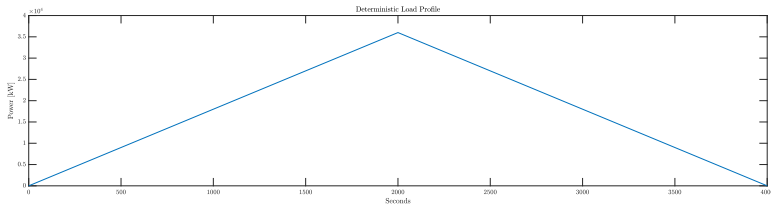

Figure 6.1: Deterministic load profile used for first step of verification of MILP optimization.

Power Plant Configuration

The configuration of the power plant used in the verification of the MILP optimization is shown in Figure 6.2. This configuration consists of six gensets with an equal capacity of 8000 kW, according to the 46-engine-family of four stroke Wärtsilä engines (Wärtsilä, 2019). The simplified marine power plant used for verification is not a simulation model, and only the static behavior of the power plant is modeled, i.e. no engine dynamics are

included. The bus is subject to a load, P_{load}, which is represented by instantaneous values of the deterministic load profile from Figure 6.1.

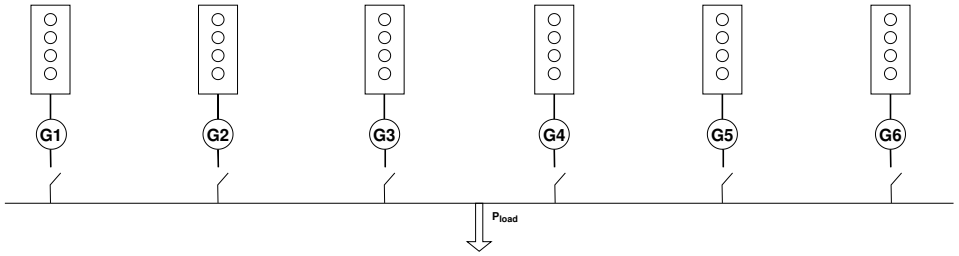

Figure 6.2: Simplified marine power plant configuration used for optimization verification.

The SFOC-curve used for optimizing the load sharing of the active gensets is constructed using regression analysis on the working points of the 46-engine-family of four stroke Wärtsilä engines (Wärtsilä, 2019). The data set contains measured fuel oil consumption as a function of the engine load, in per-unit. The SFOC curve does not necessarily provide an accurate representation of the realistic fuel consumption, as the curve is constructed using regression analysis from a set of data points, in addition to the measurements typically being steady state measurements in a laboratory environment (Thorat and Skjetne, 2018). However, for the use as a data foundation in this thesis, the data from the estimated SFOC-curve are good enough. The measurements used in the regression analysis are the data points presented in (Jalkanen et al., 2011), provided by Wärtsilä product guide for the 46-engine-family (Wärtsilä, 2019). The resulting SFOC curve can be seen in Figure 6.3.

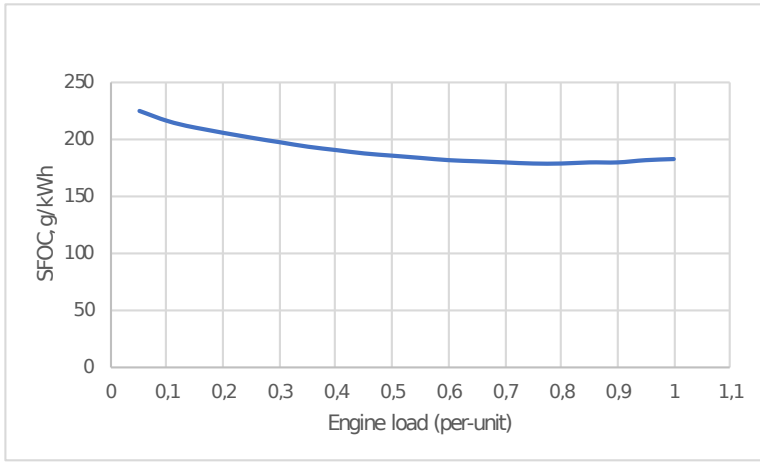

Figure 6.3: SFOC as a function of engine load following from regression analysis of data points of the 46-engine-family of four stroke Wärtsilä engines.

The SFOC-curve presented in Figure 6.3 is used to create the PWL curves which are

implemented into the MILP optimization algorithm and used for minimization of the fuel consumption for each genset.

Optimization Objectives

Four simulations are conducted, each with a different optimization objective. Demonstrating the performance of the optimization algorithm, four optimizations using different optimization objectives regarding the scheduling of the gensets are explored. The different optimization objectives are described in Table 6.1. The MILP formulation presented in Equation (4.11) includes weights of the different optimization objectives. The weights used in the algorithm for each optimization objective are shown in Table 6.2. In addition to optimizing the scheduling of the gensets, the load sharing between the active gensets is optimized by minimizing the fuel consumption. This minimization is executed regardless of the chosen optimization objective.

Optimization objective	**Description**
Opt. Obj. 1	Minimizing online capacity of the connected gensets.
Opt. Obj. 2	Minimizing online capacity and running time of the connected gensets.
Opt. Obj. 3	Minimizing online capacity and number of connections/disconnections of the gensets.
Opt. Obj. 4	Combining all of the above objectives.

Table 6.1: Description of optimization objectives in the MILP optimization algorithm.

Optimization objective	w_1	w_2	w_3	w_4
Opt. Obj. 1	1	0	0	0
Opt. Obj. 2	1	1	0	0
Opt. Obj. 3	1	0	1	1
Opt. Obj. 4	1	10	10	10

Table 6.2: Weighting scheme used in the MILP formulation of Equation 4.11 for the four different optimization objectives in verification of optimization of a simplified marine power plant.

The optimal loading factor is set to 0.80, according to the optimal running condition for the gensets from Figure 6.3. Technical specifications of the gensets are presented in (Wärtsilä, 2019), using a maximum output of active power of 8000 kW. Using an optimal loading factor of 0.80 means that the MILP optimization algorithm will connect a new genset when the demanded load increases to over 80 % MCR of the connected gensets. The periodic execution of the optimization is ten seconds. The optimization algorithm is implemented in Matlab, and the code used for running the genset scheduling and load sharing optimization is presented in Appendix appendix A.1.

6.1.2 Simulations

Optimization Objective 1

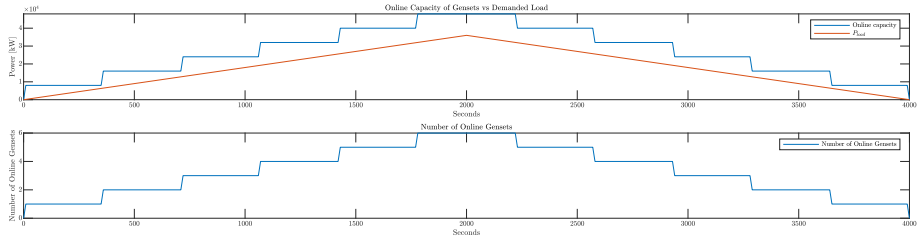

Figure 6.4: Online capacity of gensets and demanded load (top), and number of connected gensets (bottom) when optimizing genset scheduling and load sharing of a simplified marine power plant using Optimization Objective 1.

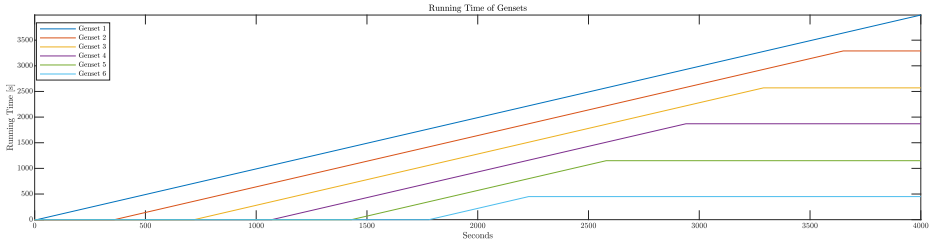

Figure 6.5: Running time of gensets when optimizing genset scheduling and load sharing of a simplified marine power plant using Optimization Objective 1.

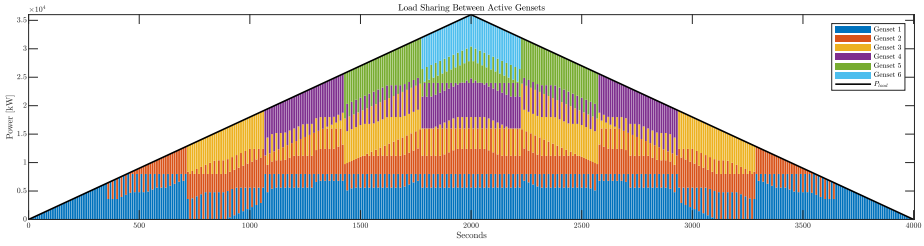

Figure 6.6: Load sharing between gensets when optimizing genset scheduling and load sharing of a simplified marine power plant using Optimization Objective 1.

Optimization Objective 2

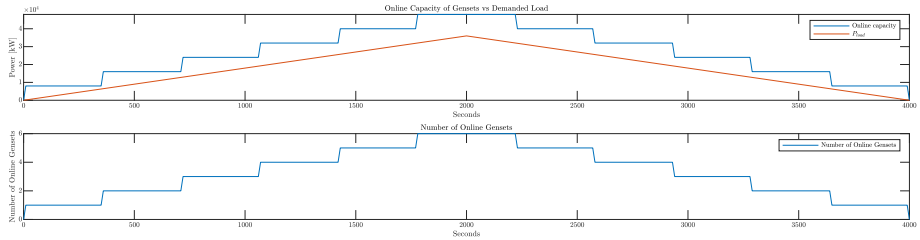

Figure 6.7: Online capacity of gensets and demanded load (top), and number of connected gensets (bottom) when optimizing genset scheduling and load sharing of a simplified marine power plant using Optimization Objective 2.

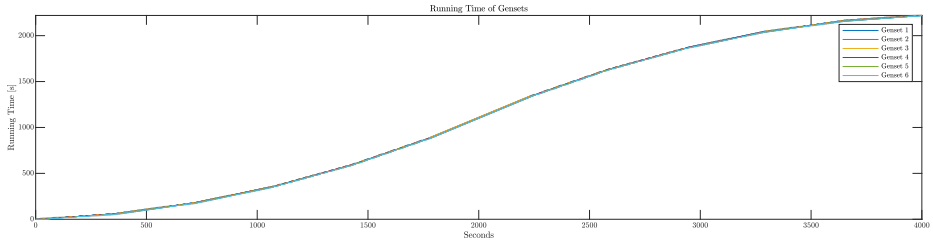

Figure 6.8: Running time of gensets when optimizing genset scheduling and load sharing of a simplified marine power plant using Optimization Objective 2.

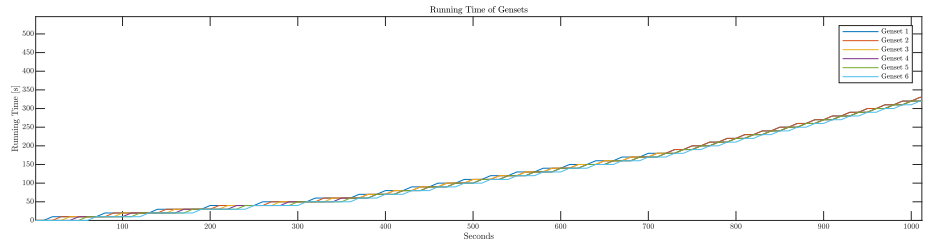

Figure 6.9: Close up of the running time of the gensets when optimizing genset scheduling and load sharing of a simplified marine power plant using Optimization Objective 2.

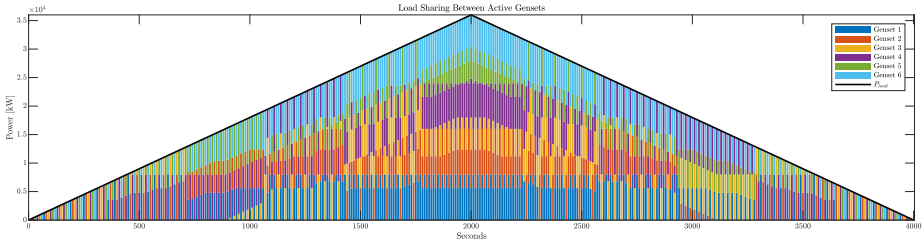

Figure 6.10: Load sharing between gensets when optimizing genset scheduling and load sharing of a simplified marine power plant using Optimization Objective 2.

Optimization Objective 3

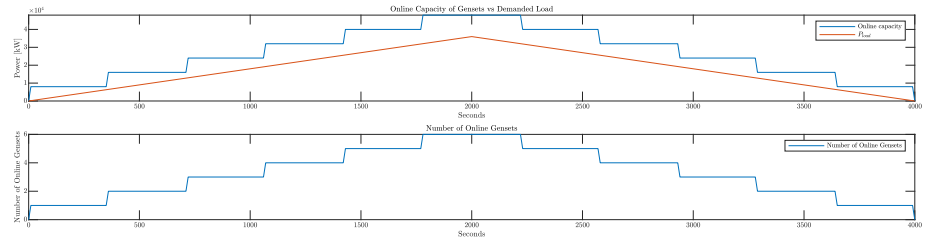

Figure 6.11: Online capacity of gensets and demanded load (top), and number of connected gensets (bottom) when optimizing genset scheduling and load sharing of a simplified marine power plant using Optimization Objective 3.

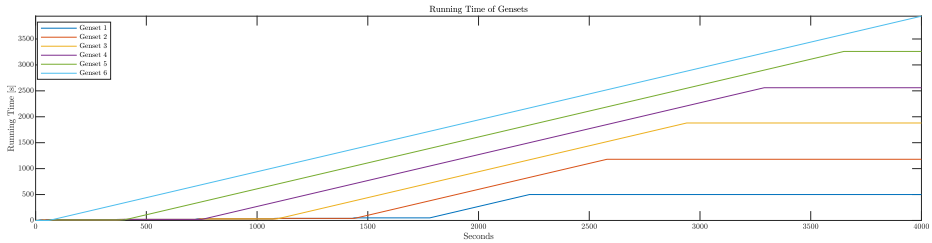

Figure 6.12: Running time of gensets when optimizing genset scheduling and load sharing of a simplified marine power plant using Optimization Objective 3.

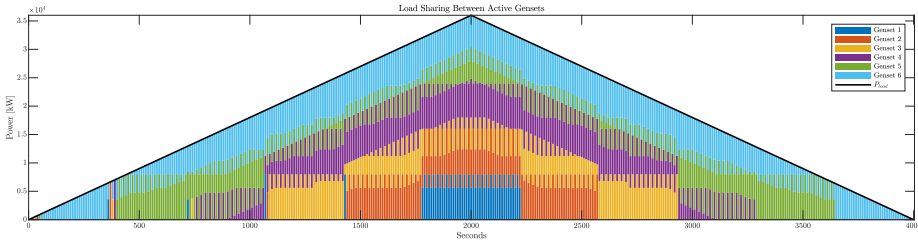

Figure 6.13: Load sharing between gensets when optimizing genset scheduling and load sharing of a simplified marine power plant using Optimization Objective 3.

Optimization Objective 4

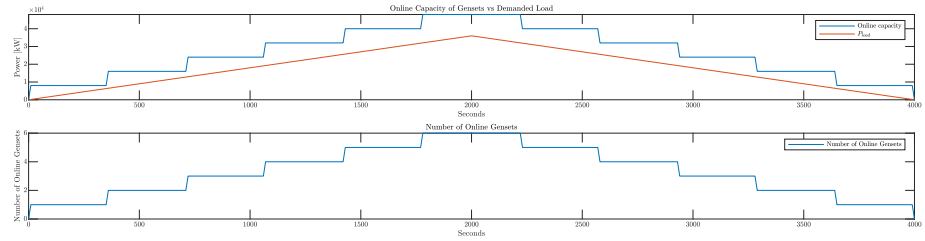

Figure 6.14: Online capacity of gensets and demanded load (top), and number of connected gensets (bottom) when optimizing genset scheduling and load sharing of a simplified marine power plant using Optimization Objective 4.

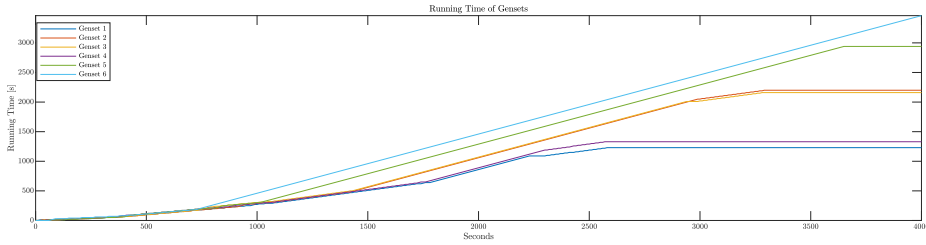

Figure 6.15: Running time of gensets when optimizing genset scheduling and load sharing of a simplified marine power plant using Optimization Objective 4.

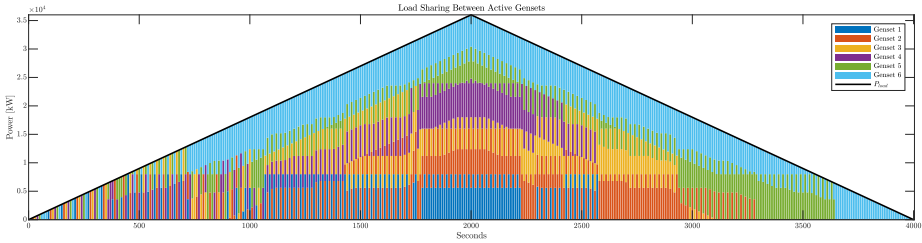

Figure 6.16: Load sharing between gensets when optimizing genset scheduling and load sharing of a simplified marine power plant using Optimization Objective 4.

6.1.3 Discussion

In Figures 6.4, 6.7, 6.11 and 6.14 the online capacity and demanded load, and the number of online gensets are shown for Optimization Objective 1, 2, 3 and 4. The figures show that gensets are connected/disconnected as the demanded load increases/decreases and that this happens when the demanded load is 80 % of the online capacity. This is as expected when the optimal loading factor is set to 0.80.

Figure 6.5 shows how the running time of the gensets develops throughout the simulation when using Optimization Objective 1. As expected from using this optimization objective, the gensets are connected/disconnected consecutively, one by one, as the demanded load increases/decreases, which can be seen in Figure 6.5. This characteristic can also be seen in Figure 6.6 which shows the load contribution from each genset.

Figure 6.6 shows the load sharing between the active gensets when using Optimization Objective 1. This figure also illustrates how the gensets are connected/disconnected consecutively as the load increases/decreases. One can see the load share of certain gensets alternating between zero and a distinct load share not equal to zero. This happens for Genset 2 right after the time Genset 2 is connected (approx. at 350 s) and right before Genset 2 is disconnected (approx. at 3650 s). The same happens with Genset 4 after Genset 5 is connected (approx. at 1400 s) and before Genset 5 is disconnected (approx. at 2600 s). While this may seem like Genset 2 and Genset 4 are being connected and disconnected every other execution of the optimization, they are however connected for the whole time. The reason why they are not providing any power every other optimization execution is that the optimization of the load sharing between the active gensets chooses the optimal operating point at 0 % MCR.

In Figure 6.8, the running time of gensets when using Optimization Objective 2 is shown. This optimization objective results in multiple connections/disconnections of the gensets. This happens since the goal of the optimization is to minimize the number of running time for each genset, such that the algorithm connects and disconnects gensets in a manner which ensures the running time is kept as low as possible. Thus, if a genset has accumulated a long running time, the optimization of the scheduling variable, C, will choose a different connection scheme than one that contains the connection of the long running

genset. Figure 6.8 shows that the gensets are operated in a way which equally distributes the running time between them, which gives the somewhat interconnected gathering of the plots of the running time. This can be seen in greater detail in Figure 6.9, which shows a close up of this characteristic. The illustration of the load sharing between the gensets, shown in Figure 6.10, depicts the same behavior, as the optimization algorithm constantly connects different gensets. This can be seen by which of the gensets that contribute with power to the bus. However, when the demanded load is highest (approx. 1800-2200 s), all gensets provide power, since the load is so high that all gensets are required to be connected.

The running time of the gensets when using Optimization Objective 3 can be seen in Figure 6.12. Optimization Objective 3 seeks to minimize the number of connections and disconnections, thus a development of the running time of the gensets as depicted in Figure 6.5 (using Optimization Objective 1) is expected. This is in fact the case, however with a minor difference, which can be identified even easier in Figure 6.13, which shows the load sharing between the active gensets. When the optimization algorithm is going to connect a new genset, the algorithm connects and disconnects all gensets, one by one, before the last one is connected "permanently". This is due to the way the objective function and constraints are formulated in the MILP optimization problem. An elaborate explanation and illustration of what happens mathematically is included in Appendix A.5. Other than this, the results indicate that using Optimization Objective 3 fulfills the goal of minimizing the connections and disconnections.

Figures 6.15 and 6.16 show the running time of gensets and load sharing between gensets, respectively, when using Optimization Objective 4. This optimization objective seeks to combine the characteristics of Optimization Objective 1, 2 and 3, with equal weights for minimizing running time and connections/disconnections (see Tables 6.1 and 6.2. The development of the running time and the connections/disconnections of gensets seen from Figures 6.15 and 6.16 show that there actually is a trade off between minimizing running time and connections/disconnections of the gensets. Comparing Figure 6.15 with Figure 6.8, which illustrates the running time of gensets when using Optimization Objective 2, one can see that the connections and disconnections happen much less frequently when Optimization Objective 4 is applied. This is as expected since the minimization of the connections/disconnections are added as a term to the objective function by giving w_3 and w_4 non-zero positive values. Figure 6.15 shows that the gensets are frequently connected/disconnected in the beginning of the simulation, indicating that the optimization algorithm prioritizes minimizing the running time of the gensets rather than the connections/disconnections of the gensets. Later in the simulation, the optimization algorithm seems to prioritize minimizing the connections/disconnections rather than the running time of the gensets. This can be explained by investigating the objective function of the MILP optimization problem, Equation 4.11. The term related to minimizing the running time of the gensets, the second term in Equation 4.11, will decrease with time due to $|d|$ growing large with time, as it sums up the running time of all of the gensets. This means that

$$\lim_{t\to\infty} w_2 \frac{d(t)}{|d(t)| + \varepsilon} = 0, \tag{6.1}$$

thus showing that as the time of the simulation goes by, the term related to minimizing the running hours will be lighter weighted than the terms related to minimizing connections and disconnections. This happens because $|d|$ increases faster than $|S_{on}|$ and $|S_{off}|$, unless gensets are connected and disconnected several times per second, which is an unlikely scenario.

Aspects of the optimization which could be improved are:

- The rate of change of the power level for a genset is not included in the optimization. This means that a genset's optimal power level in theory could go from 0 % MCR to 100 % MCR from one optimization to the next. To provide a more realistic optimal operation of the components, the rate of change allowed for each genset should be included as constraints in the LP calculating the optimal power levels.
- The periodic execution of the optimization is frequent, often ranging from 1 second to 10 seconds. This is done for illustrational purposes in this thesis, but realistically, an optimization of a marine power plant would not be executed this often.
- As discussed, some gensets experience being put in the operating point of 0 % MCR, or idle. As 0 % MCR is a highly inefficient operating point for a single genset, alterations to the optimization algorithm could be made, ensuring that no genset is put in idle. This would reduce the number of connected gensets, which in turn would decrease the wear and tear of the equipment. This said however, the algorithm does minimize the fuel consumption even when one genset is operated very inefficiently. This single genset does contribute with a high fuel consumption, but the system as a whole has its lowest fuel consumption when this engine is put in idle. This can be viewed as a matter of local vs global minima.
- The discussed characteristic of the algorithm "working through" non-connected gensets before connecting the last one tried could be altered to make this behavior disappear, as it truly does not minimize the connections and disconnections of gensets when they previously have been connected/disconnected an equal amount of times.

6.2 Verification of Optimization of a Simulated Marine Power Plant

6.2.1 Background and Problem Formulation

The second step of the verification of the MILP optimization algorithm is to use the optimization algorithm on a simulation model of a marine power plant in the MVPPSS. This verifies that the optimization is implemented correctly within the simulation environment of the MVPPSS and shows that the algorithm produces the optimal genset scheduling and load sharing also when it is connected to the MVPPSS. Also, this stage verifies that the MVPPSS is able to be controlled by the optimization algorithm and that the simulated marine power plant follows the setpoints of scheduling and power loads from the optimization. Thus, the second step verification confirms that the developed MILP optimization algorithm is able to function as an online optimization algorithm of a simulated marine power plant.

Load Profile

For the verification of the MILP optimization algorithm connected with the MVPPSS, a deterministic load profile is used. Following the reasoning in Section 6.1.1, using a deterministic load profile provides the opportunity of recognizing the expected and desired behavior of the optimization algorithm. However, for this stage of the verification, the deterministic load profile contains steps of constant load levels after a new genset is connected or disconnected. This ensures that the gensets have time to reach steady state operation in between the connection or disconnection of new gensets, thus providing stable power load levels and frequency and voltage levels. The deterministic load profile used for the verification of the optimization algorithm implemented together with the MVPPSS can be seen in Figure 6.17. A deterministic load profile with a shorter time horizon is used for Optimization Objective 2. This is due to unexpected behavior of the MVPPSS when connecting and disconnecting gensets frequently, and forces the load profile to be altered in order to run a complete simulation when using Optimization Objective 2. This is discussed further in Section 6.2.3. The load profile used when Optimization Objective 2 is the objective is presented in Figure 6.18.

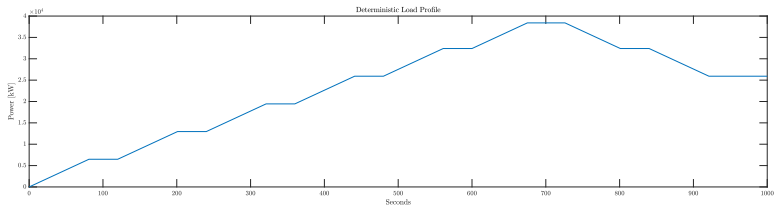

Figure 6.17: Deterministic load profile used for Opt. Obj. 1, 3 and 4 in verification of MILP optimization in the MVPPSS.

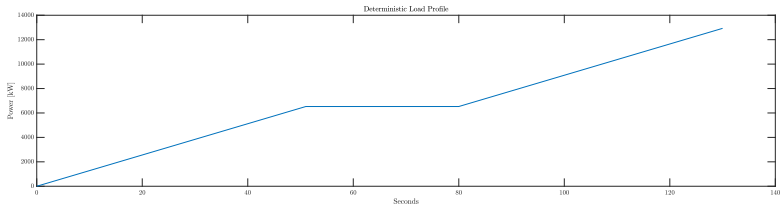

Figure 6.18: Deterministic load profile used for Opt. Obj. 2 in verification of MILP optimization in the MVPPSS.

Power Plant Configuration

The configuration of the power plant coincides with the configuration described in Section 6.1.1, however, the marine power plant is a simulation model and not just a static simplified marine power plant. The simulation model consists of six gensets with an equal capacity of 8000 kW. The SFOC-curve described in Section 6.1.1 is used for the creation of PWL curves which are used for minimization of the fuel consumption of the gensets.

Optimization Objectives

To verify that the MILP optimization algorithm has been implemented correctly in the MVPPSS, four different optimization objectives are used for the simulations. The optimization objectives are the same as those used in the optimization of the simplified marine power plant, as shown in Table 6.1. However, some of the weights used in the objective function of Equation 4.11 are different for the optimization objectives. The difference in the weighting schemes is due to some unexpected behavior of the MVPPSS when optimizing with certain weights. This is further discussed in Section 6.2.3. The weights used in the optimization for each optimization objective are shown in Table 6.3.

Optimization objective	w_1	w_2	w_3	w_4
Opt. Obj. 1	1	0	0	0
Opt. Obj. 2	1000	0.1	0	0
Opt. Obj. 3	1	0	1	1
Opt. Obj. 4	1000	0.1	1000	1000

Table 6.3: Weighting scheme used in the MILP formulation of Equation 4.11 for the four different optimization objectives in verification of optimization of a simulation model.

When implementing the MILP optimization algorithm in the MVPPSS, the conditional execution of the algorithm depends on both the time variable itself and the time since the last optimization was executed, as described in Section 5.3. For Optimization Objectives 1, the first optimization is executed after 0.1 s, and for Optimization Objectives 2, 3 and 4, after 1 s. The periodic execution of the optimization is for Optimization Objective 1 and 3 ten seconds, for Optimization Objective 2 four seconds, and for Optimization Objective 4 one second. The periodic execution of the optimization differs for the different

optimization objectives because of problems that occurred when including minimization of running hours in the optimization, i.e. Optimization Objectives 2 and 4. This is addressed in Section 6.2.3. For all optimization objectives, Genset 1 is always initialized as connected and providing power according to 80 % MCR. This is done to ensure that there is always enough power available when the simulation is started and before the optimization algorithm provides optimal setpoints to the simulator.

6.2.2 Simulations

Optimization Objective 1

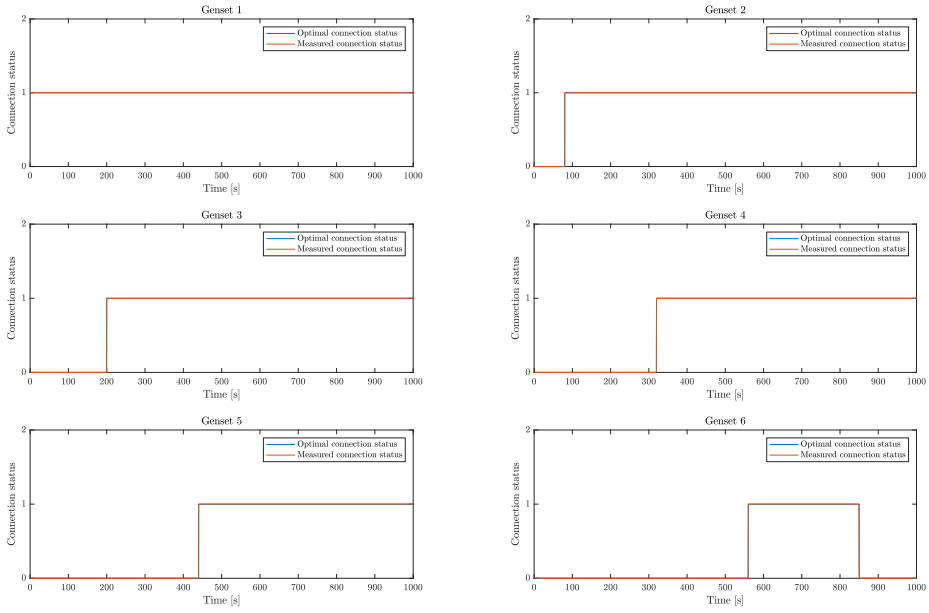

Figure 6.19: Connection status of gensets when optimizing genset scheduling and load sharing using Optimization Objective 1 on a simulation model in the MVPPSS.

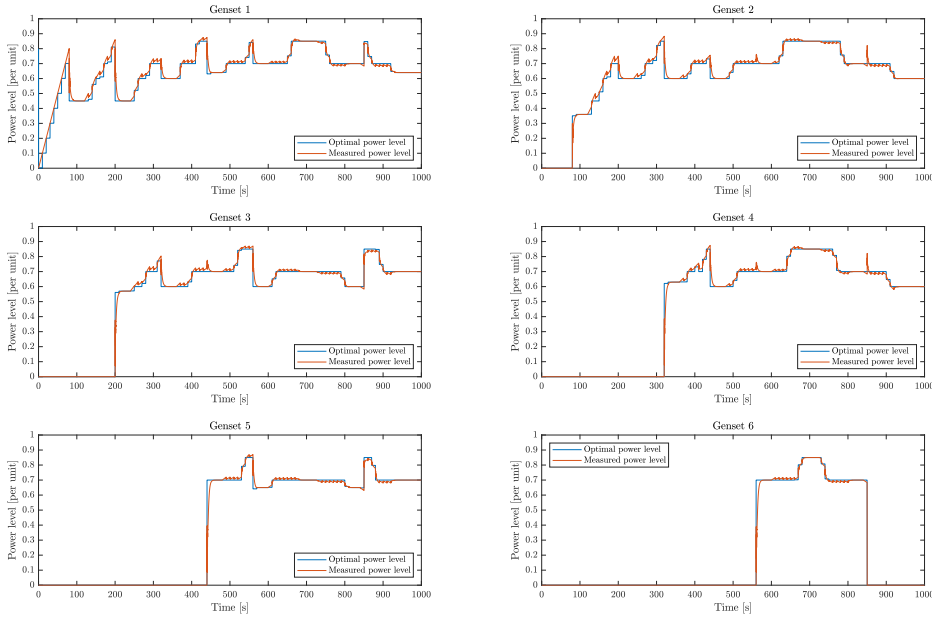

Figure 6.20: Active power delivered by gensets when optimizing genset scheduling and load sharing using Optimization Objective 1 on a simulation model in the MVPPSS.

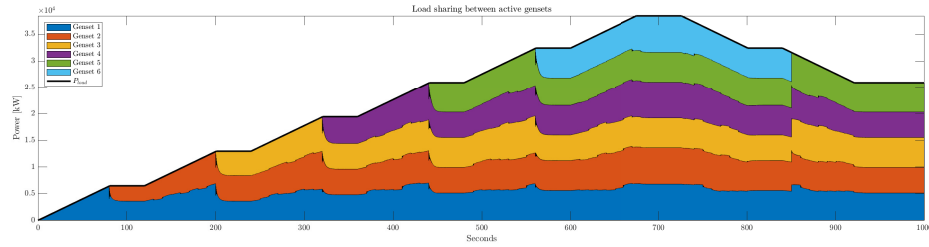

Figure 6.21: Load sharing between gensets when optimizing genset scheduling and load sharing using Optimization Objective 1 on a simulation model in the MVPPSS.

Optimization Objective 2

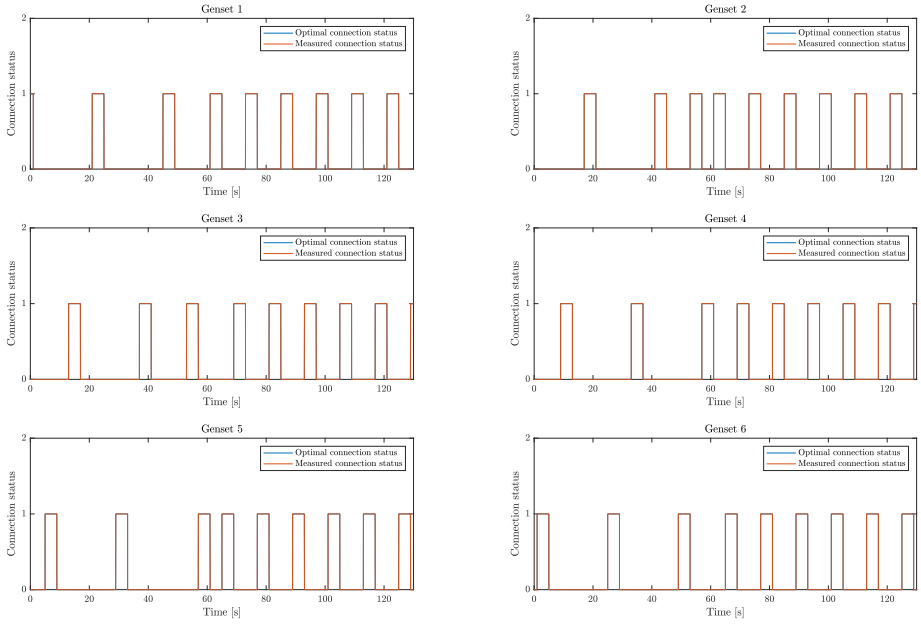

Figure 6.22: Connection status of gensets when optimizing genset scheduling and load sharing using Optimization Objective 2 on a simulation model in the MVPPSS.

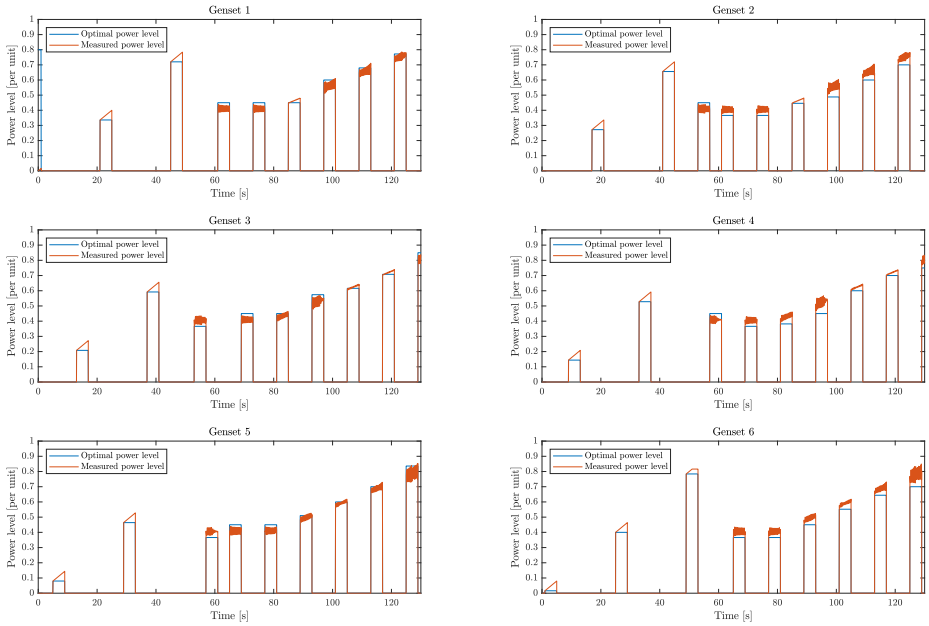

Figure 6.23: Active power delivered by gensets when optimizing genset scheduling and load sharing using Optimization Objective 2 on a simulation model in the MVPPSS.

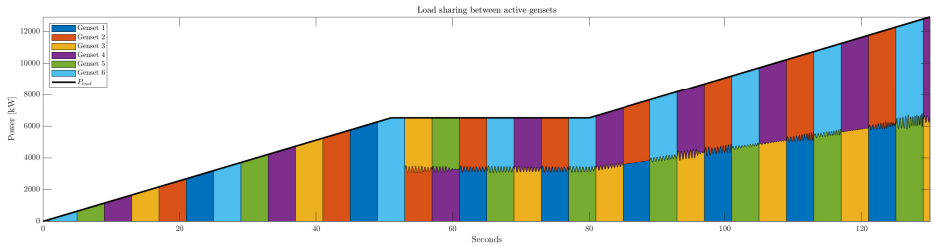

Figure 6.24: Load sharing between gensets when optimizing genset scheduling and load sharing using Optimization Objective 2 on a simulation model in the MVPPSS.

Optimization Objective 3

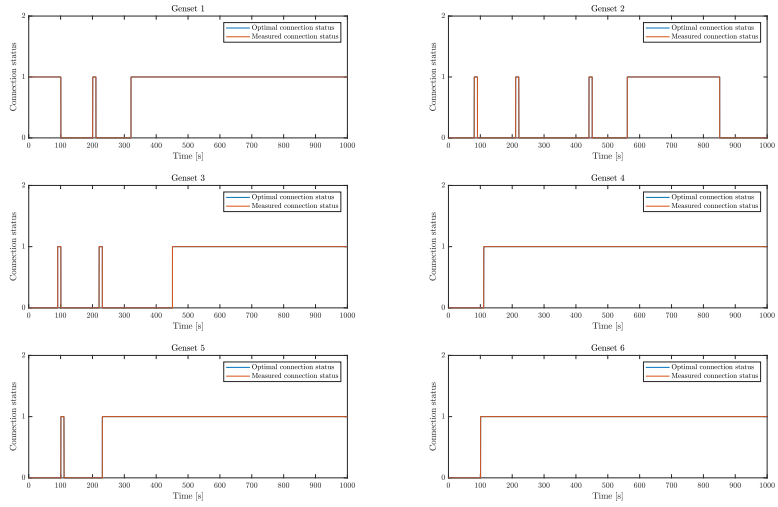

Figure 6.25: Connection status of gensets when optimizing genset scheduling and load sharing using Optimization Objective 3 on a simulation model in the MVPPSS.

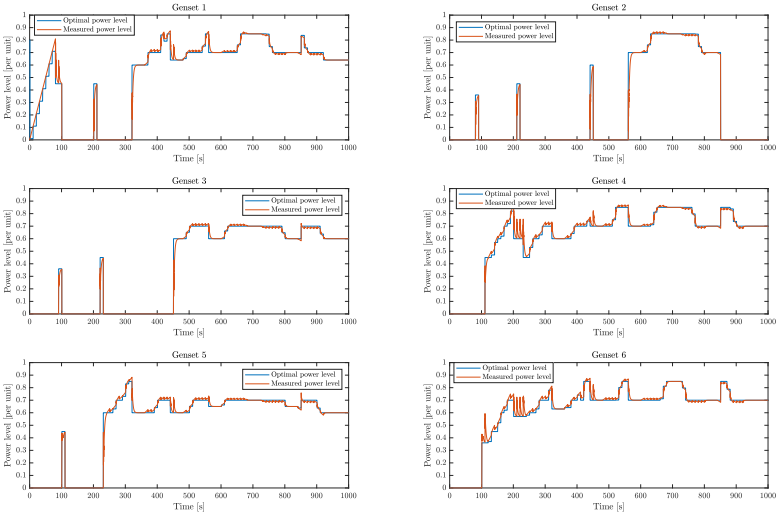

Figure 6.26: Active power delivered by gensets when optimizing genset scheduling and load sharing using Optimization Objective 3 on a simulation model in the MVPPSS.

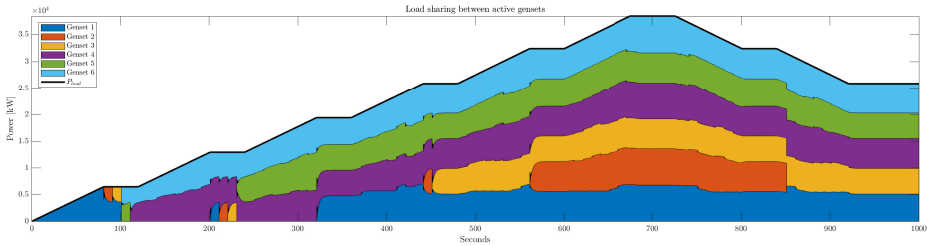

Figure 6.27: Load sharing between gensets when optimizing genset scheduling and load sharing using Optimization Objective 3 on a simulation model in the MVPPSS.

Optimization Objective 4

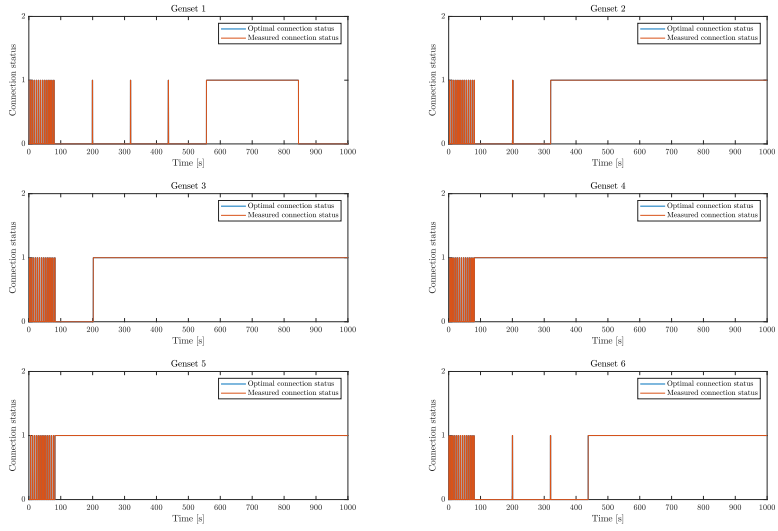

Figure 6.28: Connection status of gensets when optimizing genset scheduling and load sharing using Optimization Objective 4 on a simulation model in the MVPPSS.

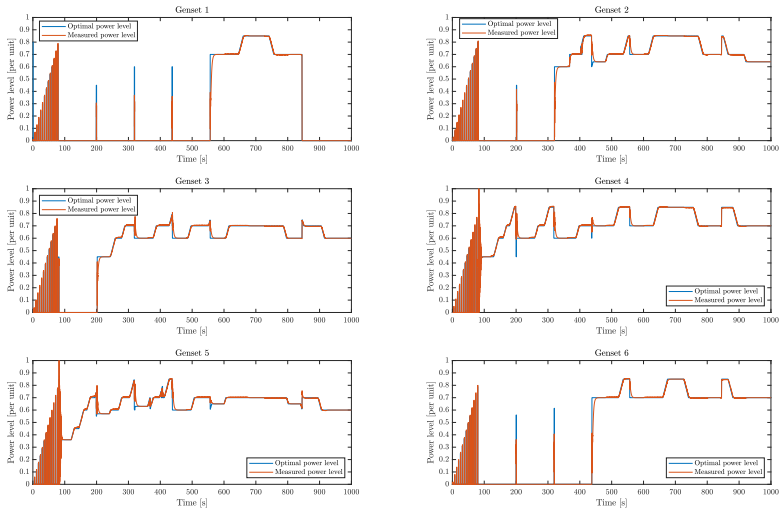

Figure 6.29: Active power delivered by gensets when optimizing genset scheduling and load sharing using Optimization Objective 4 on a simulation model in the MVPPSS.

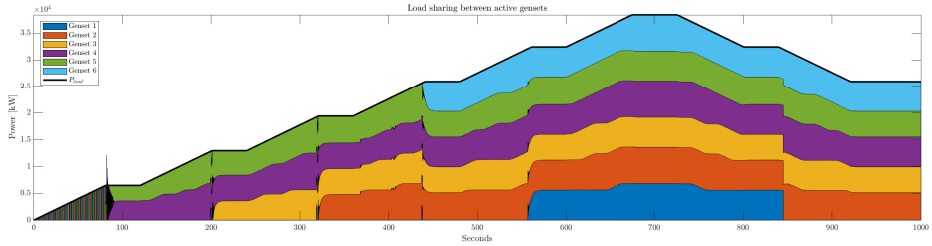

Figure 6.30: Load sharing between gensets when optimizing genset scheduling and load sharing using Optimization Objective 4 on a simulation model in the MVPPSS.

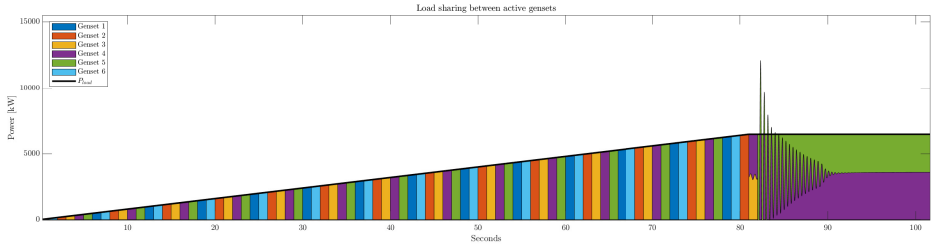

Figure 6.31: Detail image of load sharing between gensets when optimizing genset scheduling and load sharing using Optimization Objective 4 on a simulation model in the MVPPSS.

6.2.3 Discussion

Figures 6.19, 6.22, 6.25 and 6.28 show the plotted optimal connection status with the measured connection status for the marine power plant when using Optimization Objective 1, 2, 3 and 4, respectively. All figures show that the connection statuses of the gensets in the power plants perfectly follow the optimal connection statuses. Thus, the optimal scheduling setpoints of the power plant are successfully implemented in the simulation model, and the scheduling of gensets works as desired also within the simulation environment of the MVPPSS.

The optimal power level and measured power level for each genset when using Optimization Objective 1, 2, 3 and 4 are plotted in Figures 6.20, 6.23, 6.26 and 6.29, respectively. The measured power levels mostly follow the optimal power levels, though with some fluctuations and time delays, especially when gensets are ramped up. Due to the modeled engine dynamics, some transients occur together with load fluctuations, as would be expected in a simulation model. This is the case for all optimization objectives, though the measured power level of the gensets in the simulations using Optimization Objective 2 experience larger fluctuations than when using the other optimization objectives. This might be due to the frequent connections and disconnections of the gensets which happens for this optimization objective. The MVPPSS seems to have problems handling frequent connections and disconnections of gensets.

Figure 6.21 shows the load sharing between the active gensets when using Optimization Objective 1. The illustration confirms that the connections and disconnections of gensets happen according to when the load gets too big to be handled by the previous gensets, which happens right before each plateau in the load profile. The way the new gensets are connected when the load increases is as expected with the desired behavior of Optimization Objective 1, which simply chooses ”next genset on the list” when choosing which genset to connect, since all gensets have the same capacity. Had the gensets been of different capacity, using this optimization objective would to some degree lead to a favorization of connecting the gensets with the smallest capacity, as discussed in Section 4.1.

Figure 6.24 shows the load sharing between gensets when using Optimization Objective 2. The scheduling of the gensets is in accordance with the expected behavior of this optimization objective, as new gensets are connected each time the optimization is performed. The power levels of the gensets can be seen to fluctuate a bit when there are two gensets connected at the same time. This matches the results found in 6.23, which showed significant fluctuations in the active power level of the gensets.

In Figure 6.27, the load sharing between gensets when using Optimization Objective 3 is presented. The behavior of both scheduling and load sharing is in accordance with Optimization Objective 3, and follows from the discussion and reasoning in Section 6.1.3 regarding the optimization algorithm’s results for this optimization objective.

The load sharing between gensets when using Optimization Objective 4 can be seen in Figure 6.30. One can see that the scheduling in the start of the simulation is done accord-

ing to minimizing the running time of the gensets, as there are frequent connections and disconnections of gensets. After approximately 80 seconds, the optimization algorithm no longer connects and disconnects gensets with minimization of running time in mind, but rather with minimization of connections and disconnections. This can be explained by the same line of thought and reasoning as in Section 6.1.3, regarding the fact that $|d|$ grows large quick and hence other terms in the objective function from Equation 4.11 dominate. After the period where gensets are connected and disconnected every other optimization period, when Genset 4 and Genset 5 are connected, they both experience big fluctuations in the power level. This can be seen in Figure 6.31, and is probably an effect of the frequent connection and disconnection of gensets.

Some problems were encountered when optimization by using Optimization Objective 2 was performed. The simulation of an optimized power plant using the MILP optimization algorithm had troubles with implementing the optimal scheduling scheme in the MVPPSS. The simulator would shut down and give an error stating that the Simulink has reached its minimium step size and is unable to reduce step size further. By further investigating the variable outputs from the simulator, it was detected that when this error occured, the frequency of the gensets had been fluctuating with an increasing amplitude. This indicates unstability in the model. An investigation of the scheduling scheme provided from the MILP optimization algorithm was also done. The produced connection and disconnection plan created from the optimization of the power plant was tried to be fed in manually to the simulation model, i.e. without the use of online optimization during the simulation. The MILP algorithm was disconnected and the connections and disconnections schemes were sent in as step functions to the simulator. This resulted in the same error and shutdown of the simulation. This indicates that there are certain scheduling schemes not accepted by the MVPPSS. From the thorough investigation of this problem, there seems to be a problem for the MVPPSS when gensets are being connected and disconnected frequently. These problems are the reason why a different deterministic load profile was used when using Optimization Objective 2 compared to Optimization Objective 1, 3 and 4. The simulation model with the MILP optimization algorithm using Optimization Objective 2 would not complete the simulation using the load profile used for the other optimization objectives, even trying with several different execution periods of the optimization.

The robustness of the simulation model with implemented MILP optimization can be questioned, as its ability to run through a simulation without the mentioned error depends on the periodic execution of the optimization and chosen optimization objectives. The fact that the simulation model highly depends on the scheduling scheme, i.e. the connection and disconnection of the gensets, is a drawback to the simulation model including optimization. Especially, the frequent connections and disconnections seemed to provide trouble. This could be avoided by increasing the execution period of the optimization, i.e. performing the optimization less frequently. One drawback of doing this however, is the risk of the demanded load changing in between the optimizations, such that the demanded load becomes too high for the connected gensets, leading to a fault in the simulator.

Using a deterministic load profile is very advantageous when verifying the MILP op-

timization algorithm, due to the easy way of recognizing and validating desired results. Performing the simulations with a realistic load profile as well could serve as a stress test and robustness test of the simulation model. By letting the simulation model run with the MILP optimization as an optimization layer of the power plant for several hours could verify a robust optimization method of the simulation method. A realistic load profile is also meaningful to use when determining the performance of a power plant because of the resemblance with an actual marine operation and a realistic operation scenario.

For initialization of the simulation model, Genset 1 is always intitialized with as connected and an active power setpoint of 0.8 per unit. This can be seen in Figure 6.23, as the time horizon is short enough for it to be visible in the plots. However, this is the case for all simulations. This is done in order to ensure that the power plant has enough provided power when a new simulation is initialized.

Chapter 7

Case Study - Online Optimization and Optimal Design of Marine Power Plants Using MILP Optimization

In this chapter, a case study using the developed MILP optimization algorithm in a simulation environment, the MVPPSS, is conducted. The case study explores the optimization of the control of three marine power plants. The three different configurations are then evaluated with respect to chosen KPIs, and from this evaluation, the optimal design of the marine power plant is proposed. This demonstrates the ability of using the optimization for design purposes of marine power plants.

7.1 Problem Formulation and Marine Power Plant Configurations

This section describes in detail the set up of the different simulations performed.

The case study presented in this chapter is a study of three different marine power plant configurations, where each configuration is evaluated with respect to chosen KPIs. Each marine power system is simulated in a fixed configuration, where all gensets are connected throughout the whole time horizon of the simulation. Then, the three marine power systems are simulated in a non-fixed configuration, using the MILP optimization algorithm for connecting/disconnecting gensets and load sharing between gensets. The three power systems' performance are determined by using the chosen KPIs, and using these results

the optimal marine power plant configuration for this operation is proposed.

This case study demonstrates the ability of the MILP optimization algorithm to be used in the online optimization layer of a marine power plant during a marine operation. This feature is simulated by optimizing the operation of the power plant while feeding the power system with a realistic load profile, resembling how the EEMS would be fed with instantaneous power demands from power consumers aboard the ship during a real operation. In addition, using the MILP optimization as a design tool when designing a marine power plant is simulated by using the predetermined realistic load profile as power demands. A so called offline optimization, which optimizes the operation of a marine power plant with a predetermined or estimated load profile, is an important design tool for an optimal power plant configuration (Reddy et al., 2019). By using multiple probable load profiles of the vessel in combination with safety and reliability requirements for the power plant, an optimal power plant configuration can be obtained (Reddy et al., 2019). The simulations conducted in this case study actually resembles the method of using offline optimization for the design of a marine power plant, as the load profile is predetermined. The realistic load profile used for the simulations in this case study could be one of several likely load profiles used in a real offline optimization of a power plant. In addition to using several likely load profiles, some safety, reliability and performance requirements would also be included in a real design optimization.

The objective of this case study is to demonstrate the MILP optimization algorithm's ability of optimizing a marine power plant online and to be used as part of an offline optimization of the power plant configuration. The results of the case study can be used to further investigate features and developments of the optimization algorithm, as well as to make an informed decision of which of the proposed power plant configurations should be installed on a vessel with the given load profile.

7.1.1 Power Plant Configurations

The three different power plant configurations have different qualities and characteristics in terms of types of power sources, number of power producers and power capacity per power producer. However, the combined total capacity of all the gensets are the same for each configuration. The configurations are denoted $Power\ plant\ 1$, $Power\ plant\ 2$ and $Power\ plant\ 3$.

$Power\ plant\ 1$ consists of six gensets and one battery ESD, i.e. a hybrid electric marine power plant, connected to one bus. The gensets each have a base value capacity of 8000 kW. The battery is a Corvus Energy Storage System, a battery package of several Corvus Energy AT6500 Modules connected to the power plant, thought to have a total amount of energy of 2.6 MWh, with a capacity of 8 MW. See Appendix B.4. The battery is used in a simplified manner in this case study, in which the battery simply is put in "discharge mode", providing a constant delivered power of 8 MW throughout the whole simulation. See Appendix B.1 for an illustration of the simulation model in the MVPPSS.

$Power\ plant\ 2$ is a power plant configuration with three gensets connected to one bus. This is a configuration with few high-power gensets. Thus, each genset has a base value capacity of 16000 kW. The simulation model of the configuration can be seen in Appendix B.2.

$Power\ plant\ 3$ has twelve gensets connected to one bus. Each genset has a base value capacity of 3000 kW, meaning that this is a configuration with many low-power gensets. The configuration can be seen in Appendix B.3.

All configurations calculate the fuel consumption using the SFOC-curve presented in Figure 6.3.

7.1.2 Optimization Objectives

Using the developed MILP optimization algorithm as optimization of the marine power plant, there are several optimization objectives implemented in the algorithm that can be used, as shown in Chapter 4. Optimization Objective 1, minimizing online capacity of gensets, is the chosen optimization objective for the case study. The description of the optimization objectives, as well as the corresponding weights in the objective function of Equation 4.11, can be found in Table 6.1 and Table 6.2, respectively.

7.1.3 Load Profile

The load profile used in the case study should be a realistic load profile. Using a realistic load profile makes the results transferable to a real marine operation. The realistic load profile is based on the operation of a real vessel under construction. The vessel operates within the conditions shown in Table 7.1. The data have been provided by ABB.

Operating Conditions	Operating Code	Annualized Operation Time	Total Power Demand [kW]
Alongside, berthed	A	10 %	4695
Cargo Handling,Alongside	B	25 %	6335
Cargo Handling LitM	C	5 %	6788
Slow-Speed transit, 8 kts	D	7.5 %	11081
Slow-Speed transit, 10 kts	E	7.5 %	12534
Mid-Speed transit, 12 kts	F	10 %	14770
Mid-Speed RAS, 12 kts, 2 Tx stations	G	10 %	17219
Mid-Speed RAS, 12 kts, 4 Tx stations	H	10 %	17792
High-Speed RAS, 14 kts, 2 Tx stations	I	3.33 %	20557
High-Speed RAS, 14 kts, 4 Tx stations	J	3.33 %	21129
High-Speed transit, 18 kts	K	3.33 %	29083
Max speed, 20 kts	L	5 %	37668

Table 7.1: Operational conditions of the vessel of interest used for simulations of marine power plant cases.

It is assumed that the time scale of the operation is one week, or in other words 86400 seconds. There exists no information of the actual load profile of the vessel, other than the

different operating conditions and the annualized operation time. Therefore, a somewhat realistic load profile is made for the marine power plant by randomizing the load conditions from Table 7.1. Since the time scale of one week, or 86400 seconds, is a relatively long time horizon for simulation purposes, the time scale of the load profile is scaled down to use in simulations in the MVPPSS. Thus, the scaled down load profile has a duration of 4700 seconds. In addition, the load profile is made such that the change from one operating condition to another happens over the course of 10 seconds. This is done in order to avoid too rapid load fluctuations, which could be unacceptable for the simulation model in the MVPPSS and lead to the generators tripping. The scaled down load profile is presented in Figure 7.1.

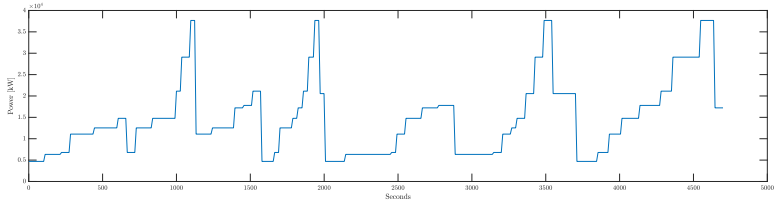

Figure 7.1: Load profile with scaled down time.

The realistic load profile presented in Figure 7.1 is used for simulations of all power plant configurations, i.e. $Power\ plant\ 1$, $Power\ plant\ 2$ and $Power\ plant\ 3$.

7.1.4 Key Performance Indicators

A marine power plant can be evaluated by several performance indicators that can be measured and optimized. Such performance indicators can be fuel consumption, total emission, total cost, running hours of engines, number of starts/stops or other characteristics. Given the implemented optimization objectives in the MILP optimization algorithm, the chosen KPIs for the case study are running hours of gensets, connections/disconnections of gensets and total fuel consumption, denoted d, S_{on}/S_{off} and FC, respectively. The KPIs will be presented for each of the three power plants, for both the fixed and the non-fixed configurations.

7.2 Simulations of Marine Power Plants in the MVPPSS

7.2.1 Power plant 1 - Fixed Configuration

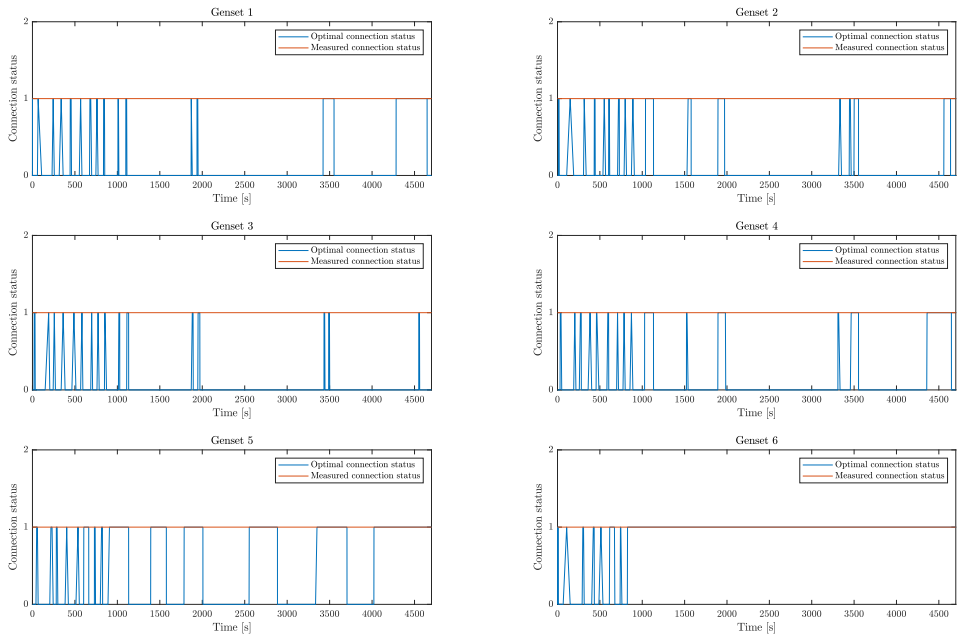

Figure 7.2: Connection status of gensets for $Power\ plant\ 1$ in fixed configuration.

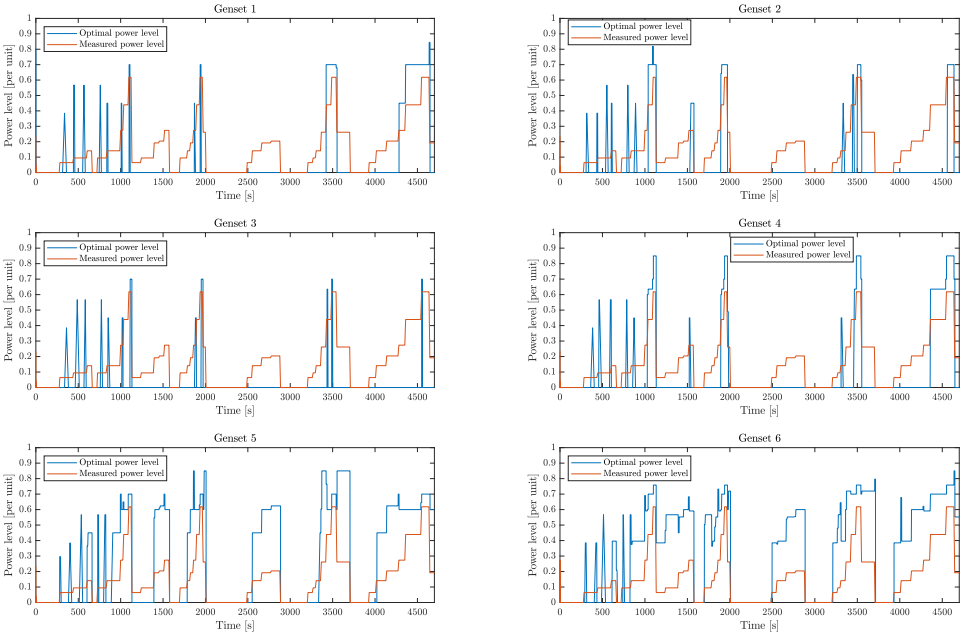

Figure 7.3: Power level of gensets for $Power\ plant\ 1$ in fixed configuration.

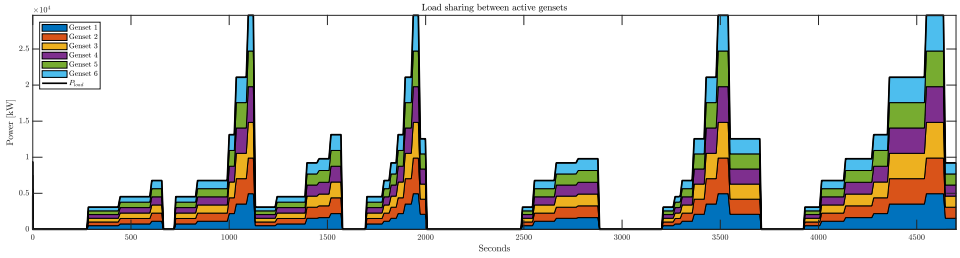

Figure 7.4: Load sharing between gensets for $Power\ plant\ 1$ in fixed configuration.

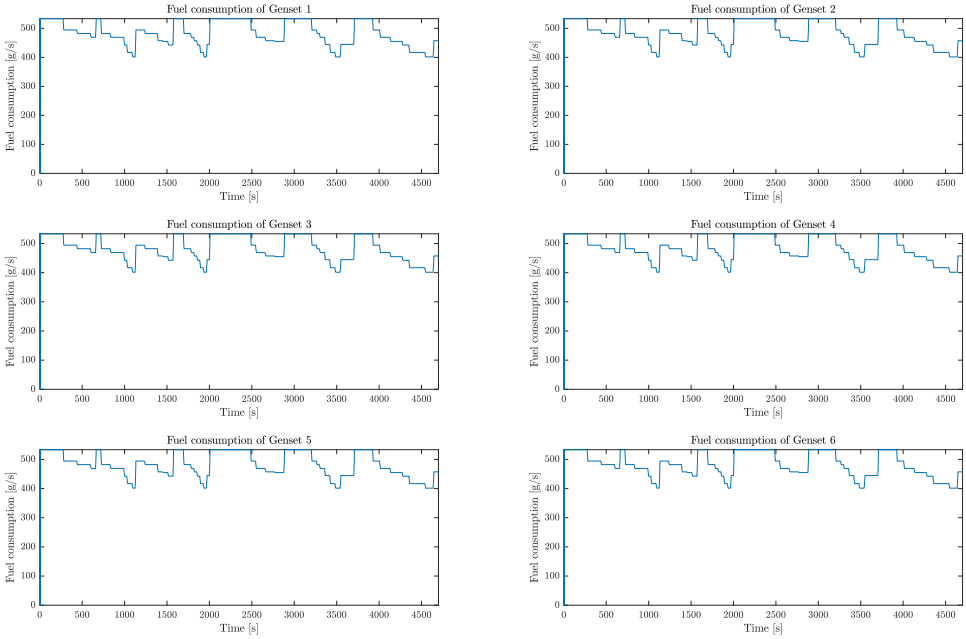

Figure 7.5: Fuel consumption of gensets for *Power plant* 1 in fixed configuration.

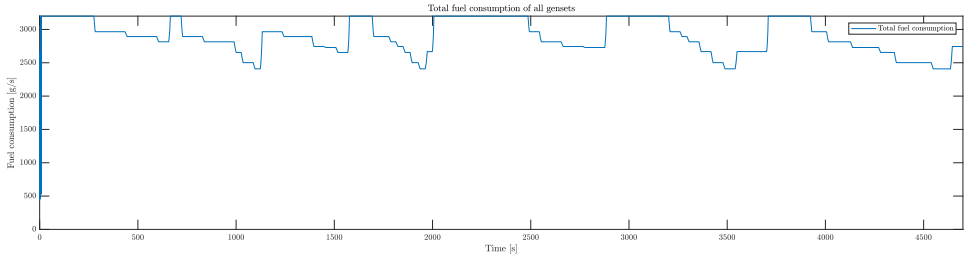

Figure 7.6: Total fuel consumption of gensets for *Power plant* 1 in fixed configuration.

7.2.2 Power plant 1 - Non-Fixed Configuration

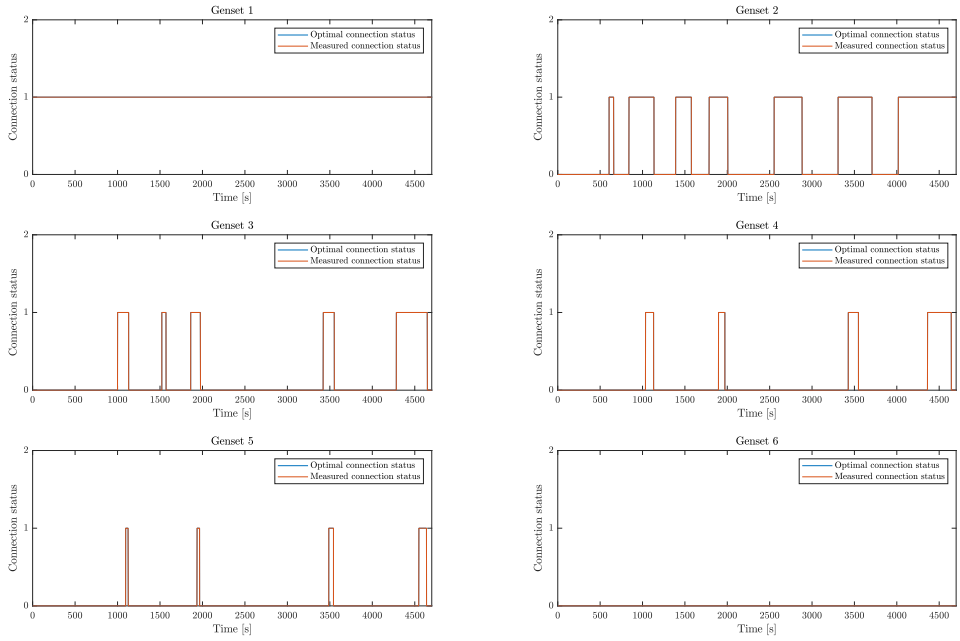

Figure 7.7: Connection status of gensets for $Power\ plant\ 1$ in non-fixed configuration.

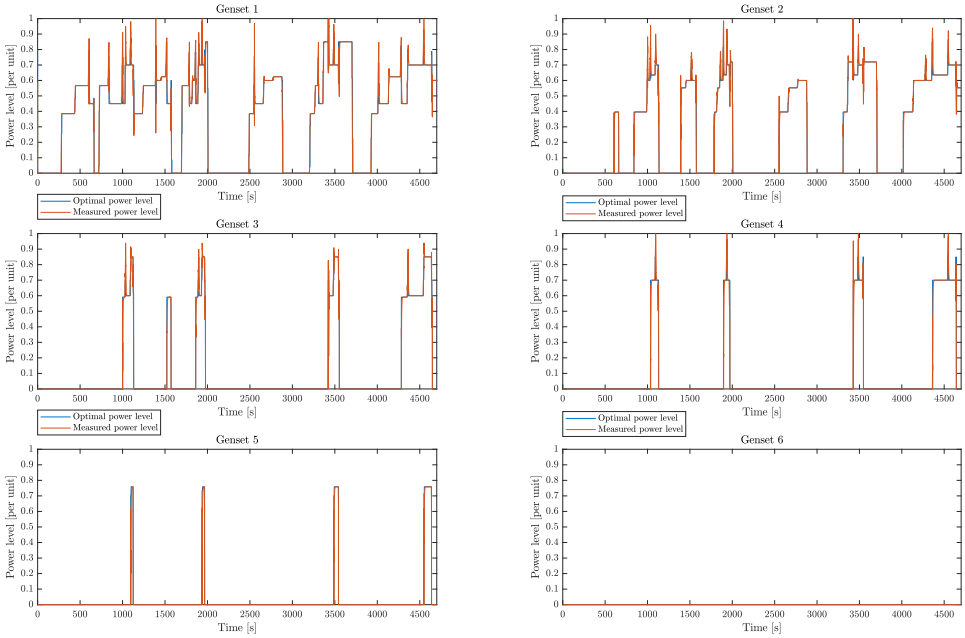

Figure 7.8: Power level of gensets for $Power\ plant\ 1$ in non-fixed configuration.

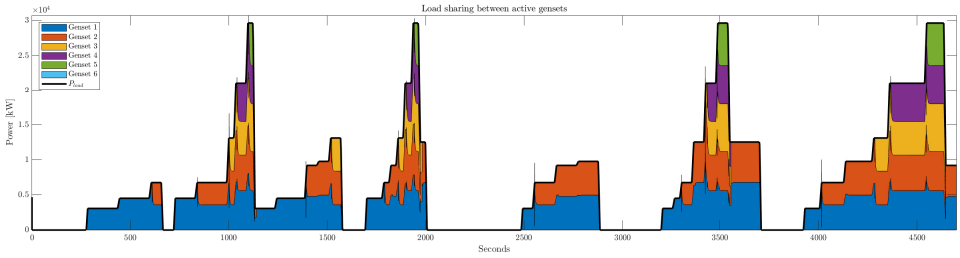

Figure 7.9: Load sharing between gensets for $Power\ plant\ 1$ in non-fixed configuration.

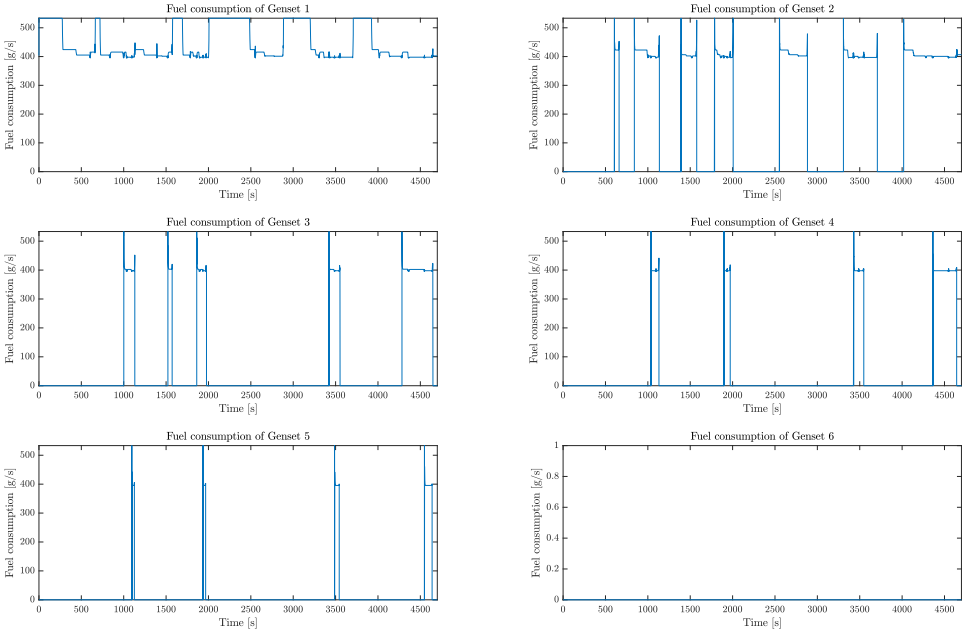

Figure 7.10: Fuel consumption of gensets for $Power\ plant\ 1$ in non-fixed configuration.

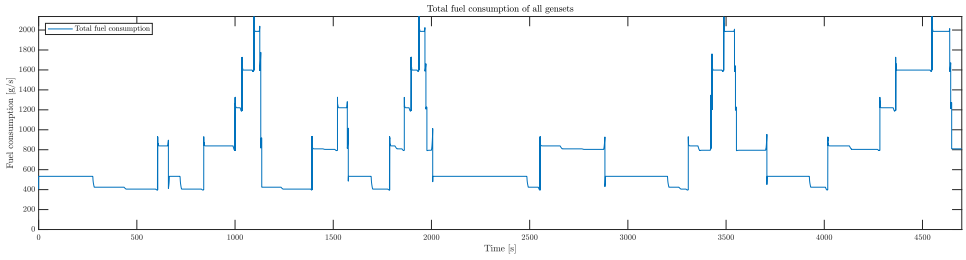

Figure 7.11: Total fuel consumption of gensets for $Power\ plant\ 1$ in non-fixed configuration.

7.2.3 Power plant 2 - Fixed Configuration

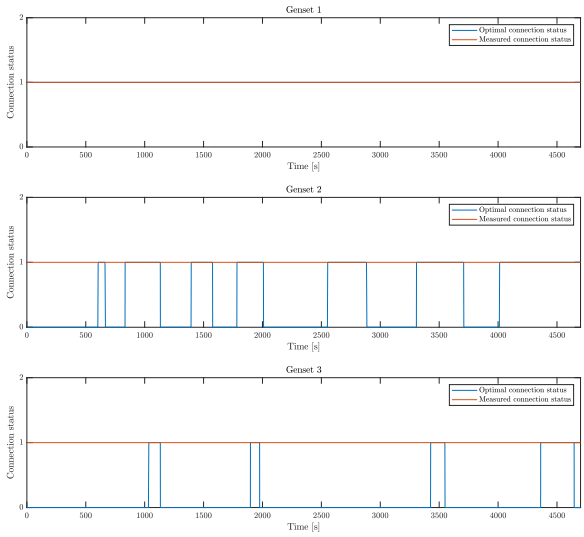

Figure 7.12: Connection status of gensets for $Power\ plant\ 2$ in fixed configuration.

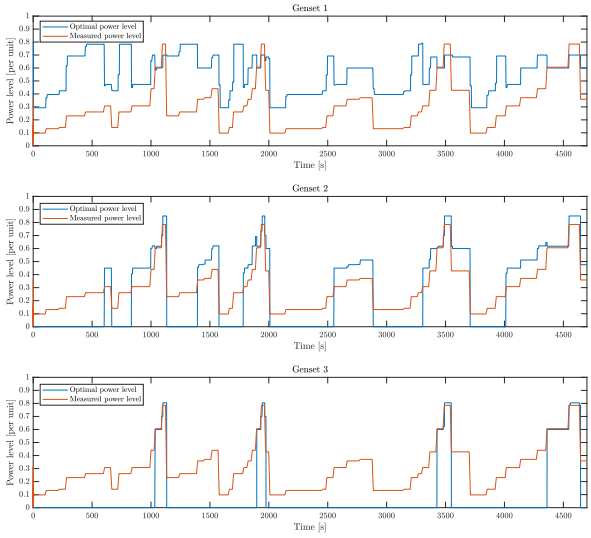

Figure 7.13: Power level of gensets for $Power\ plant\ 2$ in fixed configuration.

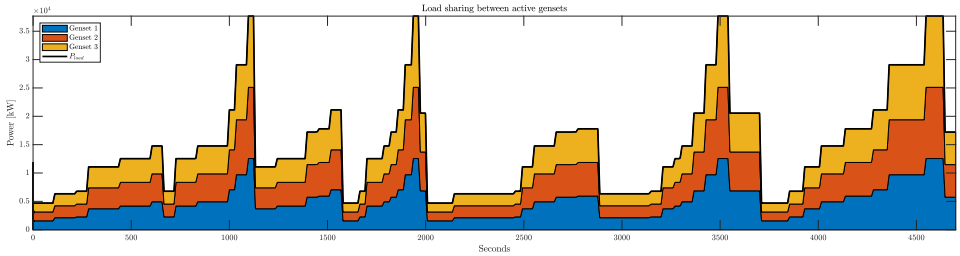

Figure 7.14: Load sharing between gensets for $Power\ plant\ 2$ in fixed configuration.

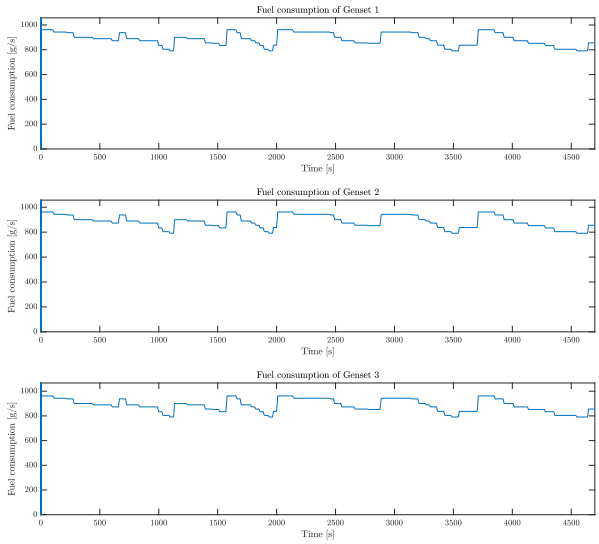

Figure 7.15: Fuel consumption of gensets for $Power\ plant\ 2$ in fixed configuration.

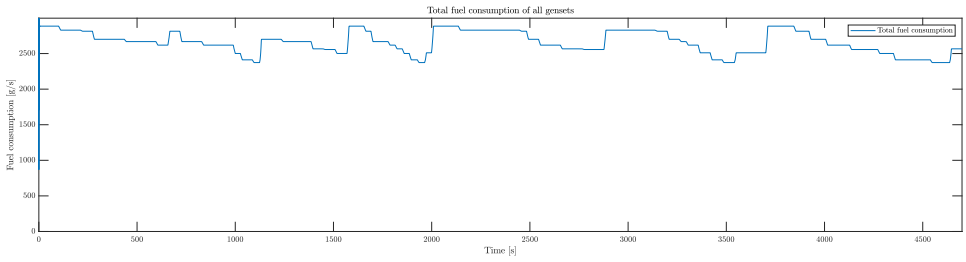

Figure 7.16: Total fuel consumption of gensets for $Power\ plant\ 2$ in fixed configuration.

7.2.4 Power plant 2 - Non-Fixed Configuration

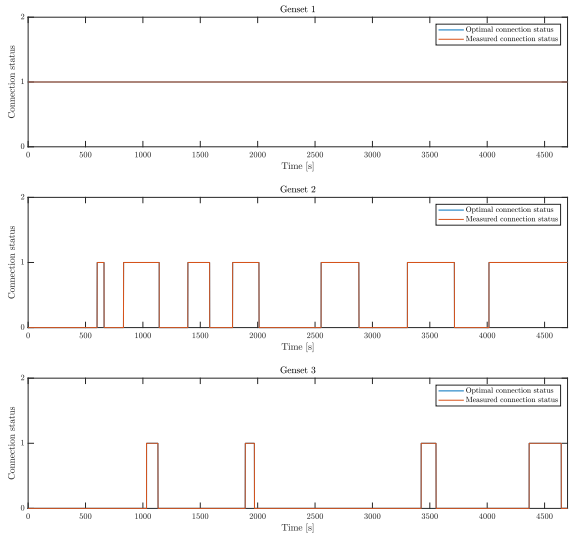

Figure 7.17: Connection status of gensets for *Power plant* 2 in non-fixed configuration.

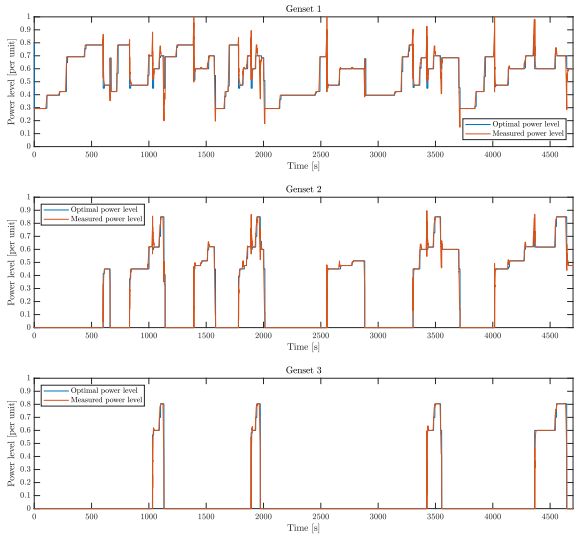

Figure 7.18: Power level of gensets for *Power plant* 2 in non-fixed configuration.

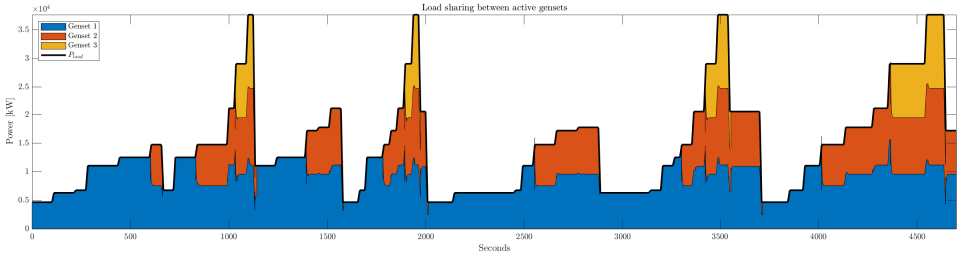

Figure 7.19: Load sharing between gensets for $Power\ plant\ 2$ in non-fixed configuration.

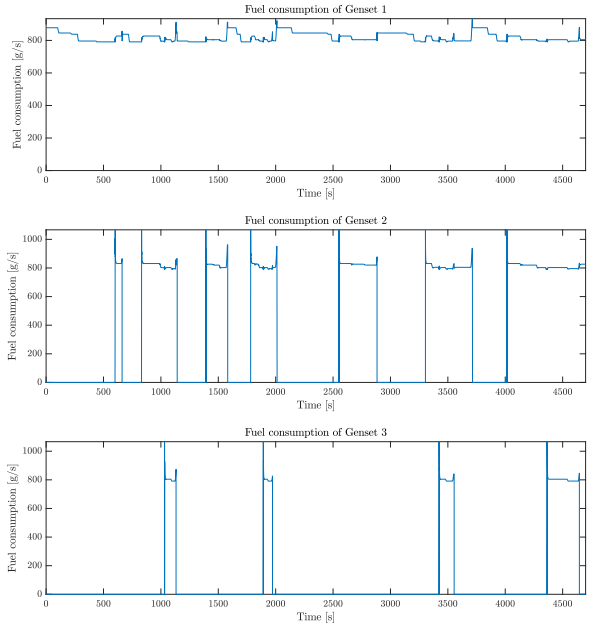

Figure 7.20: Fuel consumption of gensets for $Power\ plant\ 2$ in non-fixed configuration.

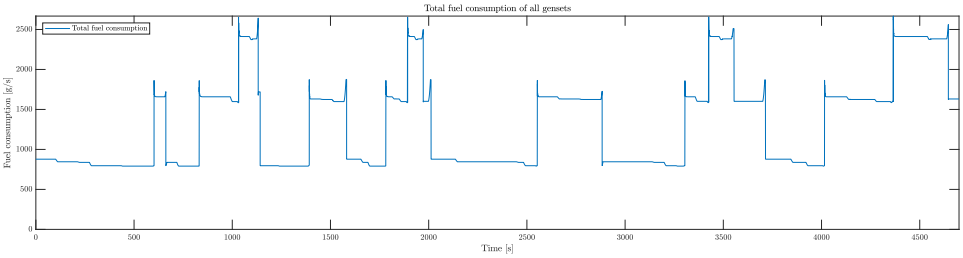

Figure 7.21: Total fuel consumption of gensets for *Power plant* 2 in non-fixed configuration.

7.2.5 Power plant 3 - Fixed Configuration

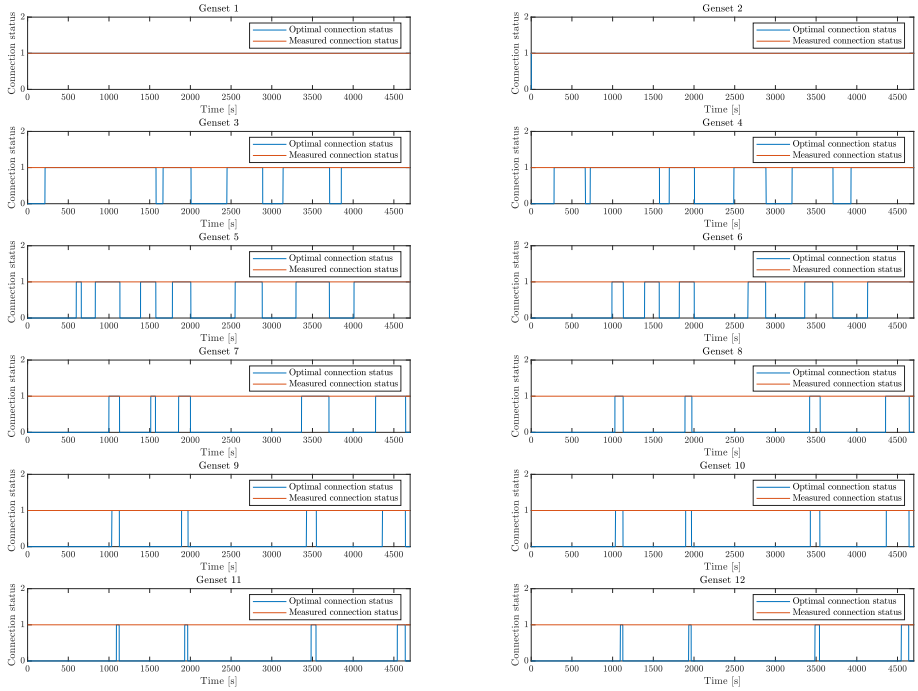

Figure 7.22: Connection status of gensets for *Power plant* 3 in fixed configuration.

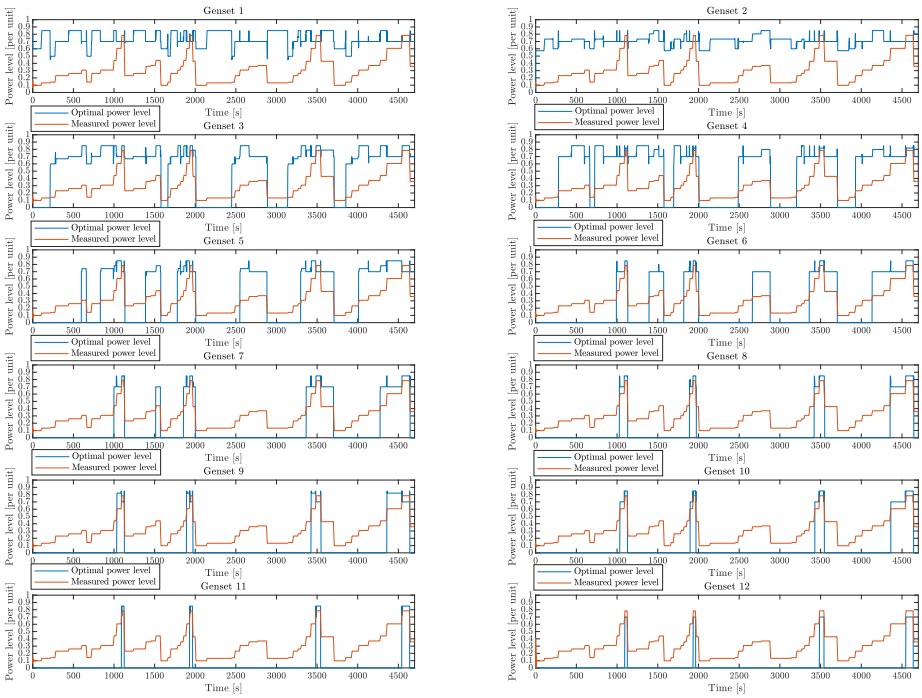

Figure 7.23: Power level of gensets for *Power plant* 3 in fixed configuration.

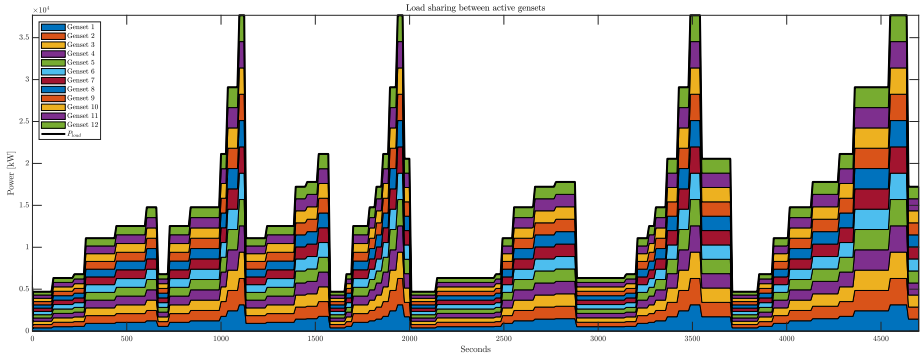

Figure 7.24: Load sharing between gensets for *Power plant* 3 in fixed configuration.

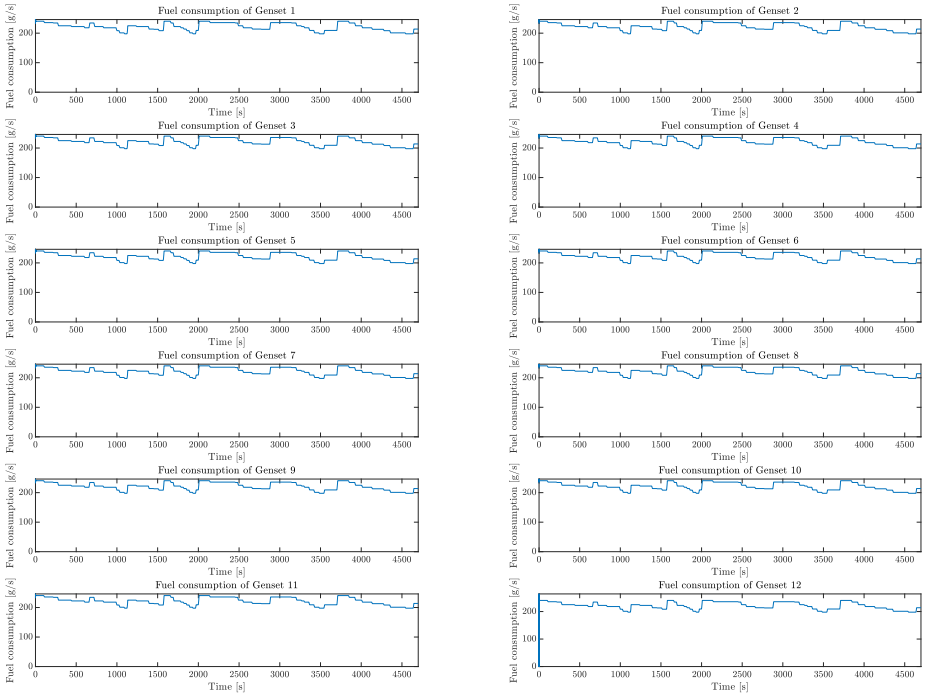

Figure 7.25: Fuel consumption of gensets for $Power\ plant\ 3$ in fixed configuration.

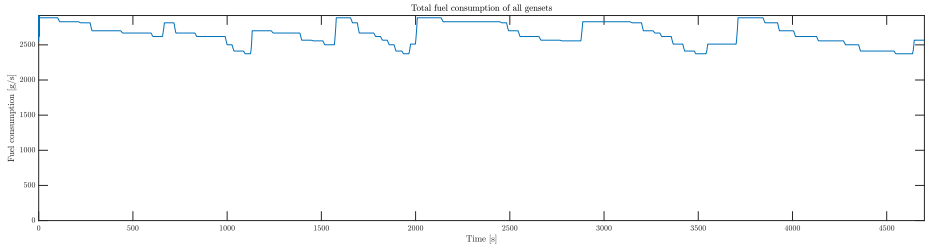

Figure 7.26: Total fuel consumption of gensets for $Power\ plant\ 3$ in fixed configuration.

7.2.6 Power plant 3 - Non-Fixed Configuration

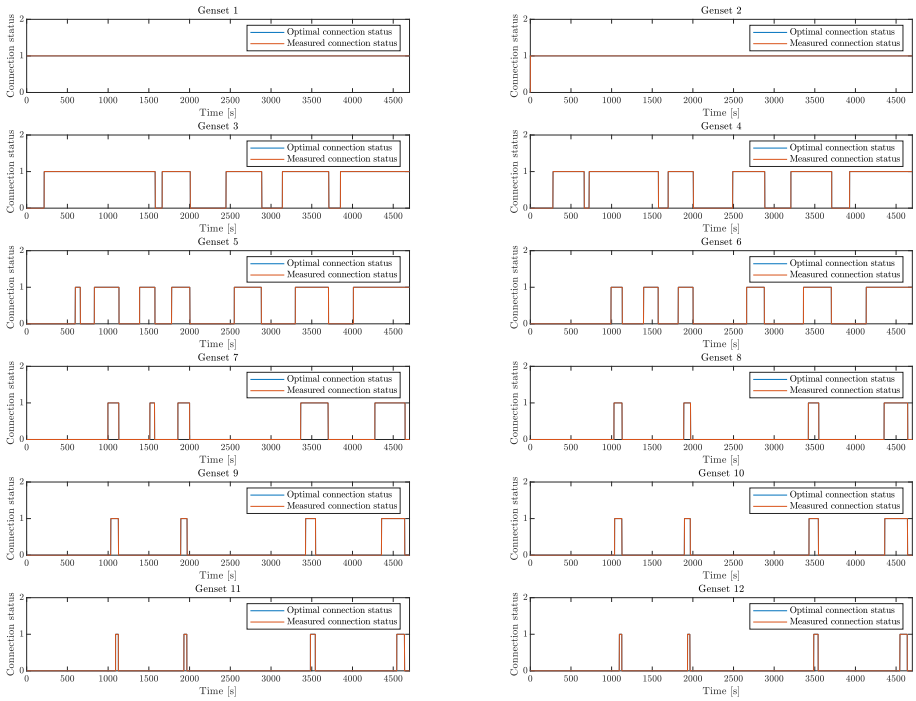

Figure 7.27: Connection status of gensets for *Power plant* 3 in non-fixed configuration.

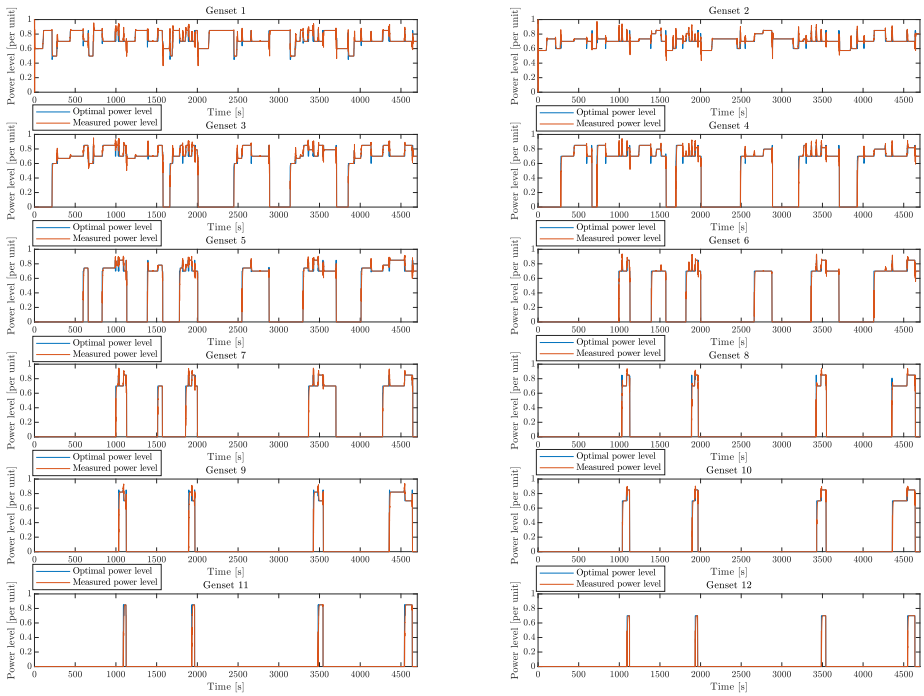

Figure 7.28: Power level of gensets for *Power plant* 3 in non-fixed configuration.

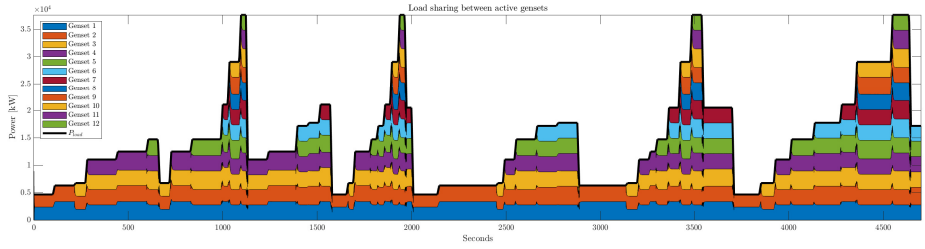

Figure 7.29: Load sharing between gensets for *Power plant* 3 in non-fixed configuration.

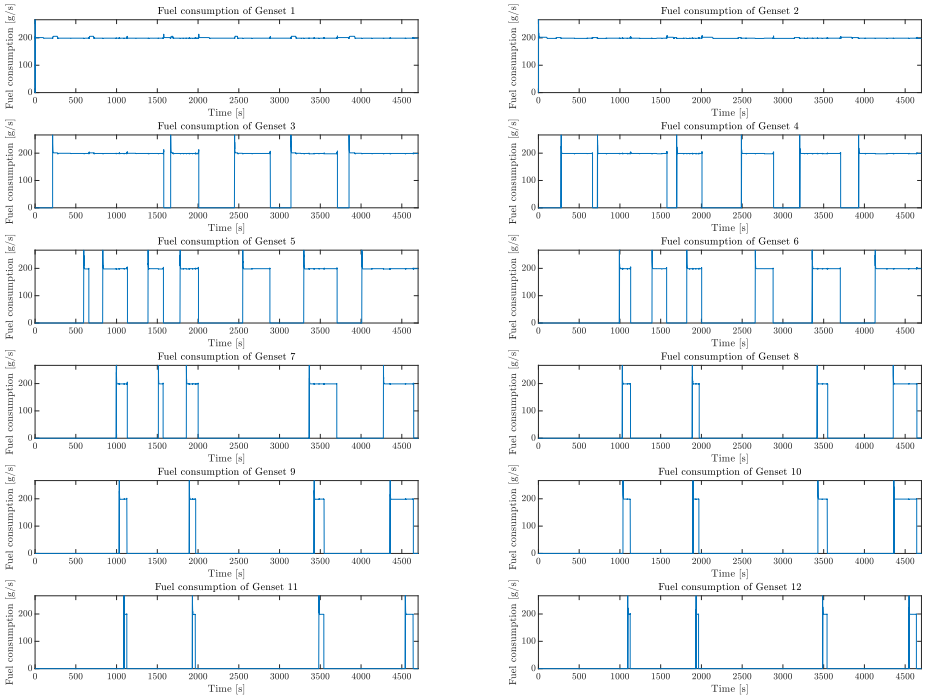

Figure 7.30: Fuel consumption of gensets for $Power\ plant$ 3 in non-fixed configuration.

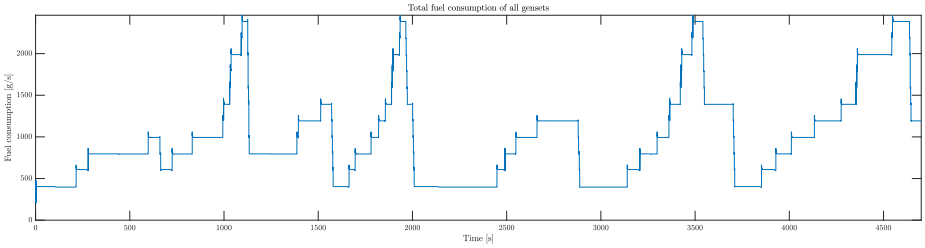

Figure 7.31: Total fuel consumption of gensets for $Power\ plant$ 3 in non-fixed configuration.

7.3 Comments, Evaluation and Discussion

7.3.1 Comments

The connection status of gensets in the power plants in fixed configuration can be seen in Figures 7.2, 7.12 and 7.22. One can see that all gensets are connected at all times, which shows that there is no difference in connection status for any genset throughout the simulation, and thus that the configuration of $Power\ plant\ 1$, $Power\ plant\ 2$ and $Power\ plant\ 3$ is fixed.

The measured power levels of the gensets in the power plants in fixed configuration, shown in Figures 7.3, 7.12 and 7.22, do not resemble the optimal power levels. This is in accordance with the power plant being set in a fixed position, where there is no active load sharing. Thus, the gensets all have the same droop curve, meaning they produce the same amount of active power. The fact that all gensets produce the same amount of active power when the power plants are in fixed configuration can also be seen in Figures 7.4, 7.14 and 7.24, where the load sharing between the active gensets are shown. The load share contribution from each genset all add up to the required active power load, P_{load}, which is a desired characteristic.

Load sharing between active gensets in $Power\ plant\ 1$, $Power\ plant\ 2$ and $Power\ plant\ 3$ in fixed configuration is shown in Figures 7.4, 7.14 and 7.24, respectively. The area plots depicting the amount of power delivered from each genset show that all gensets are connected at all times, and are equally sharing the required power load between each other. This makes the gensets often operate in very inefficient operating conditions, most often with a percentage of MCR much lower than its optimal operating point.

Figures 7.5, 7.15 and 7.25 show the fuel consumption of gensets in $Power\ plant\ 1$, $Power\ plant\ 2$ and $Power\ plant\ 3$, respectively, in fixed configuration. The figures show that the fuel consumption is the same for all gensets, due to the power plants' fixed configuration. This is as expected.

The total fuel consumption of all gensets in $Power\ plant\ 1$, $Power\ plant\ 2$ and $Power\ plant\ 3$ operating in fixed condition can be seen in Figures 7.6, 7.16 and 7.26, respectively. The total fuel consumption is found by superpositioning the fuel consumption of each genset.

Figures 7.7, 7.17 and 7.27 show the measured connection status plotted against the optimal connection status of all gensets in $Power\ plant\ 1$, $Power\ plant\ 2$ and $Power\ plant\ 3$, respectively, in non-fixed configuration. One can see that the measured connection status of the gensets in all power plants follow the optimal setpoint of the connection status perfectly, indicating that the simulation model correctly connects and disconnects gensets according to the MILP optimization algorithm's output.

The measured power level is plotted against the optimal power level of each genset in $Power\ plant\ 1$, $Power\ plant\ 2$ and $Power\ plant\ 3$ in non-fixed configuration. See Fig-

ures 7.8, 7.18 and 7.28 respectively. These plots show that the gensets provide the desired optimal power and that the measured power level curve follows the optimal power level curve, though with some fluctuations and delays. This happens because of the dynamics in the modeled gensets, and is expected behavior of a simulation model like the one used in this case study.

Figures 7.9, 7.19 and 7.29 show the load sharing between the active gensets in $Power\ plant\ 1$, $Power\ plant\ 2$ and $Power\ plant\ 3$, respectively, in non-fixed configuration. As one can see in the figures, not all gensets provide active power to the main bus. This is due to the optimal scheduling and load sharing which is calculated by the MILP optimization algorithm, and ensures that only the necessary gensets for the given load are connected. The figures depicting the load sharing between the active gensets are in accordance with Figures 7.7, 7.17 and 7.27 and Figures 7.8, 7.18 and 7.28 in terms of the gensets' connection statuses and power levels.

Fuel consumption for each genset in $Power\ plant\ 1$, $Power\ plant\ 2$ and $Power\ plant\ 3$ in non-fixed configuration are presented in Figures 7.10, 7.20 and 7.30, respectively. Studying the corresponding connection status plots, i.e. Figures 7.7, 7.17 and 7.27, and power level plots, i.e. 7.8, 7.18 and 7.28, one can conclude that the fuel consumption curves correlate with the connection status and power levels of each genset. By correlation, it is meant that the fuel consumption curves develop according to the connection status of the gensets, i.e. when connection status is disconnected, then the fuel consumption is zero, and according to the power level of the gensets, i.e. fuel consumption decreases when a genset is operated near its optimal MCR. Elaboration follows in the next paragraph.

Figure 7.10 shows the fuel consumption for each genset in $Power\ plant\ 1$ in non-fixed configuration. As expected, $Genset\ 6$ has zero fuel consumption, as it is disconnected (seen from Figure 7.7) and provides zero active power. The remaining gensets consume fuel as expected when comparing Figure 7.10 with Figures 7.7 and 7.8, both in terms of when gensets are switched on and off and when power levels increase or decrease, provided that a known minimum fuel consumption occurs around 0.8 MCR. One example of this can be seen for $Genset\ 2$ which at approximately 2500 s is connected and providing a power level of about 0.4, before its provided power level increases to around 0.6. The response of this in Figure 7.10 can be seen as a sudden increase in fuel connsumption for $Genset\ 2$ when the genset is turned on and operated at a power level of 0.4, before it decreases little by little when the power level increases to around 0.6, implying that the genset is being operated closer to its optimal level of MCR.

The total fuel consumption of the gensets in $Power\ plant\ 1$, $Power\ plant\ 2$ and $Power\ plant\ 3$ in non-fixed configuration is seen in Figures 7.11, 7.21 and 7.31. Again, the total fuel consumption for each power plant is found by superpositioning the fuel consumption of each genset.

$Power\ plant\ 1$ is a hybrid electric marine power plant with a battery ESD. The battery

is implemented in the simulation model in a way where the power contribution from the battery simply reduces the required active power load, P_{load}, accordingly to the delivered power from the battery. This can be seen as a reduction in the load profile of the simulation. Figures 7.4 and 7.9 show a reduced P_{load} which sometimes is close to zero (1 kW) for both the fixed and non-fixed configuration of $Power\ plant\ 1$. P_{load} is close to zero because of a simplification in the battery power contribution which sets P_{load} to 1 kW if the demanded load from the load profile is less than the contribution of supplied power from the battery. Had this feature not been implemented, the required load would become negative, making the optimization problem infeasible. For $Power\ plant\ 1$ in non-fixed configuration, when the required load is close to zero, $Genset\ 1$ is kept connected, but providing power according to 1 kW. Thus, $Genset\ 1$ consumes fuel according to 1 kW load demand, which is approximately at 0.01 % MCR, which is a very inefficient operating point for the gensets. Hence, the fuel consumption of $Genset\ 1$ is high in the periods where P_{load} is close to zero, as can be seen in Figure 7.10. The total fuel consumption, shown in Figure 7.11, is not very high in these periods compared to other periods of the operation, however considering that only one genset is connected and that the demanded power is low, the fuel consumption is considered high. This has room for improvement and will be addressed further in Section 7.3.3.

7.3.2 Evaluation

The results from the simulations of the different marine power plants are evaluated by the KPIs described in Section 7.1.4. In Table 7.2, the measured KPIs for each power plant and configuration are shown.

Power plant configuration	Power plant 1		Power plant 2		Power plant 3	
	Fixed	Non-fixed	Fixed	Non-fixed	Fixed	Non-fixed
Running time of gensets [s]	28200	8433	14100	7509	56400	23227
Connections	6	21	3	12	12	51
Disconnections	0	19	0	10	0	45
Total fuel consumption [kg]	$1.3581 \cdot 10^4$	$3.6095 \cdot 10^3$	$1.2490 \cdot 10^4$	$6.1327 \cdot 10^3$	$1.2490 \cdot 10^4$	$4.6261 \cdot 10^3$

Table 7.2: Performance of marine power plant configurations measured by chosen KPIs.

The KPIs are measured or calculated during the simulations of the marine power plants. The running time of the gensets represents the total combined time that all gensets are connected. For example, a genset connected the whole time of the simulation will have a contribution of 4700 s. The connections and disconnections variables are incremented each time a genset is connected or disconnected and thus count the total amount of connections and disconnections of all gensets. The total fuel consumption for each power plant is calculated by integrating the total fuel consumption curve of the respective power plant configuration, shown in Figures 7.6, 7.11, 7.16, 7.21, 7.26 and 7.31, over the time horizon of the simulation.

From Table 7.2, one can see that each marine power plant in its non-fixed configuration has less total fuel consumption compared to its fixed configuration counterpart. This shows that optimizing the power plant using the MILP optimization algorithm indeed leads to a reduction in fuel consumption using this simulation model. The power plant configuration with the lowest fuel consumption is $Power\ plant\ 1$ with a total fuel consumption of $4.6095 \cdot 10^3$ kgs, when optimized with the MILP optimization algorithm.

The running time of gensets for the different configurations presented in Table 7.2 shows that the running time generally increases with the number of gensets in the power plant. This is as expected, as the inclusion of more gensets in the marine power plants mean that more gensets will be connected at the same times, introducing a multiplication of the running hours. The increase in running time with the increase in number of gensets applies to both the fixed and the non-fixed configurations of the marine power plants.

Considering the connections and disconnections of gensets for each power plant, one can see from Table 7.2 that the connections for the fixed configurations of the power plants coincide with the number of gensets. The disconnections for the fixed configurations are all zero, as expected, as the gensets only are connected once and stay connected the entire simulation. For the non-fixed configurations, the connections and disconnections generally increase with the number of gensets in the power plants, which is as expected.

Considering all KPIs, $Power\ plant\ 1$ is the power plant configuration that shows the most promising measurements. It has a total fuel consumption of 3.6095 tonnes, 1.0166 tonnes less than the second lowest total fuel consumption, which is achieved by $Power\ plant\ 3$. $Power\ plant\ 1$'s running time of gensets is also short, second shortest of all, with a total of 8433 seconds, only 924 seconds longer than the shortest running time of gensets of 7509 seconds, achieved by $Power\ plant\ 2$. The number of connections and disconnections of $Power\ plant\ 1$ are the second lowest among the three non-fixed, i.e. optimized, configurations. $Power\ plant\ 3$ has a total of 96 connections and disconnections, whereas $Power\ plant\ 1$ has a total of 40 connections and disconnections. $Power\ plant\ 2$ only has 22 connections and disconnections throughout the time horizon of the simulation. From these KPIs follows that a natural choice of configuration of a marine power plant with a probable realistic load profile as shown in Figure 7.1 and Optimization Objective 1 shown in Table 6.3 would be $Power\ plant\ 1$. Thus, by using the MILP optimization algorithm in an offline optimization of three different power plant configurations, $Power\ plant\ 1$ is proposed as the optimal design of a marine power plant with a realistic load profile as seen in Figure 7.1 when the desired optimization behavior is according to Optimization Objective 1.

The load profile used for the simulations of the marine power plants has been fed to the simulation model, and its values have been read at instantaneous points in time, during the time horizon of the simulation. In a real operation of a marine power plant, the loads would be fed to the EEMS in a similar manner, only from calculations of demanded load from the power system itself. By implementing the optimization algorithm in the EEMS of a marine power plant and using it as an optimization layer of the power system, the process

of getting demanded load, finding the optimal genset scheduling and sending setpoints to the generators will resemble the process in these simulations of optimizing marine power plants. Thus, one can conclude that an online optimization method of marine power plants has been developed using the MILP optimization algorithm in the simulation environment of the MVPPSS.

As a side note, comparing $Power\ plant\ 2$ with $Power\ plant\ 3$, shows that $Power\ plant\ 3$ has a lower fuel consumption than $Power\ plant\ 2$, when both are optimized, and everything else than the sizing and number of gensets is the same. This finding is in accordance with the findings of Wu (2017), who found that a marine power plant configuration with more but smaller gensets outperformed a marine power plant configuration with less but bigger gensets with respect to the fuel consumption.

7.3.3 Discussion

The results from the simulations presented in Table 7.2 represent the performance of each power plant configuration, using the chosen KPIs. The fuel consumption is of course of great interest when a marine power plant is designed, due to the costs related to this post. However, the other KPIs such as running time and connections/disconnections also represent an important aspect when evaluating the performance of a power plant. These KPIs directly affect the wear and tear of the equipment, which can lead to great expenses for the ship owner. The proposed marine power plant, $Power\ plant\ 1$, is the power plant with the most promising performance using the defined KPIs. This is a simplified evaluation of an optimal power plant, which in itself could be its own master's thesis. For example, finding an optimal marine power plant regarding the power plant's economic performance was done by Simonsen (2019). It is also important to emphasize that the proposed optimal marine power plant depends highly on the chosen optimization objective in the MILP optimization algorithm. As described in Section 6.2.1, the optimization can be performed using four different optimization objectives. While this case study performed the optimization using Optimization Objective 1, using other optimization objectives could lead to a different result. In addition, the performance indicators could be of different importance for different operations or different vessels, where in one case the fuel consumption must be considered the most, while another case might have strict requirements for the running time of gensets. Thus, the optimization objective should be chosen carefully with respect to the wanted behavior and characteristics of the power plant.

Using offline optimization to choose an optimal design of a marine power plant should include using several probable load profiles together with the performance and safety requirements for the power plant (Reddy et al., 2019). Such requirements could be a minimum number of gensets or a minimum total capacity etc. The load profile used in this case study is realistic in the way that the operating conditions are probable and taken from a real marine operation, but the combination of these could be more realistic. The load profile could be altered to not include such big load fluctuations over short amounts of time, in addition to including some white noise or other high frequent fluctuations for a more probable load variation.

Other improvements in the case study would be to tweak the MILP optimization algorithm in a way which makes the optimization problem for when P_{load} is equal to zero feasible. By doing this, one could set the required load equal to zero instead of 1 kW when the battery contributes with more delivered power than is required. This would mean that the marine power plant could operate in all electric operation and even greater fuel savings could be introduced for $Power\ plant\ 1$ since there would be no need to run a genset in an inefficient operating point. Another way to bypass this problem would be to include the battery in the MILP optimization algorithm. By including an ESD in the MILP optimization, the presence of the battery could be utilized in a much better way than it is now, and different usage strategies of the battery could be used, depending on what is the wanted characteristics of the power plant configuration. This is considered as the most promising addition to the MILP optimization algorithm regarding further fuel consumption reductions and reduction of wear and tear on the equipment. Including a battery in the simulation model could easily be done by using the already established battery model in the MVPPSS, which makes it possible to implement different usage strategies of the battery. Thus, the only thing needed for including a battery in the optimization is code written for the usage strategy of the battery, and the inclusion of a battery in the MILP optimization algorithm. This could be done following the method of (Skjong et al., 2017).

The estimation of fuel consumption could be made more accurate and realistic, as its current implementation does not take transients and dynamics into account, e.g. costs of starting and stopping a genset or revving the engine up to another operating level. Due to this simplified estimation of fuel consumption, which only uses SFOC-curves as a lookup table, the fuel consumption of $Power\ plant\ 2$ and $Power\ plant\ 3$ are exactly the same, since all other parameters are equal, including the SFOC-curves of the engines. The fuel consumption of $Power\ plant\ 1$ would also have been the same, had it not been for the load reduction introduced by the presence of the battery ESD. Since the same SFOC curves are used for engines of different capacity, this could be a source of error in calculation of the total fuel consumption for different power plant configurations. For a real case with different engine sizes and numbers of engines, the SFOC curves would most likely not be the same.

An interesting addition to the MILP optimization algorithm would be to use online values of fuel consumption instead of using predetermined SFOC-curves for the optimization. Exact measurements of fuel consumption could constantly be updating the data on which the optimization should be performed, thus improving the optimal load sharing of the connected gensets. This could further be explored by using machine learning to make a ”smart” optimization layer to recognize and decide the most optimal operating point of each genset.

There are also other optimization algorithms that could be better suited for an offline optimization used for finding the optimal design of a power plant. This could for instance be a genetic algorithm, dynamic programming or particle swarm optimization (PSO).

Chapter 8

Conclusions and Recommendations for Further Work

8.1 Conclusions

This thesis has explored the wide field of optimization of marine power plants. Many methods are applicable for the purpose of operating a marine power plant in a more optimal manner, and this thesis has contributed to exploring the possibility of using MILP as an optimization method of a marine power plant. MILP is especially well fitted for unit commitment and scheduling problems, which makes it highly applicable for genset scheduling and load sharing in a marine power plant.

A formulation of the optimization problem corresponding to genset scheduling and load sharing has been made and implemented in Matlab. The MILP formulation used in this thesis is based on the method presented by Thorat and Skjetne (2018). This resulted in the proposed MILP optimization algorithm, which optimizes the scheduling of the gensets in a marine power plant with respect to either minimizing online capacity, minimizing running time of gensets, minimizing the connections/disconnections of gensets or a weighted combination of all of these. The MILP optimization algorithm also optimized the load sharing between the active gensets, such that fuel consumption is minimized. The MILP optimization algorithm has through verification proven capable of controlling a simplified marine power plant with satisfactory and expected results according to the optimization objectives.

A simulation model of a marine power plant has been established in the MVPPSS. Using the MVPPSS as a simulation environment, the MILP optimization algorithm has been implemented in the simulation model. This provides the possibility of performing realistic simulations of the optimization of a marine power plant. The calculated optimal scheduling scheme of gensets is used as a setpoint to the control of connection status for

the gensets. The power level of each genset is controlled by using the calculated optimal active power level as setpoint to the droop based speed governor, where the control input is the no-load frequency. Based on the droop equation, a guidance function for mapping the active power setpoints to the commanded no-load frequency has been included for the purpose of power control. A verification of the implemented MILP algorithm in the MVPPSS environment has been conducted, and showed that the simulation model is possible to control using optimal setpoints from the optimization algorithm. Optimizing the power plant using the optimization objective of minimizing the running time of gensets was challenging, and required alterations of the experimental setup in order to simulate properly. Most likely, the simulation model reacts like this due to frequent connections/disconnections of gensets. Simulation models using the other optimization objectives worked satisfactorily.

A case study has been conducted, comparing the performance of three different configurations of marine power plants. Using the MILP optimization algorithm for control of the power plants, compared to running the power plants in fixed configuration, i.e. all gensets connected, showed that the fuel consumption was significantly reduced for all power plants. $Power\ plant\ 1$ showed the best performance through simulations and was proposed as the optimal design for the given vessel and operation. This power plant was a hybrid power plant, consisting of six gensets and a battery ESD. The case study demonstrated how the optimization can be used for optimal design purposes when projecting and designing a marine power plant.

8.2 Recommendations for Further Work

- While there are several features that can be further developed in the MILP optimization algorithm, such as including a redundancy margin (Thorat and Skjetne, 2018) or the use of variable speed gensets (Skjong et al., 2017), the most natural extension to the algorithm would be the possibility to include ESDs, such as batteries, in the MILP optimization algorithm. This has a big potential to further reducing fuel consumption and introduce the possibility to use different battery usage strategies. This means increasing the complexity of the optimization algorithm, and probably will lead to a further improvement of performance. A battery could be included in the MILP optimization algorithm using a method similar to that of (Skjong et al., 2017).
- Including an online optimization of continuously updated SFOC for each genset could improve the accuracy of the fuel consumption and lead to more optimal loading conditions of each genset. This could be an improvement because the actual SFOC can vary with several variables, e.g. temperature and wear and tear of equipment.
- In order to fully utilize the extents of the MVPPSS, a simulation model of a vessel including the DP system as well as environmental modeling and electrical system could be made, including the implemented MILP optimization algorithm. This could simulate complex marine operations and provide accurate estimations of KPIs.

Bibliography

ABB, 2019. Azipod gearless propulsors | ABB Marine & Ports. URL: https://new.abb.com/marine/systems-and-solutions/azipod.

Al-Falahi, M.D.A., Nimma, K.S., Jayasinghe, S.D.G., Enshaei, H., Guerrero, J.M., 2018. Power management optimization of hybrid power systems in electric ferries. Energy Conversion and Management 172, 50–66. URL: http://www.sciencedirect.com/science/article/pii/S0196890418307362, doi:10.1016/j.enconman.2018.07.012.

Andrea, D., 2010. Battery Management Systems for Large Lithium Ion Battery Packs. Artech House.

Blaabjerg, F., 2018. Control of Power Electronic Converters and Systems. Elsevier. doi:10.1016/C2017-0-04756-0.

Blanke, M., 1981. Ship propulsion losses related to automatic steering and prime mover control /. Ph.D. thesis.

Bosich, D., Filippo, M., Giulivo, D., Sulligoi, G., Tessarolo, A., 2012. Thruster motor start-up transient in an all-electric cruise-liner: Numerical simulation and experimental assessment, in: Railway and Ship Propulsion 2012 Electrical Systems for Aircraft, pp. 1–5. doi:10.1109/ESARS.2012.6387447. iSSN: 2165-9400.

Bø, T.I., 2016. Scenario- and Optimization-Based Control of Marine Electric Power Systems. Ph.D. thesis. NTNU. URL: https://ntnuopen.ntnu.no/ntnu-xmlui/handle/11250/2382342.

Bø, T.I., Dahl, A.R., Johansen, T.A., Mathiesen, E., Miyazaki, M.R., Pedersen, E., Skjetne, R., Sørensen, A.J., Thorat, L., Yum, K.K., 2015a. Marine Vessel and Power Plant System Simulator. IEEE Access 3, 2065–2079. doi:10.1109/ACCESS.2015.2496122.

Bø, T.I., Johansen, T.A., Dahl, A.R., Miyazaki, M.R., Pedersen, E., Rokseth, B., Skjetne, R., Sørensen, A.J., Thorat, L., Utne, I.B., Yum, K.K., Mathiesen, E.,

2015b. Real-Time Marine Vessel and Power Plant Simulation, in: Volume 1: Offshore Technology; Offshore Geotechnics, American Society of Mechanical Engineers, St. John's, Newfoundland, Canada. p. V001T01A007. URL: https://asmedigitalcollection.asme.org/OMAE/proceedings/OMAE2015/56475/St.%20John%E2%80%99s,%20Newfoundland,%20Canada/279680, doi:10.1115/OMAE2015-41479.

Cosse, R.E., Alford, M.D., Hajiaghajani, M., Hamilton, E.R., 2011. Turbine/generator governor droop/isochronous fundamentals - A graphical approach, in: 2011 Record of Conference Papers Industry Applications Society 58th Annual IEEE Petroleum and Chemical Industry Conference (PCIC), pp. 1–8. doi:10.1109/PCICon.2011.6085887. iSSN: 2161-8127.

Dinh, T., Bui, T., Marco, J., Watts, C., Yoon, J., 2018. Optimal Energy Management for Hybrid Electric Dynamic Positioning Vessels. IFAC-PapersOnLine 51, 98–103. doi:10.1016/j.ifacol.2018.09.476.

DNV GL, 2015. Ship rules for classification. Technical report, DNV GL.

Ferris, M.C., Mangasarian, O.L., Wright, S.J., 2007. Linear Programming with MATLAB. MOS-SIAM Series on Optimization, Society for Industrial and Applied Mathematics. URL: https://epubs.siam.org/doi/book/10.1137/1.9780898718775, doi:10.1137/1.9780898718775.

Fiksdahl, O., 2020. Model-based optimization for energy and emission management of a marine hybrid electric power system (Master thesis at NTNU, Department of Marine Technology.

Foss, B., Heirung, T.A.N., 2016. Merging Optimization and Control .

Fossen, T.I., Perez, T., 2009. Kalman filtering for positioning and heading control of ships and offshore rigs. IEEE Control Systems Magazine 29, 32–46. doi:10.1109/MCS.2009.934408.

Glover, J.D., Sarma, M.S., Overbye, T., 2007. Power Systems Analysis and Design. 4 edition ed., CL Engineering, Australia ; Toronto, Ont.

Gulsvik, K.A.K., 2017. Battery Management System for a low-cost ROV (Master thesis at NTNU, Department of Marine Technology). 134 URL: https://ntnuopen.ntnu.no/ntnu-xmlui/handle/11250/2615036. accepted: 2019-09-11T08:51:01Z Publisher: NTNU.

Gönen, T., 2011. Electrical Machines with MATLAB®. 2 edition ed., CRC Press, Boca Raton, FL.

Hansen, J.F., 2000. Modelling and Control of Marine Power Systems. Ph.D. thesis.

Hansen, J.F., 2019. ABB ship electric propulsion: Guest lecture in TMR4240 Marine Control Systems I (lecture 11).

Hansen, J.F., Wendt, F., 2015. History and State of the Art in Commercial Electric Ship Propulsion, Integrated Power Systems, and Future Trends. Proceedings of the IEEE 103, 2229–2242. doi:10.1109/JPROC.2015.2458990.

Hansen, J.F., Ådnanes, A.K., Fossen, T.I., 2001. Mathematical Modelling of Diesel-Electric Propulsion Systems for Marine Vessels. Mathematical and Computer Modelling of Dynamical Systems 00. doi:10.1076/mcmd.7.3.323.3641.

Herskind, C.C., Morack, M.M., 1987. A History of Mercury-arc Rectifiers in North America. IEEE. Google-Books-ID: EyQ6HAAACAAJ.

Hou, J., Sun, J., Hofmann, H., 2014. Mitigating power fluctuations in electrical ship propulsion using model predictive control with hybrid energy storage system, in: 2014 American Control Conference, pp. 4366–4371. doi:10.1109/ACC.2014.6858803. iSSN: 2378-5861.

Jalkanen, J.P., Johansson, L., Kukkonen, J., Brink, A., Kalli, J., Stipa, T., 2011. Extension of an assessment model of ship traffic exhaust emissions for particulate matter and carbon monoxide. Atmospheric Chemistry and Physics Discussions 11, 22129–22172. doi:10.5194/acpd-11-22129-2011.

Lindtjørn, J.O., Wendt, F., Gundersen, B., Fredrik, J., 2014. Demonstrating the Benefits of Advanced Power Systems and Energy Storage for DP Vessels , 24.

Lund, K., 2019. Optimal Design and Configuration of Marine Power Systems for Hybrid Electric Vessels (Project Thesis at NTNU, Department of Marine Technology).

Mayne, D.Q., Rawlings, J.B., Rao, C.V., Scokaert, P.O.M., 2000. Constrained model predictive control: Stability and optimality. Automatica 36, 789–814.

Mirjalili, S., Mirjalili, S.M., Lewis, A., 2014. Grey Wolf Optimizer. Advances in Engineering Software 69, 46–61. URL: http://www.sciencedirect.com/science/article/pii/S0965997813001853, doi:10.1016/j.advengsoft.2013.12.007.

Miyazaki, M.R., 2017. Modeling and Control of Hybrid Marine Power Plants. Ph.D. thesis. URL: https://ntnuopen.ntnu.no/ntnu-xmlui/handle/11250/2450905. accepted: 2017-08-16T11:14:44Z ISBN: 9788232624713 Publisher: NTNU.

Miyazaki, M.R., Sørensen, A.J., Vartdal, B.J., 2016. Reduction of Fuel Consumption on Hybrid Marine Power Plants by Strategic Loading With Energy Storage Devices. IEEE Power and Energy Technology Systems Journal 3, 207–217. doi:10.1109/JPETS.2016.2621117.

MSS, 2010. Marine Systems Simulator. URL: http://marinecontrol.org/.

Pedersen, T.A., Pedersen, E., 2012. Bond graph modelling of marine power systems. Mathematical and Computer Modelling of Dynamical Systems 18, 153–173. doi:10.1080/13873954.2011.603735.

Planakis, N., Papalambrou, G., Kyrtatos, N., 2018. Predictive Control for a Marine Hybrid Diesel-Electric Plant During Transient Operation, in: 2018 5th International Conference on Control, Decision and Information Technologies (CoDIT), pp. 989–994. doi:10.1109/CoDIT.2018.8394939. iSSN: 2576-3555.

Radan, D., 2008. Integrated Control of Marine Electrical Power Systems. Ph.D. thesis. Fakultet for ingeniørvitenskap og teknologi. URL: https://ntnuopen.ntnu.no/ntnu-xmlui/handle/11250/231176.

Reddy, N.P., Zadeh, M.K., Thieme, C.A., Skjetne, R., Sorensen, A.J., Aanondsen, S.A., Breivik, M., Eide, E., 2019. Zero-Emission Autonomous Ferries for Urban Water Transport: Cheaper, Cleaner Alternative to Bridges and Manned Vessels. IEEE Electrification Magazine 7, 32–45. doi:10.1109/MELE.2019.2943954. conference Name: IEEE Electrification Magazine.

Rejani Miyazaki, M., Sørensen, A.J., Lefebvre, N., Yum, K., Pedersen, E., 2016. Hybrid modeling of strategic loading of a marine hybrid power plant with experimental validation. 8793-8804 URL: https://ntnuopen.ntnu.no/ntnu-xmlui/handle/11250/2474204, doi:10.1109/ACCESS.2016.2629000.

Seenumani, G., Sun, J., Peng, H., 2010. A hierarchical optimal control strategy for power management of hybrid power systems in all electric ships applications, in: 49th IEEE Conference on Decision and Control (CDC), pp. 3972–3977. doi:10.1109/CDC.2010.5717035. iSSN: 0743-1546.

Simonsen, E.B., 2019. Modeling and Optimization of a Hybrid Electric Ship Power System (Master thesis at NTNU, Department of Marine Technology) URL: https://ntnuopen.ntnu.no/ntnu-xmlui/handle/11250/2625268. accepted: 2019-10-29T15:01:00Z Publisher: NTNU.

Skjetne, R., 2012. Lecture notes in TMR4243 - Marine Control Systems II.

Skjetne, R., 2017. Report: Power system simulator design. Technical Report.

Skjong, E., 2017. Optimization-based Control in Shipboard Electric Systems. Ph.D. thesis. NTNU. URL: https://ntnuopen.ntnu.no/ntnu-xmlui/handle/11250/2444268.

Skjong, E., Johansen, T.A., Molinas, M., Sorensen, A.J., 2017. Approaches to Economic Energy Management in Diesel–Electric Marine Vessels. IEEE Transactions on Transportation Electrification 3, 22–35. URL: http://ieeexplore.ieee.org/document/7807341/, doi:10.1109/TTE.2017.2648178.

Skjong, E., Rødskar, E., Molinas, M., Johansen, T.A., Cunningham, J., 2015. The Marine Vessel's Electrical Power System: From its Birth to Present Day. Proceedings of the IEEE 103, 2410–2424. doi:10.1109/JPROC.2015.2496722.

Skjong, E., Volden, R., Rodskar, E., Molinas, M., Johansen, T.A., Cunningham, J., 2016. Past, Present, and Future Challenges of the Marine Vessel's Electrical Power System.

IEEE Transactions on Transportation Electrification 2, 522–537. URL: http://ieeexplore.ieee.org/document/7451276/, doi:10.1109/TTE.2016.2552720.

Smith, E.C., 2013. A Short History of Naval and Marine Engineering. Cambridge University Press. Google-Books-ID: zfvXAAAAQBAJ.

Sorensen, A.J., Skjetne, R., Bo, T., Miyazaki, M.R., Johansen, T.A., Utne, I.B., Pedersen, E., 2017. Towards Safer, Smarter, and Greener Ships: Using Hybrid Marine Power Plants. IEEE Electrification Magazine 5, 68–73. doi:10.1109/MELE.2017.2718861.

Thorat, L., Skjetne, R., 2018. Optimal Online Configuration and Load-Sharing in a Redundant Electric Power System for an Offshore Vessel Using Mixed Integer Linear Programming. ASME. URL: https://ntnuopen.ntnu.no/ntnu-xmlui/handle/11250/2577041, doi:10.1115/OMAE2018-77955. accepted: 2018-12-11T08:53:14Z.

Tristan, P., Smogeli, O., Fossen, T., Sørensen, A., 2006. An Overview of the Marine Systems Simulator (MSS): A Simulink Toolbox for Marine Control Systems. Modeling, Identification and Control 27. doi:10.4173/mic.2006.4.4.

Wilson, T., 2000. The evolution of power electronics. IEEE Transactions on Power Electronics 15, 439–446. doi:10.1109/63.844503.

Wu, Z., 2017. Comparison of Fuel Consumption on A Hybrid Marine Power Plant with Low-Power versus High-Power Engines. Ph.D. thesis. URL: https://ntnuopen.ntnu.no/ntnu-xmlui/handle/11250/2455248.

Wu, Z., Thorat, L., Skjetne, R., 2018. Comparison of Fuel Consumption on a Hybrid Marine Power Plant With Low-Power Versus High-Power Engines. ASME. URL: https://ntnuopen.ntnu.no/ntnu-xmlui/handle/11250/2587636, doi:10.1115/OMAE2018-77959.

Wärtsilä, F.P.G., 2019. Wärtsilä 46F - diesel engine. URL: https://www.wartsila.com/marine/build/engines-and-generating-sets/diesel-engines/wartsila-46f. library Catalog: www.wartsila.com.

Xie, Y., Sun, J., Miz, C., Freudenbergy, J.S., 2009. Analysis and modeling of a DC hybrid power system testbed for power management strategy development, in: 2009 IEEE Vehicle Power and Propulsion Conference, pp. 926–933. doi:10.1109/VPPC.2009.5289746. iSSN: 1938-8756.

Zahedi, B., Norum, L.E., Ludvigsen, K.B., 2014. Optimized efficiency of all-electric ships by dc hybrid power systems. Journal of Power Sources 255, 341–354. URL: http://adsabs.harvard.edu/abs/2014JPS...255..341Z, doi:10.1016/j.jpowsour.2014.01.031.

Ådnanes, A.K., 2003. Maritime Electrical Installations And Diesel Electric Propulsion. ABB AS, Norway .

Appendix

Appendix A

MILP Optimization Algorithm

A.1 Implementation in Matlab

```
% clear;
% clc;
%%                    Load Profile Selection
%%%%%%%%%%%%%%%%%%%%                          %%%%%%%%%%%%%%%%%

%Choose the deterministic load profile by uncommenting the
%following two lines.
operation_time = 4000; %4373
load_profile = deterministicLoadProfile(operation_time);


%load_profile = deterministicLoadProfile3;
% The load profile can be altered in the function
% "deterministicLoadProfile.m"


%Choose the realistic load profile by uncommenting the
%following two lines
%load_profile = plotLoadProfile;
operation_time = length(load_profile);
%The load profile can be altered in the function
%"plotLoadProfile.m"

%%%%%%%%%%%%%%%%%%%%%%%%%%%%%%%%%%%%%%%%%%%%%%%%%%%%%%%%%%%%%%%%%%%%%%%

%%             Variables Used for Genset Scheduling
%%%%%%%%%%%%%%%                                            %%%%%%%%%%

T_s = 10; %Periodic execution of optimization
epsilon = 0.1;
P_b = [8000, 8000, 8000, 8000, 8000, 8000];

n_gensets = length(P_b);
P_b_onenorm = sum(P_b);
optimal_loading_factor = 0.80; %Optimal running condition
Gamma = optimal_loading_factor*eye(n_gensets);
ones_vector = ones(n_gensets, 1);
N_min = 0;
intcon = zeros(1, n_gensets);
for i = 1:n_gensets
    intcon(i) = i;
end

```

```
%Boundaries ensure c-variables binary
lb_gs = zeros(n_gensets,1);
ub_gs = ones(n_gensets,1);

%Weighting scheme of objective function - chooses
%optimization objective
w1 = 1;
w2 = 0;
w3 = 0;
w4 = 0;

%%%%%%%%%%%%%%%%%%%%%%%%%%%%%%%%%%%%%%%%%%%%%%%%%%%%%%%%%%%%%%%%%%%%%%%

%%              Variables Used for Load Sharing
%%%%%%%%%%%%%%%%                                      %%%%%%%%%%%%%

%Defining SFOC-curves for each genset:

f_sfoc =      [0.00, 0.05, 0.10, 0.15, 0.20, 0.25, 0.30, ...
               0.35, 0.40, 0.45, 0.50, 0.55, 0.60, 0.65, ...
               0.70, 0.75, 0.80, 0.85, 0.90, 0.95, 1.00; ...
               240,  225,  216,  210,  205,  201,  197, ...
               193,  190,  187,  185,  183,  181,  180, ...
               179,  178,  178,  179, 179,  181,  182];

%For GENSET 1
f_sfoc_1 = f_sfoc;

%For GENSET 2
f_sfoc_2 = f_sfoc;

%For GENSET 3
f_sfoc_3 = f_sfoc;

%For GENSET 4
f_sfoc_4 = f_sfoc;

%For GENSET 5
f_sfoc_5 = f_sfoc;

%For GENSET 6
f_sfoc_6 = f_sfoc;

%Using fuel consumption data points to form matrix constraints
%for the minimization of fuel consumption
```

```
89
90  m = length(f_sfoc_1) - 1;
91
92  %Preallocating for speed
93  a_1 = zeros(m,1);
94  b_1 = zeros(m,1);
95
96  a_2 = zeros(m,1);
97  b_2 = zeros(m,1);
98
99  a_3 = zeros(m,1);
100 b_3 = zeros(m,1);
101
102 a_4 = zeros(m,1);
103 b_4 = zeros(m,1);
104
105 a_5 = zeros(m,1);
106 b_5 = zeros(m,1);
107
108 a_6 = zeros(m,1);
109 b_6 = zeros(m,1);
110
111 for k = 2:m+1
112     a_1(k-1) = (f_sfoc_1(2, k) - ...
113         f_sfoc_1(2, k-1))/(f_sfoc_1(1, k) - f_sfoc_1(1, k-1));
114     b_1(k-1) = f_sfoc_1(2, k-1) - a_1(k-1)*f_sfoc_1(1, k-1);
115 end
116
117 for k = 2:m+1
118     a_2(k-1) = (f_sfoc_2(2, k) - ...
119         f_sfoc_2(2, k-1))/(f_sfoc_2(1, k) - f_sfoc_2(1, k-1));
120     b_2(k-1) = f_sfoc_2(2, k-1) - a_2(k-1)*f_sfoc_2(1, k-1);
121 end
122
123 for k = 2:m+1
124     a_3(k-1) = (f_sfoc_3(2, k) - ...
125         f_sfoc_3(2, k-1))/(f_sfoc_3(1, k) - f_sfoc_3(1, k-1));
126     b_3(k-1) = f_sfoc_3(2, k-1) - a_3(k-1)*f_sfoc_3(1, k-1);
127 end
128
129 for k = 2:m+1
130     a_4(k-1) = (f_sfoc_4(2, k) - ...
131         f_sfoc_4(2, k-1))/(f_sfoc_4(1, k) - f_sfoc_4(1, k-1));
132     b_4(k-1) = f_sfoc_4(2, k-1) - a_4(k-1)*f_sfoc_4(1, k-1);
133 end
```

```
134
135 for k = 2:m+1
136     a_5(k-1) = (f_sfoc_5(2, k) - ...
137         f_sfoc_5(2, k-1))/(f_sfoc_5(1, k) - f_sfoc_5(1, k-1));
138     b_5(k-1) = f_sfoc_5(2, k-1) - a_5(k-1)*f_sfoc_5(1, k-1);
139 end
140
141 for k = 2:m+1
142     a_6(k-1) = (f_sfoc_6(2, k) - ...
143         f_sfoc_6(2, k-1))/(f_sfoc_6(1, k) - f_sfoc_6(1, k-1));
144     b_6(k-1) = f_sfoc_6(2, k-1) - a_6(k-1)*f_sfoc_6(1, k-1);
145 end
146
147 A_ls = [a_1, zeros(m, 1), zeros(m, 1), zeros(m, 1), ...
148         zeros(m, 1), zeros(m, 1); ...
149         zeros(m, 1), a_2, zeros(m, 1), zeros(m, 1), ...
150         zeros(m, 1), zeros(m, 1);
151         zeros(m, 1), zeros(m, 1), a_3, zeros(m, 1), ...
152         zeros(m, 1), zeros(m, 1);
153         zeros(m, 1), zeros(m, 1), zeros(m, 1), a_4, ...
154         zeros(m, 1), zeros(m, 1);
155         zeros(m, 1), zeros(m, 1), zeros(m, 1), zeros(m, 1), ...
156         a_5, zeros(m, 1);
157         zeros(m, 1), zeros(m, 1), zeros(m, 1), zeros(m, 1), ...
158         zeros(m, 1), a_6];
159
160 E_ls = [-1*ones(m, 1), zeros(m, 1), zeros(m, 1), ...
161         zeros(m, 1), zeros(m, 1), zeros(m, 1);
162         zeros(m, 1), -1*ones(m, 1), zeros(m, 1), ...
163         zeros(m, 1), zeros(m, 1), zeros(m, 1);
164      zeros(m, 1), zeros(m, 1), -1*ones(m, 1), zeros(m, 1), ...
165      zeros(m, 1), zeros(m, 1);
166      zeros(m, 1), zeros(m, 1), zeros(m, 1), -1*ones(m, 1), ...
167      zeros(m, 1), zeros(m, 1);
168      zeros(m, 1), zeros(m, 1), zeros(m, 1), zeros(m, 1), ...
169      -1*ones(m, 1), zeros(m, 1);
170      zeros(m, 1), zeros(m, 1), zeros(m, 1), zeros(m, 1), ...
171      zeros(m, 1), -1*ones(m, 1)];
172
173 b_ls = [b_1;
174         b_2;
175         b_3;
176         b_4;
177         b_5;
178         b_6];
```

```
179
180 %Defining upper and lower values of p-value for each engine
181 p_min = [f_sfoc_1(1, 1);
182          f_sfoc_2(1, 1);
183          f_sfoc_3(1, 1);
184          f_sfoc_4(1, 1);
185          f_sfoc_5(1, 1);
186          f_sfoc_6(1, 1)];
187
188 p_max = [f_sfoc_1(1, m+1);
189          f_sfoc_2(1, m+1);
190          f_sfoc_3(1, m+1);
191          f_sfoc_4(1, m+1);
192          f_sfoc_5(1, m+1);
193          f_sfoc_6(1, m+1)];
194
195 %%%%%%%%%%%%%%%%%%%%%%%%%%%%%%%%%%%%%%%%%%%%%%%%%%%%%%%%%%%%%%%%%%%%%%%
196
197 %%          Initialization of Optimization Variables
198 %%%%%%%%%%                                              %%%%%%%%
199
200 Son = zeros(n_gensets, 1);
201 Soff = zeros(n_gensets, 1);
202
203 d = zeros(n_gensets, 1); %Variable counting running hour of
204                          %gensets
205
206 d_prev = zeros(n_gensets, 1);
207 C_prev = zeros(n_gensets, 1);
208 C = zeros(n_gensets, 1);
209
210 DeltaCPlus = zeros(n_gensets, 1);
211 DeltaCMinus = zeros(n_gensets, 1);
212
213 d_onenorm = sum(d);
214 Son_onenorm = sum(Son);
215 Soff_onenorm = sum(Soff);
216
217 %%%%%%%%%%%%%%%%%%%%%%%%%%%%%%%%%%%%%%%%%%%%%%%%%%%%%%%%%%%%%%%%%%%%%%%
218
219 %%        Preallocation of Data Storage Variables
220 %%%%%%%%%%                                          %%%%%%%%%%
221
222 online_capacity_vector = zeros(1, ceil(operation_time/T_s));
223 no_online_gs_vector = zeros(1, ceil(operation_time/T_s));
```

```
224 running_time_gs_matrix = zeros(n_gensets, ...
225                                ceil(operation_time/T_s));
226 switches_on_vector = zeros(n_gensets, ...
227                            ceil(operation_time/T_s));
228 switches_off_vector = zeros(n_gensets, ...
229                             ceil(operation_time/T_s));
230
231 %d_matrix = zeros(n_gensets, ceil(operation_time/T_s));
232 C_matrix = zeros(n_gensets, ceil(operation_time/T_s));
233 p_matrix = zeros(n_gensets, ceil(operation_time/T_s));
234
235 %%%%%%%%%%%%%%%%%%%%%%%%%%%%%%%%%%%%%%%%%%%%%%%%%%%%%%%%%%%%%%%%%%%%%%%
236
237 %%    Simulation of Optimization of Marine Power Plant
238 %%%%%                                                          %%%%%
239
240  for i = 1:T_s:operation_time
241 %%         Optimization Stage 1 - Genset Scheduling
242 %%%%%%%%%%%                                                 %%%%%%%%%
243      %Solving mixed integer linear program for
244      %scheduling // STAGE 1
245      P_load = load_profile(1,i);
246
247      A_gs = [-P_b*Gamma;
248           -ones_vector'];
249      b_gs = [-P_load; -N_min];
250
251      d_prev = d;
252      C_prev = C;
253
254      d = d_prev + T_s*C_prev;
255
256      d_onenorm = sum(d);
257
258      obj_function_gs = (w1*(1/P_b_onenorm)*P_b' + ...
259                         w2*(d/(d_onenorm + epsilon)) + ...
260                         w3*(Son/(Son_onenorm + epsilon)) + ...
261                         w4*(Soff/(Soff_onenorm + epsilon)))';
262
263      C = intlinprog(obj_function_gs, intcon, A_gs, b_gs, ...
264                     [], [], lb_gs, ub_gs);
265
266      DeltaC = C - C_prev;
267
268      for j = 1:n_gensets
```

```
269             if DeltaC(j) > 0.99
270                 DeltaCPlus(j) = DeltaCPlus(j) + 1;
271             end
272
273             if DeltaC(j) < -0.99
274                 DeltaCMinus(j) = DeltaCMinus(j) + 1;
275             end
276         end
277
278         Son = DeltaCPlus;
279         Soff = DeltaCMinus;
280
281         Son_onenorm = sum(Son);
282         Soff_onenorm = sum(Soff);
283
284 %%%%%%%%%%%%%%%%%%%%%%%%%%%%%%%%%%%%%%%%%%%%%%%%%%%%%%%%%%%%%%%%%%%%%%%
285
286 %%            Optimization Stage 2 - Load Sharing
287 %%%%%%%%%%%%%%                                          %%%%%%%%%%%
288
289         %Objective function
290         c_ls_star_1 = [C; 0; 0; 0; 0; 0; 0];
291
292         obj_function_ls = c_ls_star_1';
293
294         %Inequality constraint: A_star * my_star <= -b
295         A_ls_star = [E_ls, A_ls];
296         b_ls = -b_ls;
297
298         %Equality constraint:
299         %(c_star_2    P_b_star)'
300         %* mu_star = P_load
301
302         c_ls_star_2 = [0; 0; 0; 0; 0; 0; C];
303
304         P_b_ls_star = [0; 0; 0; 0; 0; 0; P_b'];
305
306         A_eq_star = [c_ls_star_2(1)*P_b_ls_star(1);
307                      c_ls_star_2(2)*P_b_ls_star(2);
308                      c_ls_star_2(3)*P_b_ls_star(3);
309                      c_ls_star_2(4)*P_b_ls_star(4);
310                      c_ls_star_2(5)*P_b_ls_star(5);
311                      c_ls_star_2(6)*P_b_ls_star(6);
312                      c_ls_star_2(7)*P_b_ls_star(7);
313                      c_ls_star_2(8)*P_b_ls_star(8);
```

```
                    c_ls_star_2(9)*P_b_ls_star(9);
                    c_ls_star_2(10)*P_b_ls_star(10);
                    c_ls_star_2(11)*P_b_ls_star(11);
                    c_ls_star_2(12)*P_b_ls_star(12)]';

    b_ls_eq = P_load;

    lb_ls = [-inf;
             -inf;
             -inf;
             -inf;
             -inf;
             -inf;
             c_ls_star_2(7)*0;
             c_ls_star_2(8)*0;
             c_ls_star_2(9)*0;
             c_ls_star_2(10)*0;
             c_ls_star_2(11)*0;
             c_ls_star_2(12)*0];

    ub_ls = [inf;
             inf;
             inf;
             inf;
             inf;
             inf;
             c_ls_star_2(7)*1;
             c_ls_star_2(8)*1;
             c_ls_star_2(9)*1;
             c_ls_star_2(10)*1;
             c_ls_star_2(11)*1;
             c_ls_star_2(12)*1];

    mu_star = linprog(obj_function_ls, A_ls_star, b_ls, ...
                      A_eq_star, b_ls_eq, lb_ls, ub_ls);

    p = mu_star(7:12);

%%%%%%%%%%%%%%%%%%%%%%%%%%%%%%%%%%%%%%%%%%%%%%%%%%%%%%%%%%%%%%%%%%%%%%%

%%            Data Storage of Operation Variables
%%%%%%%%%%%%%                                          %%%%%%%%%%

    online_capacity = P_b*C; %online capacity
    no_online_gs = sum(C); %number of online gensets
```

```
359
360       online_capacity_vector(ceil(i/T_s)) = online_capacity;
361
362       no_online_gs_vector(ceil(i/T_s)) = no_online_gs;
363
364       running_time_gs_matrix(:, ceil(i/T_s)) = d;
365       switches_on_vector(:, ceil(i/T_s)) = Son;
366       switches_off_vector(:, ceil(i/T_s)) = Soff;
367
368
369       %Storing all scheduling configurations for entire time
370       %horizon
371       C_matrix(:, ceil(i/T_s)) = C;
372
373       %Storing all load sharing configurations for entire
374       %time horizon
375       p_matrix(:, ceil(i/T_s)) = p;
376
377       fprintf('%f %% Complete\n', 100*(i/operation_time));
378
379 %%%%%%%%%%%%%%%%%%%%%%%%%%%%%%%%%%%%%%%%%%%%%%%%%%%%%%%%%%%%%%%%%%%%%%%
380  end
381 %%%%%%%%%%%%%%%%%%%%%%%%%%%%%%%%%%%%%%%%%%%%%%%%%%%%%%%%%%%%%%%%%%%%%%%
382  %% Rearranging Data Sets for Plotting of Operation Variables
383  %%%
384 fprintf('Optimization complete. Enjoy results\n');
385
386 %Extended with "true" time value in bottom row, i.e. 10
387 %instead of index 1, 20 instead of index 2, because the
388 %optimization periodic execution T = 10.
389 %Preallocating for speed
390 online_capacity_vector_ext = zeros(2, ...
391                                    ceil(operation_time/T_s));
392 no_online_gs_vector_ext = zeros(2, ceil(operation_time/T_s));
393 running_time_gs_matrix_ext = zeros(n_gensets + 1, ...
394                                     ceil(operation_time/T_s));
395 p_matrix_ext = zeros(n_gensets + 1, ceil(operation_time/T_s));
396
397 for i = 1:ceil(operation_time/T_s)
398     online_capacity_vector_ext(2, i) = i*T_s - T_s;
399     no_online_gs_vector_ext(2, i) = i*T_s - T_s;
400     running_time_gs_matrix_ext(n_gensets + 1, i) = ...
401         i*T_s - T_s;
402     p_matrix_ext(n_gensets + 1, i) = i*T_s - T_s;
403 end
```

```
404 online_capacity_vector_ext(1, :) = online_capacity_vector;
405 no_online_gs_vector_ext(1, :) = no_online_gs_vector;
406 running_time_gs_matrix_ext(1:n_gensets, :) = ...
407     running_time_gs_matrix;
408 p_matrix_ext(1:n_gensets, :) = p_matrix;
409
410 P_matrix_ext = p_matrix_ext;
411
412 for i = 1:length(p_matrix_ext)
413     for j = 1:n_gensets
414         P_matrix_ext(j,i) = P_matrix_ext(j,i)*P_b(j);
415     end
416 end
417
418 plotVerificationSimpl;
419
420 %%%%%%%%%%%%%%%%%%%%%%%%%%%%%%%%%%%%%%%%%%%%%%%%%%%%%%%%%%%%%%%%%%%%%%%%%%%
```

A.2 LP Formulation Method

The LP in Equations 4.21 through 4.25 introduces the auxiliary variable μ for the minimization of the PWL SFOC-curves.

Matlab needs a linear program to be on the form

$$\begin{aligned} &\min_{x} f^\top x \\ &\text{s.t.} \quad Ax \leq b \\ &\qquad A_{eq}x = b_{eq} \end{aligned}$$

Our linear program is formulated as

$$\begin{aligned} \min_{p,\mu} \quad & C^\top \mu \\ \text{s.t.} \quad & Ap + E\mu \leq -b \\ & (C \circ P_b)^\top p = P_{load} \\ & C \circ (p_j^- - \Delta p) \leq p \leq C \circ (p_j^- + \Delta p) \\ & C \circ p_{min} \leq p \leq C \circ p_{max} \end{aligned}$$

This introduces the problem: how can p be included as an optimization variable when it is not part of the objective function? The following is a suggested method which has proven to provide correct optimization and reasonable results from the LP. The method includes introducing μ^*, which contains both μ and p: $\mu^* := [\mu \quad p]^\top$. Then, the objective function and constraints are converted to fit with the new optimization variable, μ^*. For illustrational purposes, an imaginary configuration of four gensets are used as a basis for derivation of equations, in order to illustrate the dimensions of the matrices and vectors.

In the following steps, explanations of the needed alterations and conversions of the linear program are presented.

1.)
Concerning a power plant with four gensets, $\mu^* = [\mu_1 \quad \mu_2 \quad \mu_3 \quad \mu_4 \quad p_1 \quad p_2 \quad p_3 \quad p_4]^\top$. The first necessary conversion is to convert the constraint in Equation 4.22, the inequality constraint. This is done by introducing a new inequality:

$$Ap + E\mu \leq -b \quad \longrightarrow \quad A^*\mu^* \leq -b$$

where

$$A^* = \begin{bmatrix}[E] & [A]\end{bmatrix} \quad \text{and} \quad \mu^* = \begin{bmatrix}\mu \\ p\end{bmatrix}$$

which gives

$$\begin{bmatrix} E_{11} & E_{12} & \dots & E_{14} & A_{11} & A_{12} & \dots & A_{14} \\ E_{21} & E_{22} & & E_{24} & A_{21} & A_{22} & & A_{24} \\ \vdots & & \ddots & \vdots & \vdots & & \ddots & \vdots \\ E_{41} & \dots & \dots & E_{44} & A_{41} & \dots & \dots & A_{44} \end{bmatrix} \begin{bmatrix} \mu_1 \\ \mu_2 \\ \mu_3 \\ \mu_4 \\ p_1 \\ p_2 \\ p_3 \\ p_4 \end{bmatrix} \leq - \begin{bmatrix} b_1 \\ b_2 \\ b_3 \\ b_4 \end{bmatrix}$$

2.)
Introducing $C^* = [C^\top \quad 0 \quad 0 \quad 0 \quad 0]^\top$, gives the following conversion of the objective function:

$$\min_{p,\mu} C^\top \mu \quad \longrightarrow \quad \min_{\mu^*} {C^*}^\top \mu^*$$

which yields the new objective function.

3.)
Lastly, the equality constraint from Equation 4.23 is converted by introducing $C^{**} = [0 \quad 0 \quad 0 \quad 0 \quad C^\top]^\top$ and doing the following alterations:

$$(C \circ P_b)^\top p = P_{load} \quad \longrightarrow \quad (C^{**} \circ P_b^{**})^\top \mu^* = P_{load}$$

where

$$P_b^{**} = [0 \quad 0 \quad 0 \quad 0 \quad P_b^\top]^\top$$

which gives

$$\begin{bmatrix} 0 & 0 & 0 & 0 & C_1 P_{b1} & C_2 P_{b2} & C_3 P_{b3} & C_4 P_{b4} \end{bmatrix} \begin{bmatrix} \mu_1 \\ \mu_2 \\ \mu_3 \\ \mu_4 \\ p_1 \\ p_2 \\ p_3 \\ p_4 \end{bmatrix} = P_{load}$$

Equations 4.24 and 4.25 are corrected by using the introduced variable C^{**} and including them in the optimization solver in Matlab as upper and lower bounds of the feasible solution region.

A.3 Implementation in the MVPPSS - Simulink model

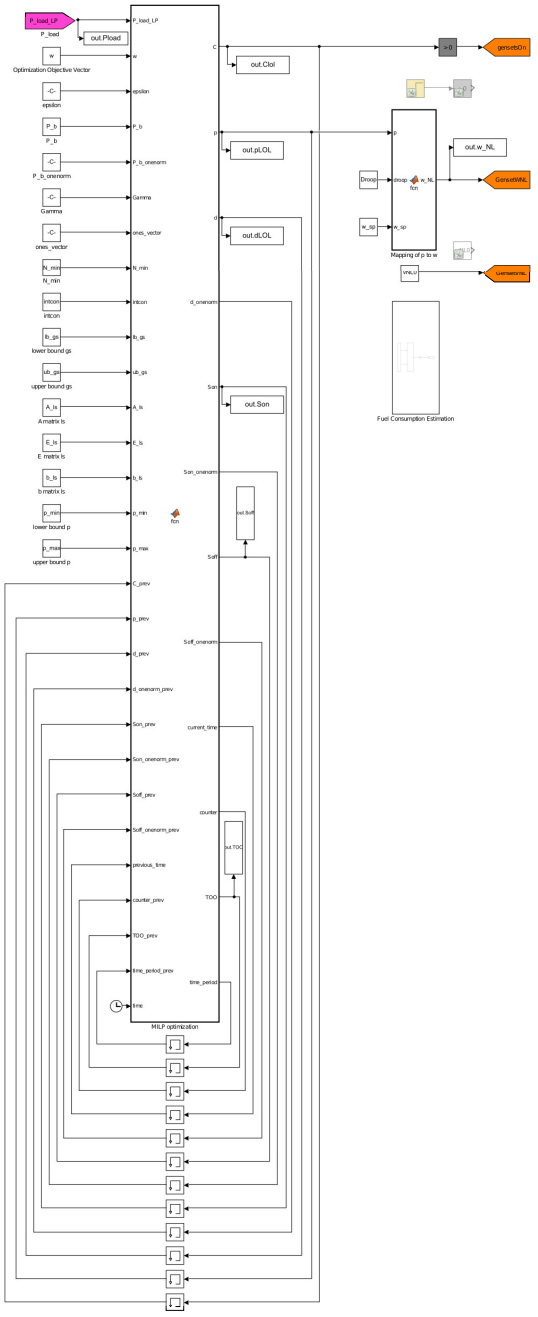

A.4 Implementation in the MVPPSS - Matlab function block

```
function [C, p, d, d_onenorm, Son, Son_onenorm, Soff, ...
          Soff_onenorm, current_time,counter, TOO, ...
          time_period] = fcn(P_load_LP, w, epsilon, P_b, ...
          P_b_onenorm, Gamma, ones_vector, N_min, intcon, ...
          lb_gs, ub_gs, A_ls, E_ls, b_ls, p_min, p_max, ...
          C_prev, p_prev, d_prev, d_onenorm_prev, ...
          Son_prev, Son_onenorm_prev, Soff_prev, ...
          Soff_onenorm_prev, previous_time, counter_prev, ...
          TOO_prev, time_period_prev, time)

coder.extrinsic('intlinprog');
coder.extrinsic('linprog');

w1 = w(1);
w2 = w(2);
w3 = w(3);
w4 = w(4);

P_load = P_load_LP;

C = C_prev;
p = p_prev;
d = d_prev;
d_onenorm = d_onenorm_prev;
Son = Son_prev;
Son_onenorm = Son_onenorm_prev;
Soff = Soff_prev;
Soff_onenorm = Soff_onenorm_prev;
current_time = time;
TOO = TOO_prev;
time_period = time_period_prev;
counter = counter_prev;


if time > 1 %to prevent that first milp genset scheduling is
            %performed at t = 0 => P_load = 0 => 0 gensets
            %activated until next periodic execution at 10 s
            %=> voltage error!

    if current_time - TOO > 10 %1

        counter = counter + 1;
```

```
        time_period = current_time - TOO;
        if counter == 1
            time_period = current_time;
        end

% MILP Optimization Stage 1 - Genset Scheduling.
        A_gs = [-P_b*Gamma;
                -ones_vector'];
        b_gs = [-P_load; -N_min];

        d = d_prev + time_period*C_prev;

        d_onenorm = sum(d);

        obj_function_gs = (w1*(1/P_b_onenorm)*P_b' + ...
                           w2*(d/(d_onenorm + epsilon)) + ...
                           w3*(Son/(Son_onenorm + epsilon)) + ...
                           w4*(Soff/(Soff_onenorm + epsilon)))';

        C = intlinprog(obj_function_gs, intcon, A_gs, ...
                           b_gs,[], [], lb_gs, ub_gs);

        DeltaC = C - C_prev;

        for j = 1:length(C)
            if DeltaC(j) > 0.99
                Son(j) = Son(j) + 1;
            end

            if DeltaC(j) < -0.99
                Soff(j) = Soff(j) + 1;
            end
        end

        Son_onenorm = sum(Son);
        Soff_onenorm = sum(Soff);


% MILP Optimization Stage 2 - Load Sharing Between Gensets.

        %Objective function for load sharing optimization
        c_ls_star_1 = [C; 0; 0; 0; 0; 0; 0];

        obj_function_ls = c_ls_star_1';

```

```
88          %Inequality constraint: A_star * my_star <= -b
89          A_ls_star = [E_ls, A_ls];
90          b_ls = -b_ls;
91
92          %Equality constraint: (c_star_2 Hadamard elementwise
93          %vector product P_b_star)'*mu_star = P_load
94
95          c_ls_star_2 = [0; 0; 0; 0; 0; 0; C];
96
97          P_b_ls_star = [0; 0; 0; 0; 0; 0; P_b'];
98
99          A_eq_star = [c_ls_star_2(1)*P_b_ls_star(1);
100                       c_ls_star_2(2)*P_b_ls_star(2);
101                       c_ls_star_2(3)*P_b_ls_star(3);
102                       c_ls_star_2(4)*P_b_ls_star(4);
103                       c_ls_star_2(5)*P_b_ls_star(5);
104                       c_ls_star_2(6)*P_b_ls_star(6);
105                       c_ls_star_2(7)*P_b_ls_star(7);
106                       c_ls_star_2(8)*P_b_ls_star(8);
107                       c_ls_star_2(9)*P_b_ls_star(9);
108                       c_ls_star_2(10)*P_b_ls_star(10);
109                       c_ls_star_2(11)*P_b_ls_star(11);
110                       c_ls_star_2(12)*P_b_ls_star(12)]';
111
112         b_ls_eq = P_load;
113
114         lb_ls = [-inf;
115                  -inf;
116                  -inf;
117                  -inf;
118                  -inf;
119                  -inf;
120                  c_ls_star_2(7)*0;
121                  c_ls_star_2(8)*0;
122                  c_ls_star_2(9)*0;
123                  c_ls_star_2(10)*0;
124                  c_ls_star_2(11)*0;
125                  c_ls_star_2(12)*0];
126
127         ub_ls = [inf;
128                  inf;
129                  inf;
130                  inf;
131                  inf;
132                  inf;
```

```
                    c_ls_star_2(7)*1;
                    c_ls_star_2(8)*1;
                    c_ls_star_2(9)*1;
                    c_ls_star_2(10)*1;
                    c_ls_star_2(11)*1;
                    c_ls_star_2(12)*1];

        mu_star = linprog(obj_function_ls, A_ls_star, ...
                        b_ls, A_eq_star, b_ls_eq, lb_ls, ub_ls);

        p = mu_star(7:12);


        TOO = current_time;
    else
        TOO = TOO;
    end


%%%%%%%%%%%%%%%%%%%%%%%%%%%%%%%%%%%%%%%%%%%%%%%%%%%%%%%%%%%%%%%%%%%%%%%
end

end
```

A.5 Optimization Objective Minimizing Connections/Disconnections

Considering only the two terms from Equation 4.11 concerning connections and disconnections, i.e. the third and fourth term yields the objective function:

$$\left(w_3 \frac{s^{on}}{|s^{on}| + \varepsilon} + w_4 \frac{s^{off}}{|s^{off}| + \varepsilon}\right)^\top C$$

Reducing this to only including the s^{on} and s^{off} variables, as these are the variables changing due to connections and disconnections yields the objective function

$$\left(s^{on} + s^{off}\right)^\top C$$

Again, using a power plant with four genset for illustrational purposes, the following will show how the optimization algorithm chooses the scheduling scheme as the optimization algorithm is executed several times. Considering a constant load corresponding to the need of connecting one genset is used as the demanded load input to the optimization algorithm. The following behavior of the algorithm will then be as follows:

Iteration 1

$$s^{on} = \begin{bmatrix}0\\0\\0\\0\end{bmatrix}, \quad s^{off} = \begin{bmatrix}0\\0\\0\\0\end{bmatrix} \quad \Rightarrow \min_C (s^{on} + s^{off})^\top C = \begin{bmatrix}1\\0\\0\\0\end{bmatrix}$$

The first genset is connected by the algorithm because it is first in line and everything else is equal for all gensets. The s^{on} variable is then updated and will look different for iteration 2, i.e. the next execution of the optimization algorithm.

Iteration 2

$$s^{on} = \begin{bmatrix}1\\0\\0\\0\end{bmatrix}, \quad s^{off} = \begin{bmatrix}0\\0\\0\\0\end{bmatrix} \quad \Rightarrow \min_C (s^{on} + s^{off})^\top C = \begin{bmatrix}0\\1\\0\\0\end{bmatrix}$$

This time, the second generation is connected by the algorithm. This is due to the first genset, connected last optimization, has been given a value of 1 in the s^{on} variable. Thus, the objective function will have the lowest value if one of the other gensets, which all have values of 0, are connected instead. After this disconnection of Genset 1 and connection of Genset 2, the s^{on} and s^{off} variables are updated accordingly, for the next execution of the optimization algorithm.

Iteration 3

$$s^{on} = \begin{bmatrix} 1 \\ 1 \\ 0 \\ 0 \end{bmatrix}, \quad s^{off} = \begin{bmatrix} 1 \\ 0 \\ 0 \\ 0 \end{bmatrix} \quad \Rightarrow \min_{C}(s^{on} + s^{off})^{\top} C = \begin{bmatrix} 0 \\ 0 \\ 1 \\ 0 \end{bmatrix}$$

For the third iteration of the optimization, Genset 3 is connected, due to the values assigned to Genset 1 and 2 in the s^{on} and s^{off} variables. As stated before, the lowest value of the objective function is accomplished by choosing one of the gensets with values of 0, i.e. Genset 3 and 4. Thus, Genset 3 is connected.

Iteration 4

$$s^{on} = \begin{bmatrix} 1 \\ 1 \\ 1 \\ 0 \end{bmatrix}, \quad s^{off} = \begin{bmatrix} 1 \\ 1 \\ 0 \\ 0 \end{bmatrix} \quad \Rightarrow \min_{C}(s^{on} + s^{off})^{\top} C = \begin{bmatrix} 0 \\ 0 \\ 0 \\ 1 \end{bmatrix}$$

Following the reasoning presented for iteration 2 and 3, the genset connected in iteration 4 is Genset 4.

Iteration 5

$$s^{on} = \begin{bmatrix} 1 \\ 1 \\ 1 \\ 1 \end{bmatrix}, \quad s^{off} = \begin{bmatrix} 1 \\ 1 \\ 1 \\ 0 \end{bmatrix} \quad \Rightarrow \min_{C}(s^{on} + s^{off})^{\top} C = \begin{bmatrix} 0 \\ 0 \\ 0 \\ 1 \end{bmatrix}$$

For this iteration, Genset 4 is again chosen to be the connected genset. This can be seen from the s^{on} and s^{off} variables. Every genset has now been connected once, and all have a value of 1 in the s^{on} variable. The difference is in the s^{off} variable, where Genset 4 has a value of 0, while every other genset has a value of 1. This makes the algorithm choose Genset 4 again, as it corresponds to the smallest value of the objective function. The optimization algorithm will continue to choose Genset 4 as the optimal genset to connect for all iterations, given the simple optimization problem illustrated here.

Thus, we see that the optimization algorithm when minimizing connections/disconnections will ”go through” all gensets, connect and disconnect them one by one, before choosing the last one in line to be connected. This happens due to the fact that the optimization algorithm needs a difference in the s^{on} and s^{off} variables in order to choose one genset to be connected permanently.

Appendix B

Case study - Equipment and Power Plant Configurations in the MVPPSS

B.1 Power plant 1

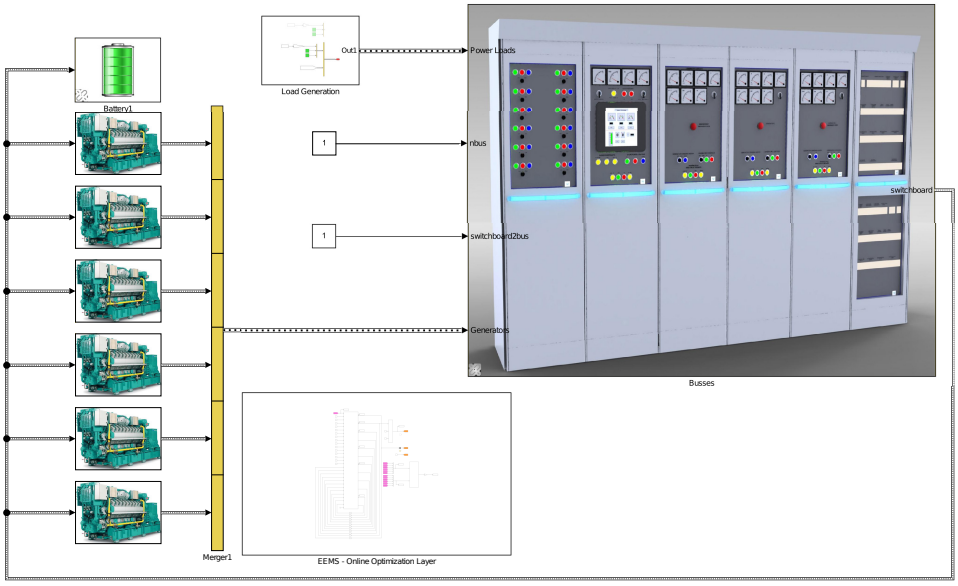

B.2 Power plant 2

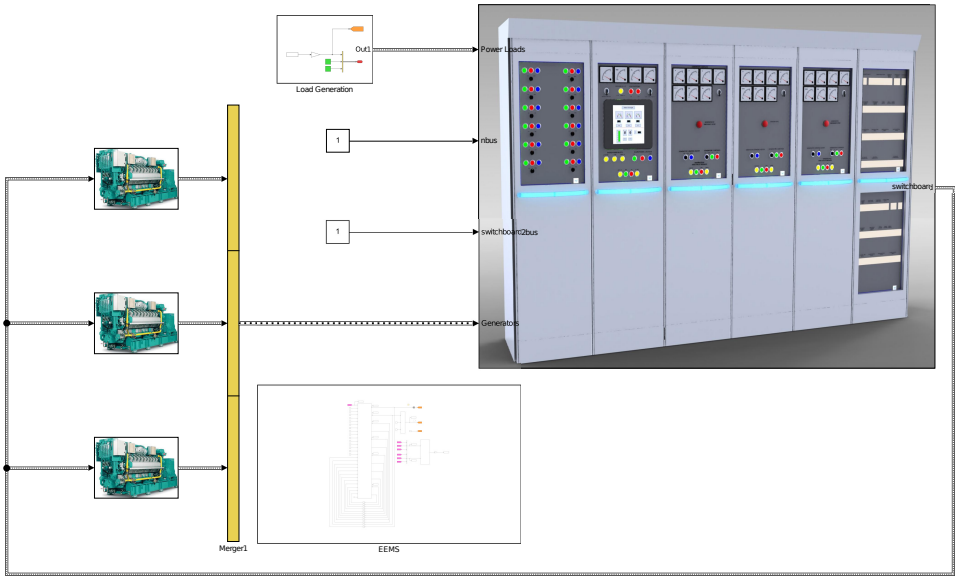

B.3 Power plant 3

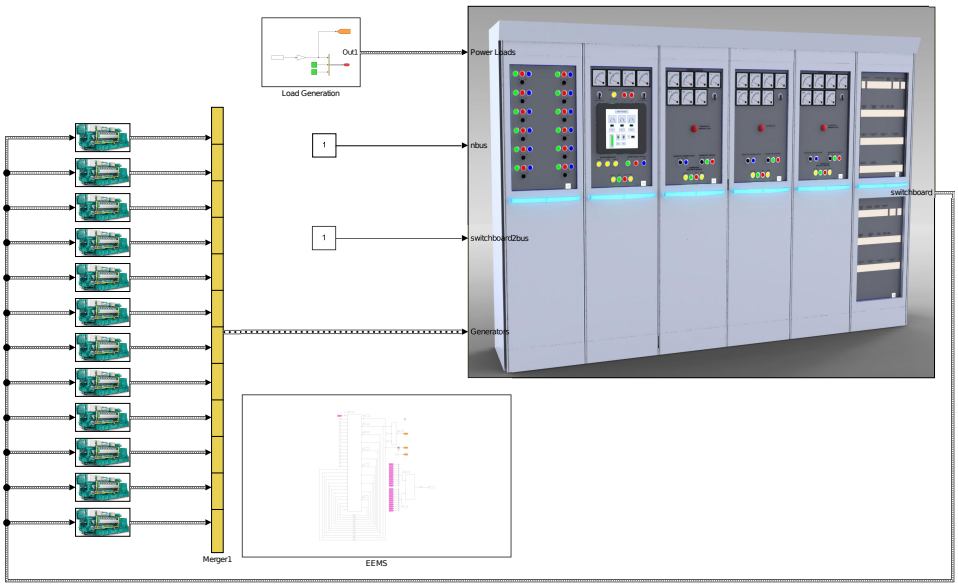

B.4 Corvus Energy System

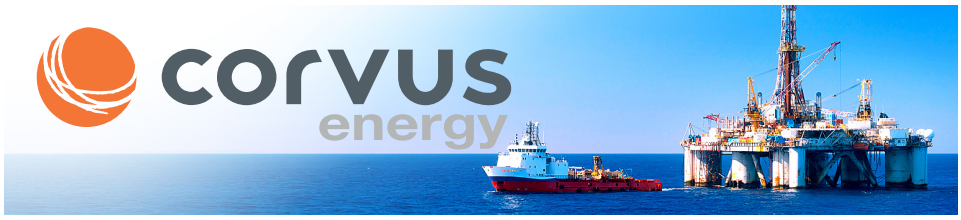

CORVUS Energy Storage Benefits

AT6500-LQ MODULE

- **Rapid return on investment**
- **Safe and proven heavy duty power**
- **Improved operating costs**
- **Better system redundancy**
- **The only lithium battery Type-Approved by DNV-GL, Lloyd's Register and ABS**
- **Reduced harmful emissions**

The Marine Industry Standard

- **COMMISSIONED PROJECTS**
  Over 24 megawatt-hours in over 30 marine systems deployed
- **SUPERIOR LIFE SPAN**
  Excellent cycle life & shelf life
- **TEMPERATURE RANGE**
  0°C to +50°C
- **WATER RESISTANT**
  IP67 enclosure
- **INDUSTRY LEADING BATTERY MANAGEMENT SYSTEM (BMS)**
  High performance rapid charge/discharge (C-Rates) for megawatt scale systems
- **COMPACT AND LIGHTWEIGHT**
  High energy and power density with a small system footprint
- **SCALABLE**
  Infinite scalability at megawatt power levels

CORVUS Energy AT6500 Module Specifications

COMPONENT	AT6500-50 AIR-COOLED	AT6500-100 AIR-COOLED	AT6500-50-LQ LIQUID-COOLED	AT6500-100-LQ LIQUID-COOLED
Maximum Voltage	50.4V	100.8V	50.4V	100.8V
Nominal Voltage	44.4V	88.8V	44.4V	88.8V
Minimum Voltage	38.4V	76.8V	38.4V	76.8V
Capacity	150Ah	75Ah	150Ah	75Ah
RMS [1] C-Rate	0.8C [2]	0.8C [2]	1.5C	1.5C
RMS [1] Current	120A	60A	225A	113A
Energy	6.5kWh	6.5kWh	6.5kWh	6.5kWh
Weight	70 kg (154 lb.)	70 kg (154 lb.)	72 kg (158 lb.)	72 kg (158 lb.)
Size	59x33x38 cm (26x13x15 in)	59x33x38 cm (26x13x15 in)	59x33x38 cm (26x13x15 in)	59x33x38 cm (26x13x15 in)

[1] RMS - True continuous operation; indefinite alternating charge and discharge
[2] Using Corvus CUBE Racking System

corvus energy

ABOUT US

Corvus Energy manufactures the world's most durable Energy Storage Systems (ESS). Designed for heavy industrial applications, a Corvus ESS will reduce fuel consumption, maintenance, emissions & increase reliability. Contact us today to learn how Corvus energy storage can improve your bottom line:

CONTACT
Toll Free: +1 (888) 390-7239
Tech Support +1 (604) 227-1932

HEAD OFFICE
#220-13155 Delf Place
Richmond, BC V6V 2A2 Canada
info@corvus-energy.com

NORWAY
Bergen Office
+47 918 25 618
sales@corvus-energy.com

2015-05-22

www.corvus-energy.com

Kristoffer Lund

Online Optimization of a Hybrid Electric Marine Power Plant Using Mixed Integer Linear Programming

NTNU
Norwegian University of
Science and Technology